REDUCING UNCERTAINTIES OF EVAPOTRANSPIRATION AND PREFERENTIAL FLOW IN THE ESTIMATION OF GROUNDWATER RECHARGE

Report to the
WATER RESEARCH COMMISSION

by

Jovanovic N[1], Bugan RDH[1], Israel S[1], Dzikiti S[1], Kapangaziwiri E[1], Le Maitre D[1], Rozanov A[2], Stander M[2], Mikes D[3], May F[1,3], C. Jarmain[4] and C. Everson[4]
[1] CSIR, Natural Resources and Environment, Stellenbosch
[2] Department of Soil Science, University of Stellenbosch
[3] Department of Earth Sciences, University of Stellenbosch
[4]University of KwaZulu Natal, School of Bioresources Engineering and Environmental Hydrology

WRC Report No. 1909/1/12
ISBN 978-4312-0272-0

March 2012

Obtainable from

Water Research Commission
Private Bag X03
Gezina, 0031

orders@wrc.org.za or download from www.wrc.org.za

DISCLAIMER

This report has been reviewed by the Water Research Commission (WRC) and approved for publication. Approval does not signify that the contents necessarily reflect the views and policies of the WRC, nor does mention of trade names or commercial products constitute endorsement or recommendation for use.

© WATER RESEARCH COMMISSION

EXECUTIVE SUMMARY

BACKGROUND

The quantification of groundwater resources is of utmost importance for future water allocations and management. Groundwater is stored in aquifers that include a static zone (permeable portion of the aquifer below the zone of natural groundwater level fluctuation) with a dynamic zone (volume of groundwater available in the zone of natural groundwater level fluctuation, above the static zone). The key variable of the dynamic storage zone that determines natural groundwater replenishment and water table fluctuations is groundwater recharge.

Several methods for the estimation of groundwater recharge were applied in the past. Results of applications of these methods showed that groundwater recharge estimates varied widely depending on methods and data used. It is widely acknowledged that groundwater recharge estimates can be improved through improved estimation of evapotranspiration (ET) and preferential flow. Uncertainties exist in the estimation of ET that would account for below-potential water use by vegetation as well as preferential flow paths of water and contaminants. Soil water fluxes determining groundwater recharge are also the main drivers of solute and contaminant transport by convection. In that sense, it is inevitable that processes like ET and preferential flow are also relevant to groundwater quality and the protection of groundwater resources. Previous research and statistical analyses of historic climatic data indicated that South Africa may be impacted severely by climate change. Little work was done, however, on the impact of climate change on groundwater resources. It is therefore necessary to investigate linkages between rainfall, ET and recharge in order to describe some possible scenarios of impacts of abstraction and climate change on groundwater resources.

RATIONALE

This project aimed at addressing the knowledge gaps identified in previous research. Improved methodologies for the estimation of recharge were proposed, as well as the use of hydrological models verified with field data to predict the effects of weather, vegetation, soil and geology on groundwater recharge. Evapotranspiration of natural vegetation, in particular Sand Plain Fynbos and Sandstone Fynbos, was never measured before. Preferential flows in the soil and vadose zone were seldom estimated/measured in previous hydrological studies. Accounting for ET and preferential flow in the estimation of the water balance and groundwater recharge provides means for more informed decisions on groundwater resources assessment and management.

OBJECTIVES AND AIMS

The general objective of this project was to develop improved process-based estimates of groundwater recharge. Attention was focused on the determination of two important components of the water balance, in particular evapotranspiration and water movement through preferential flow. The specific aims of the project were:

AIM 1

To develop improved methodologies for the estimation of recharge, by reducing uncertainties in estimates of evapotranspiration and preferential flow, at two typified locations were recharge occurs predominantly through vertical fluxes and through restricted areas on a hillslope.

AIM 2

To develop methodologies for upscaling localized estimations of evapotranspiration and recharge.

AIM 3

To assess the impacts of recharge and associated processes on groundwater quality at two typified locations, by utilizing improved methodologies for recharge estimation.

AIM 4

To use the improved estimates of groundwater recharge in order to predict the possible impacts of climate change on the groundwater resources at two typified locations.

METHODOLOGY

Two typified groundwater recharge mechanisms were considered in this research:

1) The first recharge mechanism is through vertical fluxes (diffuse). This mechanism occurs typically in coastal plain sandy aquifers, on light-textured soils and shallow groundwater tables fluctuating seasonally. A representative study site was selected in the Riverlands Nature Reserve (Western Cape).

2) The second recharge mechanism is through restricted areas that can be represented by alluvial deposits at the bottom of hillslopes or through fractured systems (localized, focused). This mechanism occurs typically on undulating terrain on hillslopes, overlaying shale layers and/or fractured aquifers. A study site representing the Table Mountain Group (TMG) fractured rock aquifer was selected in the Oudebosch catchment in the Kogelberg Biosphere Reserve (Western Cape).

The approach consisted in establishing field trials at the two study sites. The field trials were set up to monitor all components of the hydrological system, namely weather, vegetation, soil, surface water and groundwater. They included historic data collection as well as three years of new data collection in order to generate a time series sufficiently long to account for rainfall and weather variability. The following data were collected at both sites:

- Topography and geology
- Daily weather data and rainfall.
- Soil mapping and description of soil forms
- Soil physical, hydraulic and chemical properties
- Soil infiltration, water content and temperature
- Resistivity in the sub-soil (only Oudebosch)
- Vegetation description
- Fynbos evapotranspiration with scintillometry
- Canopy cover, canopy interception of rain water and root distribution
- Groundwater levels and temperature
- Groundwater quality.

It was retained that this set of monitored variables would be sufficient to generate data for estimating groundwater recharge with improved methods, for setting up and running hydrological and groundwater flow models, and ultimately to fulfil the objectives of the project.

Data collection was used to inform the applications of methods for the estimation of groundwater recharge. In particular, the following methods were applied:

1) Coupled atmospheric-unsaturated zone model (HYDRUS-2D) for the unconfined aquifer at Riverlands to determine one-dimensional water fluxes (groundwater recharge).

2) Groundwater flow model MODFLOW v. 2.8.2 for the TMG fractured rock aquifer at Oudebosch. Groundwater recharge was estimated by calibration against observed groundwater levels.
3) Rainfall Infiltration Breakthrough (RIB) based on historic fluctuations of groundwater tables both at Riverlands and Oudebosch. This approach is less data intensive than process modelling, but it requires long series of groundwater level and rainfall data.

RESULTS AND DISCUSSION

Evapotranspiration studies

The overall aim of ET studies was to improve estimates of ET of fynbos and consequently estimates of groundwater recharge. Three campaigns of ET measurements with scintillometry were performed. The first campaign was carried out on Atlantis Sand Plain Fynbos in October 2010 in the Riverlands Nature Reserve. The other two campaigns were carried out in April-June 2011 and in September-October 2011 on Kogelberg Sandstone Fynbos in the Oudebosch catchment. It was the first time that ET of these two types of endemic fynbos vegetation was measured. The window periods for the campaigns were chosen to be at season change in spring and autumn, at a time when both sunny days with high atmospheric evaporative demand and overcast days with low evapotranspiration can be expected. Measured ET ranged between 0.8 mm d^{-1} and 5.3 mm d^{-1} at Riverlands (canopy cover 39.1%). At Kogelberg, ET ranged between 0.17 mm d^{-1} and 1.40 mm d^{-1} on shallow soils on steep slopes (average canopy cover was 15.5%), and between 1.3 mm d^{-1} and 5.6 mm d^{-1} (canopy cover 32.7%-83.9%). The results of these measurements were used to inform hydrological models and improve estimates of groundwater recharge.

Preferential flow studies

In order to estimate the effects of preferential flow on groundwater recharge, investigations were carried out on soil and sub-soil. The soil studies included soil description at the two study sites as well as an investigation on soil properties, in particular hydraulic conductivity, in the spatial context. It was demonstrated that the application of remote sensing techniques, GIS and soil surveying methods can facilitate the spatial conceptualization of catchment hydrology, delineate soils based on surface features and terrain morphology and reduce the number of field observations required to conduct a comprehensive soil survey. A binary decision tree was developed that can aid in interpolating hydrological properties in unsampled observation sites.

Saturated hydraulic conductivity measured with double-ring infiltrometers ranged between 117.7 and 492.3 mm h^{-1} at Kogelberg (Fernwood and Cartref soil forms respectively) and between 148.2 and 182.6 mm h^{-1} at Riverlands (Vilafontes and Lamotte soil forms). The soil studies also included dye experiments to identify and quantify preferential flow paths. Flow paths ranged between 38% of the soil profile volume in the stony soils on the Kogelberg slopes and 82% in the alluvial plane. At Riverlands, flow paths ranged between 62% and 72% of the profile volume. As a conservative and mobile solute (KI) was used, the dye experiment served the purpose of defining the possible fate of contaminants in the environment and impacts on groundwater quality.

Given prominent preferential flow paths were observed in the soils at Kogelberg, a subsurface resistivity study was conducted in order to investigate whether paths of rapid flow occur also in the sub-soil. The investigation in the sub-soil included acquisition and processing of resistivity tomography images during and following rainfall events in order to identify any changes in resistivity due to infiltration of water through preferential pathways in the TMG fractured rock system. Preferential flow paths were estimated to be about 40% of the profile volume.

Results emanating from the preferential flow studies were also used to spatially delineate soil characteristics, to generate input data and set up hydrological models.

Case study 1: Coupled atmospheric-unsaturated zone modelling (Riverlands)

The purpose of modelling at Riverlands was to quantify evapotranspiration and recharge of an unconfined alluvial aquifer. Evapotranspiration and weather measurements were used to estimate grass reference evapotranspiration (ETo) and potential evapotranspiration of the vegetation. Potential evapotranspiration was then used as input into HYDRUS-2D to calculate the soil water balance and recharge to the shallow groundwater table. Continuous long-term records (five years) of weather, soil water content, vegetation and groundwater were used to simulate the one-dimensional (vertical) soil water balance of fynbos at Riverlands. Simulated average groundwater recharge was 25% of rainfall for five years, ranging between 15 and 35% per year. This was comparable to other studies done in the area.

Case study 2: Groundwater flow modelling (Oudebosch)

The purpose of modelling at Oudebosch was to quantify groundwater flow and to determine the effects of evapotranspiration and preferential flow on groundwater recharge using field data as inputs, and by calibration against observed groundwater levels. Given the objectives of modelling and the seasonal nature of the Oudebosch stream, MODFLOW was used to model the groundwater system. The model was set up using input data obtained mainly through data collection. As it is usually extremely difficult to simulate groundwater flow in complex geological environments, like fractured sandstone, with MODFLOW, the model was calibrated for localized areas surrounding two boreholes, where good conceptual knowledge of the system existed. Simulated data of groundwater heads were compared to observations for calibration purposes. Input data of groundwater recharge were varied until a satisfactory statistical performance of model simulations was obtained compared to observations. Calibrated groundwater recharge for the simulated period of about three years was 20% of total rainfall. It should be noted that the calibrated estimate of groundwater recharge was based on two boreholes that displayed distinct fluctuations in groundwater level. Other boreholes did not display fluctuations in groundwater level and, if used for calibration, they would have likely resulted in much lower values of calibrated recharge. Estimates of recharge therefore depend on the specific boreholes used in the calibration. A more realistic estimate of recharge would have been obtained by averaging responses of boreholes over the whole study area.

Case study 3: Rainfall infiltration breakthrough (Riverlands and Oudebosch)

The coupling and use of process models (e.g. atmospheric, unsaturated zone, saturated zone) is usually very data-intensive. A simpler method, called Rainfall Infiltration Breakthrough (RIB) was therefore proposed in this study in addition to complex physical process models. The method calculates groundwater recharge based on historic rainfall and fluctuations of groundwater tables. The model is applicable at locations where groundwater levels respond distinctly to rainfall and infiltration. This approach is less data-intensive but it requires long series of groundwater level and rainfall data, as well as sound knowledge of aquifer characteristics. The RIB software, written in Excel, was applied both at Riverlands and Oudebosch to estimate daily recharge. The main purpose of using this model was to obtain quick estimates of groundwater recharge time series with a limited amount of input data.

Daily simulations of groundwater recharge were done with the RIB model for boreholes that displayed distinct seasonal groundwater level fluctuations. Depending on input data (in particular specific yield) groundwater recharge estimates ranged between 8% and 41% of annual ranifall at Riverlands and between 5% and 26% at Oudebosch. Assuming a normal probability distribution of groundwater levels, an uncertainty analysis was carried out by propagating input uncertainty through the model to generate an ensemble of outputs whose range represents the uncertainty in groundwater recharge. A perturbation of the groundwater level time series by a factor 20% resulted in a maximum groundwater recharge of 26.9% of mean annual rainfall at Riverlands and 51.7% at Oudebosch.

The Kogelberg Nature Reserve is currently part of the TMG groundwater exploration programme run by the City of Cape Town. Simulations were therefore run with RIB in order to predict trends of groundwater level under different scenarios of abstraction. Abstraction of 3 ML d^{-1} did not affect the groundwater level drastically. However, if the draining area for a borehole is reduced by 1/10 (i.e. 10 abstraction boreholes are used over the same area), the groundwater level was predicted to drop by 0.21 m compared to no abstraction. A second set of scenario simulations was run for Kogelberg in order to predict the effects of climate change on groundwater levels, in particular changes in rainfall. The simulations indicated that the groundwater level could drop by 0.07 m with 10% rainfall reduction and by 0.13 m with 20% rainfall reduction after 3 years.

CONCLUSIONS

Evapotranspiration measurements were invaluable in gaining understanding of the water use and water balance of two types of fynbos. It was the first time that measurements of ET were done on Atlantis Sand Plain Fynbos and Kogelberg Sandstone Fynbos. Evapotranspiration depended on weather conditions, vegetation (root distribution and canopy cover) and soil water storage capacity.

Soil hydraulic properties, in particular saturated hydraulic conductivity and preferential flow patterns, play a large role in groundwater recharge. Hydraulic conductivities are essential inputs in hydrological models and they need to account for preferential flow characteristics. Preferential flow may affect a substantial portion of soil profiles and the plant available water is thus expected to be low as the profile drains and contributes to groundwater recharge. Less variability in the hydraulic properties of Riverlands soils was evident compared to Kogelberg.

The continuous long-term monitoring of weather, soil water content, vegetation and groundwater was very beneficial in terms of model calibration. Both process models used in the case studies were successful in predicting water balance components (both absolute values and temporal trends). In particular, HYDRUS-2D predicted well seasonal variations in soil water content at Riverlands, whilst MODFLOW was calibrated for two localized areas where conceptual knowledge of the system existed. The RIB model proved to be useful for quick estimates of groundwater recharge at locations where groundwater levels respond distinctly to rainfall. The values of groundwater recharge obtained with three selected methods (HYDRUS-2D, MODFLOW and RIB) were within the range of those obtained in other studies. Scenario simulations with the RIB model allowed to quantify possible impacts of abstraction and climate change (reduction in rainfall) on the groundwater resource. The selection of boreholes to be used for calibration is fundamental as the measurements need to be representative of the entire area.

Uncertainty in the estimation of groundwater recharge has implications not only on the recharge estimation, but also on management decision-making and risk associated with the groundwater resource. The uncertainty of the estimates of groundwater recharge depends on the accuracy of measured input data into the model (e.g. scintillometer measurements, weather instrumentation, etc.) and variability in environmental factors (rainfall, groundwater levels, vegetation, hydraulic properties, etc.). The technique used in the uncertainty analysis showed that the error propagation method can be useful for analysing the influence of input data on the simulated groundwater recharge.

RECOMMENDATIONS FOR FUTURE RESEARCH

The following recommendations for further research emanated from this project:

- Data collection and monitoring is a pre-requisite in order to gain understanding of natural systems and predict catchment processes accurately. The usefulness of continuous and long term (at least five years) monitoring was proved again in this project.
- Tools for spatial description of environmental variables (e.g. vegetation, soil properties, etc.) need to be refined and made available.
- Remote sensing tools and products are becoming more and more popular in the estimation of water cycle variables of relevance to groundwater recharge. These need to be validated and investigated further.
- Geophysical methods (e.g. resistivity tomography) showed potential in defining preferential pathways for water in the sub-soil and they should be investigated further. However, the applicability of this methodology is specific to a site because the resistivity readings also depend on salinity and geological characteristics.
- The quantification of uncertainties in catchment hydrology needs to be investigated further given the large number of tools and methods available. Long-term monitoring data are required for this purpose.

ACKNOWLEDGEMENTS

The authors would like to thank the Reference Group of the WRC Project K5/1909 for the assistance and the constructive discussions during the duration of the project:

- *Dr Shafick Adams* — *Water Research Commission*
- *Mr Matthys Dippenaar* — *University of Pretoria*
- *Mr Fortress Netili* — *Council for Geoscience*
- *Dr Hans Beekman* — *Consultant*
- *Dr Scott Sinclair* — *University of KwaZulu-Natal*
- *Dr Danie Vermeulen* — *University of the Free State*
- *Mr PJ Hobbs* — *CSIR*
- *Mr E van Wyk* — *Department of Water Affairs*

The authors wish to acknowledge Cape Nature Conservation for providing the pilot study sites at the Riverlands Nature Reserve and in the Kogelberg Biosphere Reserve. The Burgerspost farm is also acknowledged (Riverlands site).

The authors thank GEOSS (Julian Conrad and Dale Barrow) for supplying the weather time series of data for Kogelberg and the Riverlands Nature Reserve for providing rainfall data. GEOSS and the groundwater exploration programme of the City of Cape Town are acknowledged for providing groundwater level and quality data for Kogelberg. The South African Weather Services (SAWS) and the Western Cape Department of Agriculture are thanked for supplying weather data for Malmesbury and Langgewens, respectively.

The Institute for Groundwater Studies at the University of the Free State (Dr Ingrid Dennis, Dr Rainier Dennis and the student Pacome Ahokpossi) is acknowledged for their contributions in the first year of the project.

Prof Yongxin Xu and Mr Xiaobin Li (UNESCO Chair of Hydrogeology, University of the Western Cape) are thanked for the development and contribution in the application of the Rainfall Infiltration Breakthrough (RIB) model.

TABLE OF CONTENTS

LIST OF FIGURES

LIST OF TABLES

LIST OF SYMBOLS AND ACRONYMS

∆H – Height difference (m)

ΔS – Change in soil water content, usually measured continuously or manually with a variety of techniques (mm)

A – Double-ring inner surface area (m^2)

B – Baseflow

BD – Bulk density (g cm^3)

BDT – Binary decision tree

C – Conductance (m^2 d^{-1})

Cc – Concordia soil form

Cf – Cartref soil form

C_N^2 – Refractive index of air

CRD – Cumulative Rainfall Departure

D – Drainage (mm)

D – Drainage (or capillary rise), it approximates vertical recharge (mm)

Dayi – Day of simulation

dh(crd) – Calculated water level with the CRD method (m)

dh(rib) – Calculated water level with the RIB method (m)

dh_obs – Observed water level fluctuation in the RIB model (m)

DWAF – Department of Water Affairs and Forestry

E – Soil evaporation (mm)

EC – Electrical conductivity (mS m^{-1})

ET – Actual evapotranspiration (mm)

ETo – Penman-Monteith grass reference evapotranspiration (mm)

FAO – Food and Agricultural Organization of the United Nations

FC – Field capacity

Fw – Fernwood soil form

G – Soil heat flux (W m^{-2})

Gk – Groenkop soil form

GPS – Geographic Positioning System

GRA – Groundwater Resource Assessment

Gs – Glenrosa soil form

GWC – Gravimetric soil water content

H – Sensible heat flux (W m^{-2})

Hh – Houwhoek soil form

HSU – Hydrologically Similar Units

I – Current intensity (A)

i – Sequential number of rainfall events

k – Geometric factor dependent on the arrangement of resistivity electrodes

Ka – Katspruit soil form

Kc – FAO crop factor

Kc_{max} – Coefficient dependent on vegetation (i.e. height, morphology) and environmental conditions (i.e. weather variables)

K_{crd} – Parameter of the CRD method

K_{sat} – Saturated hydraulic conductivity (m d^{-1})

L – Distance, reference level (m)

lag_Days – Time delay between rainfall events and recharge (d)

LE – Latent flux of vapourization (W m^{-2})

Length_D – Parameter that characterizes rain sequences and antecedent conditions in the RIB model (d)

Lt – Lamotte soil form

M – Thickness of the river bed (m)

m, n – Start and end of time series

MAE – Mean absolute error

NDVI – Normalized difference vegetation index

OM – Organic matter content (%)

P – Precipitation (mm)

P_a – Apparent resistivity (ohm)

P_{av} – Average rainfall over the entire rainfall time series (mm)

PAW – Plant available water (mm)

PD – Porosity

PET – Potential evapotranspiration (mm)

Pg – Pinegrove soil form

PT – Potential transpiration (mm)

P_t – Threshold value representing aquifer boundary conditions, determined during the simulation process (ranging from 0 for a closed aquifer to P_{av} for an open aquifer) (mm)

$Q_{\_other}$, Q_{out}, $Q_{\_pumpage}$ – Sink/source terms in the RIB model (m^3 d^{-1})

R – Groundwater recharge (mm)

r – Recharge percentage (fraction of cumulative rainfall departure that contributes to rainfall infiltration breakthrough)

R^2 – Coefficient of determination

rain – Daily rainfall in the RIB model (mm)

R_{AV} – Average rainfall in the RIB model (mm d^{-1})

Re – Ratio of recharge to rainfall

Re(rib) – Calculated recharge in the RIB method (mm d^{-1})

Res – Electrical resistance (ohm)

RG – Reference group

RIB – Rainfall Infiltration Breakthrough model

RMSE – Root mean square error

Rn – Net radiation (W m^{-2})

Ro – Runoff or run-on (a component of lateral subsurface inflow/outflow can also be included) (mm)

R_{ref} – Threshold value representing aquifer boundary conditions in the RIB model

SPAC – Soil-plant-atmosphere continuum

S_r – Specific retention equivalent to field capacity

S_y – Specific yield

T – Plant transpiration (mm)

T – Time (s)

TMG – Table mountain group

V – Volume of water (m^3)

Vt – Voltage (V)

VWC – Volumetric soil water content

W – Width of the river (m)

Wf – Witfontein soil form

WL_{AV} – Average groundwater level in the RIB model (m)

WRC – Water Research Commission

Y – Crop yield or productivity (kg ha^{-1})

Ym – Maximum crop yield or productivity (kg ha^{-1})

1 INTRODUCTION AND OBJECTIVES

1.1 Background and rationale

The quantification of groundwater resources is of utmost importance for possible future water allocations, taking into account the legal requirements of ensuring the reserve and associated water quality. To this effect, a groundwater resource assessment exercise was commissioned by DWAF (Department of Water Affairs and Forestry), published in 2006 and commonly known as GRA II (http://www.dwaf.gov.za/Geohydrology/gra2.htm). The GRA II document was based on the quantification of a static storage zone (volume of groundwater available in the permeable portion of the aquifer below the zone of natural groundwater level fluctuation) with a dynamic storage zone (volume of groundwater available in the same aquifer in the zone of natural groundwater level fluctuation). The key variable of the dynamic storage zone that determines natural groundwater replenishment and water table fluctuations is groundwater recharge. This physical variable is therefore the basis for accurate estimation of groundwater resources, for determining the modes of water allocation and groundwater resource susceptibility to abstraction and climate change.

Several methods for the estimation of groundwater recharge were applied in the past with more or less success (Xu and Beekman, 2003). Results of applications of these methods showed that groundwater recharge estimates done by different practitioners varied widely when different methods and input data sets were used. Most of the groundwater recharge methodologies developed is applicable to the large scale, whilst little information is available describing processes at the local scale. For example, uncertainties exist in the estimation of evapotranspiration that would account for below-potential water use by vegetation as well as preferential flow paths of water and contaminants. Although methodologies for measuring water use were successfully applied in crop production (Jarmain *et al*., 2009), evapotranspiration of natural indigenous vegetation was seldom measured. Preferential flow was also neglected in the past because it is a localized process and difficult to measure under field conditions (Coppola *et al*., 2009). In addition, upscaling of both evapotranspiration and preferential flow required further investigation.

Soil water fluxes determining groundwater recharge are also the main drivers of solute and contaminant transport by convection (Saayman *et al*., 2007). In that sense, it is inevitable that processes like evapotranspiration and preferential flow are also relevant to groundwater quality and the protection of groundwater resources. Previous research and statistical analyses of historic climatic data indicated that South Africa may be impacted severely by climate change (Schulze, 2005). This may result in changes in rainfall distribution, increased/decreased annual rainfall, temperature and evapotranspiration in different areas. Possible scenarios of changes in atmospheric variables and impacts on surface waters have been done in the past. Little work was done, however, on the impact of climate change on groundwater resources. It was therefore necessary to investigate linkages between rainfall, evapotranspiration and recharge in order to describe some possible scenarios of impacts of abstraction and climate change on groundwater resources.

The innovation content of this project is in addressing these knowledge gaps that were identified in previous research. Improved methodologies for the estimation of recharge are proposed, as well as the use of hydrological models verified with field data to predict the impacts of weather, vegetation, soil and geology on groundwater recharge. Evapotranspiration of natural vegetation, in particular Sand Plain Fynbos and Sandstone Fynbos, was never measured before. Preferential flows in the soil and vadose zone were seldom estimated/measured in previous hydrological studies. The principle of monitoring the entire hydrological system, including weather, vegetation, soil, surface water and groundwater, is promoted. This is not novel, but it is seldom used due to capacity and financial constraints.

1.2 Objectives

The general aim of this project was to develop improved process-based estimates of groundwater recharge. Attention was focused on the determination of two important components of the water balance, in particular evapotranspiration and water movement through preferential flow.

The specific objectives of the project were:

1) To develop improved methodologies for the estimation of recharge, by reducing uncertainties in estimates of evapotranspiration and preferential flow, at two typified locations were recharge occurs predominantly through vertical fluxes and through restricted areas on a hillslope.
2) To develop methodologies for upscaling localized estimations of evapotranspiration and recharge.
3) To assess the impacts of recharge and associated processes on groundwater quality at two typified locations, by utilizing improved methodologies for recharge estimation.
4) To use the improved estimates of groundwater recharge in order to predict the possible impacts of climate change on the groundwater resources at two typified

locations.

1.3 Approach

Two typified groundwater recharge mechanisms were considered in this research:

3) The first recharge mechanism is through vertical fluxes (diffuse). This mechanism occurs typically in coastal plain sandy aquifers, on light-textured soils and shallow groundwater tables fluctuating seasonally. An example of this recharge mechanism is the West Coast area and the Cape Flats sandy aquifers.
4) The second recharge mechanism is through restricted areas that can be represented by alluvial deposits at the bottom of hillslopes or through fractured systems (localized, focused). This mechanism occurs typically on undulating terrain on hillslopes, overlaying shale layers and/or fractured aquifers. An example of this recharge mechanism can be found in the Table Mountain Group (TMG) aquifer (Xu *et al*., 2007).

The approach consisted in establishing field trials at two sites with aquifers representing the two typified recharge mechanisms, namely in the Riverlands Nature Reserve and in the Oudebosch catchment in the Kogelberg Biosphere Reserve, both in the Western Cape. The field trials were set up to monitor all components of the hydrological system, namely weather, vegetation, soil, surface water and groundwater. They included historic data collection as well as three years of new data collection in order to generate a time series sufficiently long to account for rainfall and weather variability.

Data collection was used to inform the applications of methods for the estimation of groundwater recharge. In particular, the following methods were applied:

4) Coupled atmospheric-unsaturated-saturated zone model for the unconfined aquifer at Riverlands to determine one-dimensional water fluxes (groundwater recharge).
5) Groundwater flow model MODFLOW v. 2.8.2 (McDonald and Harbaugh, 1988) for the TMG fractured rock aquifer at Oudebosch. Groundwater recharge was estimated by calibration against observed groundwater levels.
6) Rainfall Infiltration Breakthrough (RIB) based on historic fluctuations of groundwater tables both at Riverlands and Oudebosch. This approach is less data intensive than process modelling, but it requires long series of groundwater level and rainfall data.

2 LITERATURE REVIEW AND KNOWLEDGE GAPS

2.1 Introduction

Groundwater is a critical source of fresh water worldwide, in particular in semi-arid and arid areas (Clarke *et al*., 1996), and integral part of the hydrological cycle (Alley *et al*., 2002). A groundwater system includes the aquifer in which groundwater is stored and limited by flow boundaries, replenishment areas (recharge) and discharge (e.g. springs). The static storage zone is the volume of groundwater available in the permeable portion of the aquifer below the zone of natural groundwater level fluctuation and it can be figuratively compared to an underground water reservoir. However, groundwater is not static. It gets replenished through recharge and it flows into discharge points or areas. Flow depends on hydraulic head gradients, hydraulic conductivity and porosity (properties of the aquifer), so travel time and groundwater age may range from a few hours to millions of years (Alley *et al*., 2002). This has implications to both groundwater usage and transport of contaminants. The dynamic storage zone is the volume of groundwater available in the zone of natural groundwater level fluctuation. This is also the volume of groundwater that can be used without compromising the sustainability of the system, after replenishment and before discharge. It is therefore clear that groundwater recharge measurement or estimation is a key variable in the hydrological cycle in terms of groundwater resource assessment, management, allocation and also vulnerability to climate change.

Several methods for the estimation of groundwater recharge were applied in the past and these were comprehensively summarized in reviews by Alley *et al*. (2002), Scanlon *et al*. (2002), and Xu and Beekman (2003). More or less success was achieved in the accuracy of predicting recharge using these available methods. In addition, groundwater recharge estimates done by different practitioners varied widely when different methods and data sets were used. This was mainly due to uncertainties of methodologies applied and associated processes. Two processes that are common source of uncertainties are evapotranspiration and preferential flow.

This Chapter reviews the following:

- Mechanisms of groundwater recharge, evapotranspiration and preferential flow;
- Available methods for the estimation of groundwater recharge, evapotranspiration and preferential flow at different scales; and
- Available methods for the estimation of uncertainties concerning groundwater recharge, evapotranspiration and preferential flow.

2.2 Groundwater recharge

2.2.1 Groundwater recharge processes

Groundwater recharge can be defined as the process of water entering a groundwater body, after infiltration and percolation through the unsaturated zone, and it can be classified based on the flow mechanism through the unsaturated zone, the area on which it occurs and/or the time scale (Cave *et al*., 2002). Recharge is commonly broadly classified as diffuse (occurring over a large area) or localized (e.g. from surface ponds or through fractures in heterogeneous porous systems) based on the two typified recharge mechanisms (Alley *et al*., 2002). In natural systems, a combination of diffuse and localized recharge generally occurs. Recharge is often difficult to measure/estimate and it is subject to a certain degree of uncertainty, due to the limited accuracy of measurements and the heterogeneity of the system (Hupet *et al*., 2004). It depends on rainfall and weather patterns, topography, soil properties, vegetation, geology, as well as anthropogenic activities (e.g. land use change, irrigation, urbanization, water diversion through canals, etc.), spatial and temporal scales (e.g. short-term changes of weather are not likely to have an effect on groundwater levels). Holman (2007) indicated some specific factors affecting groundwater recharge, including changed precipitation and temperature regimes, coastal flooding, urbanization, woodland establishment, and changes in cropping rotations and management practices.

The estimation of groundwater recharge generally requires the following steps:

1) The first step in determining recharge and its mechanisms is data collection (in particular for factors affecting recharge) and development of a conceptual model for the groundwater system.
2) The second step is to use multiple techniques for quantification of the water fluxes (atmospheric, runoff, unsaturated and saturated conditions).
3) The third step is to determine uncertainties in the estimation of groundwater recharge.

A conceptual model is an important prerequisite for the description of a groundwater system. Even in the absence of data, a conceptual understanding of the aquifer/s and its dynamics can be developed based on coarser scale geohydrological information.

2.2.2 Measurement or estimation

Xu and Beekman (2003) reviewed recharge estimation methods commonly used in Southern Africa. Alley *et al*. (2002) and Scanlon *et al*. (2002) discussed measurement and estimation techniques including:

- The water balance.
- Unsaturated zone methods (zero-flux plane method, Darcy method and lysimeters; Healy and Scanlon, 2011).
- Geophysical measurements (time-domain reflectrometry, ground-penetrating radar and tomography; Huisman *et al*., 2001).
- Analytical approaches (Healy and Scanlon, 2011).
- Simulation models with manual (trial and error) or automatic parametrization (Sophocleous and Perkins, 2000; Scanlon *et al*., 2002; Healy and Scanlon, 2011):
    - Empirical models (usually based on empirical relations between groundwater recharge and some climatic and basin parameters like rainfall, temperature, runoff, elevation or vegetation cover).
    - Unsaturated zone flow (water budget tipping bucket models, Richards' equation-based models, etc.).
    - Watershed models (usually based on water storage tanks in different environmental compartments).
    - Groundwater flow models.
    - Coupled models (surface water, unsaturated zone and groundwater models).
- Chemical and isotopic tracers (chloride, stable isotopes, tritium/helium, chlorofluorocarbons) (Cook and Solomon, 1997; Cook and Bohlke, 1999; Healy and Scanlon, 2011); heat as a tracer (Healy and Scanlon, 2011).
- Use of land and satellite remote sensing applications (Pool and Eychaner, 1995; Wahr *et al*., 1998; Milewski *et al*., 2009).
- Estimation based on surface water data (stream water budget usually assuming that baseflow is equal to recharge; streamflow seepage measurements; streamflow duration curves; hydrograph analysis method; chemical hydrograph analysis through the mass balance of an injected tracer) (Healy and Scanlon, 2011) .
- Piezometer measurements (Van der Kamp and Schmidt, 1997).
- Estimation of water level rises in rainfed agriculture (Healy and Scanlon, 2011).
- Water table fluctuation method (Healy and Scanlon, 2011).

The choice of the recharge estimation technique(s) will depend on the objectives (Scanlon *et al*., 2002). For example, water resource assessment requires techniques that provide large scale information, whereas groundwater contamination requires detailed information on spatial variability and preferential flow. Scanlon *et al*. (2002) also discussed space/time scales, range, applicability in arid and humid regions, and reliability of recharge estimates for a number of methods. They classified methods according to the hydrological zones from where data are obtained (surface water, unsaturated zone and saturated zone) and the nature of the technique (physical method, tracers and numerical models).

De Vries and Simmers (2002) provided a summary of the recharge process with focus on semi-arid areas in Southern Africa, identified recurring recharge-evaluation problems and reported on some recent advances in estimation techniques. They indicated direct measurements of spring discharge or stream baseflow, water balance, Darcian approaches, tracers (chloride mass balance calculations, isotope dating) and empirical methods to be commonly used techniques for different applications.

Ebel and Nimmo (2009) adopted an empirical approach by developing a simple model (Source-Responsive Preferential-Flow, SRPF model) for conservatively-transported radionuclides to groundwater. This empirical preferential flow model was developed to estimate travel times as a function of distance of solute transport, fastest solute transport velocities measured in 64 field tests (Nimmo, 2007), mean annual precipitation and the temporal nature of water supply to preferential paths (continuous or intermittent). Fastest travel times correlated strongly with the nature of water supply but not with the nature of the porous medium based on the 64 field tests (Nimmo, 20007), so the latter was not accounted for in the simple empirical model.

Both Scanlon *et al*. (2002) and De Vries and Simmers (2002) indicated that tracer techniques are the most accurate for groundwater contamination investigation. However, these measurements refer generally to the point scale, and spatial extrapolation may be difficult because of preferential pathways. For the regional scale, De Vries and Simmers (2002) recommended multiple point scale data or area/groundwater-based estimation methods with a combination of measured data, remote sensing and GIS.

2.2.3 Spatial and temporal scales

Estimations of groundwater recharge are often difficult because rates can be highly variable in space and time. There is an inherent uncertainty in all methods for the estimation of groundwater recharge and it is often difficult to assess the accuracy of any method. The cost of the method may also play a role in the selection of the spatial and temporal application of the method. It is therefore highly recommended that more than one method be used and that these methods be consistent with the purpose of the groundwater recharge estimation. The spatial scales of interest (e.g. field site, watershed, region) and the time scale (e.g. current rates of recharge, historical, future) need to be well defined. Tables 1 and 2 summarize the spatial and temporal scales recommended for applications of different groundwater recharge estimation methods (Healy and Scanlon, 2011).

TABLE 1
SUMMARY OF GROUNDWATER RECHARGE ESTIMATION METHODS AND THEIR APPLICABILITY TO DIFFERENT TEMPORAL SCALES (after HEALY and SCANLON, 2011)

Method		Type		Recharge (R), Drainage (D), Baseflow (B)	Time scales							
		Focused	Diffuse		Event/Daily	Weekly	Seasonal	Annual	Multi-annual	Decadal	Millennial	Steady
Water budget	Aquifer	x	x	R, B	x	x	x	x				x
	Soil column		x	R, D	x	x						
	Watershed	x	x	R, D	x	x	x	x				
	Stream	x		R, D, B	x	x						
Models	Unsaturated zone – Soil tank		x	R, D	x	x						
	Unsaturated zone - Richard's equation		x	R, D	x	x						
	Watershed	x	x	R, D, B	x	x						
	Groundwater flow	x	x	R, B	x	x	x	x				x
	Coupled surface water and groundwater	x	x	R, B	x	x						
	Empirical	x	x	R			x	x				x
Darcy's method	Unsaturated zone		x	D	x	x						x
	Groundwater	x	x	R	x	x	x	x				
	Surface water and groundwater	x		R	x	x						
Unsaturated zone – Groundwater methods	Zero-flux		x	D	x	x						
	Lysimeter		x	D	x	x						
	Water table fluctuation		x	R	x	x	x					
Surface water-based methods	Seepage	x		R, D, B	x							
	Step-response function	x		R	x	x						
	Flow duration		x	B					x	x		
	Hydrograph separation		x	B					x	x		
	Recession-curve displacement		x	R, B					x	x		
	Chemical hydrograph separation		x	B	x	x	x	x	x	x		
	Tracer injection		x	B	x							
Tracer methods – Unsaturated zone	Chloride		x	D					x	x	x	x
	Tritium		x	D					x	x		
	Chlorine-36		x	D					x	x		
	Applied	x	x	D	x	x	x	x	x			
	Heat		x	D		x	x					

Tracer methods - Groundwater	Chloride	x	x	R						x	x	x
	Carbon-14	x	x	R						x	x	x
	Tritium	x	x	R					x	x		
	Chlorine-36	x	x	R					x	x		
	Chlorofluorocarbons		x	R					x	x		
	SF_6		x	R					x	x		
	Tritium/Helium-3		x	R					x	x		
	Applied	x	x	R	x	x	x	x				
Tracer method - Surface water	Heat	x		R	x	x	x					

TABLE 2
SUMMARY OF GROUNDWATER RECHARGE ESTIMATION METHODS AND THEIR APPLICABILITY TO DIFFERENT SPATIAL SCALES (after HEALY and SCANLON, 2011)

Method		Spatial scale						
		$1\ m^2$	$10\ m^2$	$100\ m^2$	1 ha	$1\ km^2$	$10^3\ m^2$	$10^8\ m^2$
Water budget	Aquifer				x	x		
	Soil column	x						
	Watershed				x	x	x	x
	Stream			x	x	x		
Models	Unsaturated zone – Soil tank	x						
	Unsaturated zone - Richard's equation	x	x	x				
	Watershed				x	x	x	x
	Groundwater flow				x	x	x	x
	Coupled surface water and groundwater				x	x		
	Empirical	x	x	x	x	x	x	x
Darcy's method	Unsaturated zone	x						
	Groundwater	x	x	x				
	Surface water and groundwater	x	x	x				
Unsaturated zone – Groundwater methods	Zero-flux	x						
	Lysimeter	x	x					
	Water table fluctuation		x	x				
Surface water-based methods	Seepage	x						
	Step-response function			x	x	x	x	
	Flow duration					x	x	x
	Hydrograph separation					x	x	x
	Recession-curve displacement					x	x	x
	Chemical hydrograph separation				x	x	x	
	Tracer injection				x	x	x	
Tracer methods – Unsaturated zone	Chloride	x	x					
	Tritium	x	x					
	Chlorine-36	x	x					
	Applied	x	x	x				
	Heat	x						
Tracer methods - Groundwater	Chloride			x	x			
	Carbon-14			x	x			
	Tritium		x	x				
	Chlorine-36		x	x				
	Chlorofluorocarbons		x	x				
	SF_6		x	x				
	Tritium/Helium-3		x	x	x			
	Applied		x	x				
Tracer method - Surface water	Heat	x						

2.3 Evapotranspiration

2.3.1 Evapotranspiration processes

Relevant definitions of the evapotranspiration terminology are reported in Box 1. These were obtained from the Irrigation and Drainage Bulletin No. 56 of the Food and Agricultural Organization (FAO) of the United Nations (Allen *et al*., 1998).

Reference evapotranspiration is the evaporation from a reference surface of the Earth and it depends on weather conditions. The reference surface can be an open water surface (open pan) or it can be related to weather variables (temperature, radiation, sunshine hours, wind speed, air humidity, etc.). Many semi-empirical equations exist that relate reference evapotranspiration to weather variables. Some of the most commonly adopted are Blaney-Criddle (Blaney and Criddle, 1950), Jensen-Haise (Jensen and Haise, 1963), Hargreaves (1983) and Thornthwaite (1948).

Theoretical equations that describe the mechanisms of the evaporation process are also available. For example, reference evaporation from an open water surface was first described by Penman (1948) and consisted of a radiation and a vapour pressure deficit term, representing the available energy for the endothermic evaporation process. Priestley and Taylor (1972) proposed the Priestley-Taylor equation, where the radiation term dominates over the advection term by a factor of 1.26, suitable for large forest catchments and humid environments. The FAO proposed the Penman-Monteith grass reference evapotranspiration (Box 1), based on decades of data and knowledge gathered. The Penman-Monteith ETo is a function of the four main factors affecting evaporation, namely temperature, solar radiation, wind speed and vapour pressure. The type of vegetation is accounted through canopy resistance to gas exchange fluxes, height determining surface roughness, and albedo.

The evapotranspiration of vegetation (crops) differs distinctly from the reference evapotranspiration (ETo) because the ground cover, canopy properties and aerodynamic resistance of vegetation may be different from grass. This difference can be integrated into a factor Kc, commonly known as crop coefficient because it is used to calculate crop water requirements (Allen *et al*., 1998). Potential evapotranspiration of vegetation can then be calculated as: PET = Kc ETo.

Box 1: Definitions of evapotranspiration terminology (Allen *et al*., 1998)

Evapotranspiration (ET)

Evapotranspiration (ET) is the combination of two separate processes whereby water is lost on the one hand from the soil surface by evaporation and on the other hand from plants by transpiration. Evaporation and transpiration occur simultaneously and there is no easy way of distinguishing between them.

In this report, ET is referred as actual evapotranspiration, i.e. the evapotranspiration affected by, and adjusted for limiting factors like water stress.

Evaporation (E)

Evaporation is the process whereby liquid water is converted to water vapour (vaporization) and removed from the evaporating surface (vapour removal), which can be lakes, rivers, pavements, soils and wet vegetation.

Transpiration (T)

Transpiration consists of the vaporization of liquid water contained in plant tissues and the vapour removal to the atmosphere. Vegetation predominantly lose their water through stomata.

Reference crop evapotranspiration (ETo)

Evapotranspiration rate from a reference surface, not short of water. The reference surface is a hypothetical grass reference crop with an assumed crop height of 0.12 m, a fixed surface resistance of 70 s m^{-1} and an albedo of 0.23.

Potential evapotranspiration (PET)

Evapotranspiration of a crop grown in large fields under excellent agronomic and soil water conditions.

In nature, PET seldom occurs, especially in semi-arid areas. When water is a limiting factor, physiological adaptation of plants occurs, stomata close and evapotranspiration rates are below potential rates. This mechanism of stomatal control is described schematically in Figure 1. In the soil-plant-atmosphere continuum (SPAC), water fluxes are driven by atmospheric demand and limited by soil water supply. Under wet soil conditions, the ratio of actual transpiration (T) and potential transpiration (PT), or relative transpiration (T/PT) is close to 1, showing that the root system is able to supply the canopy with water fast enough to keep up with the atmospheric evaporative demand and thereby preventing wilting. Under these conditions, transpiration is atmospheric demand-limited. As the soil dries beyond field capacity (FC) and beyond a threshold value of water content, T/PT drops below 1. Under these conditions, transpiration is soil water supply-limited as the root system can no longer supply water fast enough to keep up with demand and the soil water can be seen to be less available. Beyond soil water content at permanent wilting point (PWP), transpiration does not occur and T/PT = 0. The same mechanism can be represented for ratios of actual to potential evapotranspiration (ET/PET) as well as actual to maximum yield or productivity (Y/Ym). Plant available water (PAW) depends on rooting depth, soil depth, texture and structure. Similar mechanisms occur for direct evaporation from the soil surface. Canopy cover is generally used to split evaporation and transpiration, as such split approximates the available solar energy intercepted by the canopy and reaching the soil surface (Ritchie, 1972). The original publication of Denmead and Shaw (1962) included the first scientific evidence on the concept of atmospheric demand-soil water supply, and this was followed by a large number of research studies in the last few decades that culminated in the FAO revision of crop water requirements (Allen *et al*., 1998).

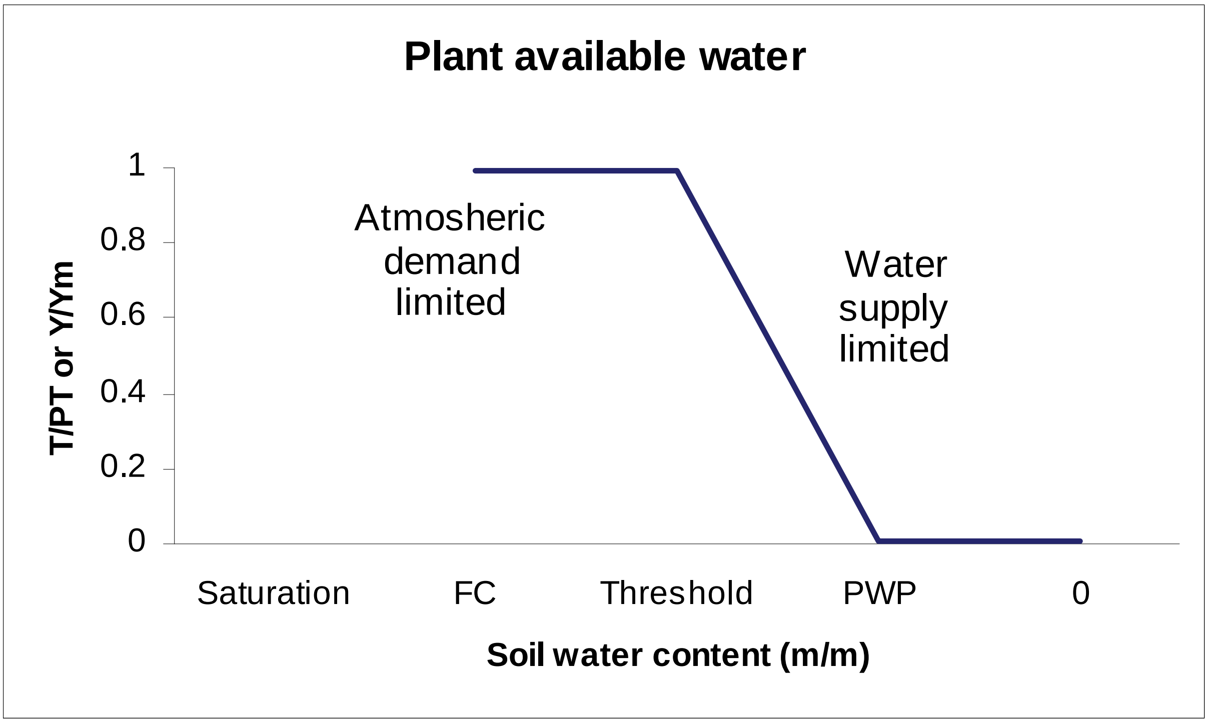

Figure 1

Schematic representation of the plant available water (PAW) graph. T – Actual transpiration; PT – Potential transpiration; Y – Actual yield or productivity; Ym – Maximum yield or productivity; FC – Soil water content at field capacity; PWP – Soil water content at permanent wilting point

2.3.2 Measurement or estimation

A large number of methods and techniques for measurements and estimation of evapotranspiration are available (Allen *et al*., 1998). These can be categorized into the following:

- Lysimeters: This is the only direct method to measure evapotranspiration.
- Atmospheric measurements

  Energy balance and micrometeorological methods: These methods are based on the computation of water fluxes based on measurements of atmospheric variables and they are therefore often referred to as direct measurements. Methods and techniques (e.g. Bowen ratio (Sanderson and Cooper, 2008), scintillometry, etc.) were widely discussed by Jarmain *et al*. (2009).

  Weather data: These methods are based on the calculation of evapotranspiration from weather data (e.g. Penman-Monteith equation for reference evapotranspiration).
- Plant measurements

  Infrared thermometry.

  Remote sensing from aircraft: Images, generally in the infrared and red band, are processed to produce a normalized difference vegetation index (NDVI) that describes the vegetation activity and its status.

  Remote sensing from satellite: These methods were not feasible in the past at high frequency; however, with the latest technological advances, these techniques show promise (e.g. SEBAL) (Bastiaansen *et al*., 1998).
- Soil measurements

  Soil water balance:

  $ET = P - Ro - D + \Delta S$

  P – Precipitation

  Ro – Runoff or run-on (a component of lateral subsurface inflow/outflow can also be included)

  D – Drainage (or capillary rise), it approximates vertical recharge

  ΔS – Change in soil water content, usually measured continuously or manually with a variety of techniques

Although methodologies for the estimation of reference and potential evapotranspiration are widely adopted, actual (below-potential) evapotranspiration is difficult to quantify. Currently, many models developed for different objectives and scales apply the concept of atmospheric demand-soil water supply limited evapotranspiration. These were described in Deliverable 3 of this project. As a result of this modelling review, it was recommended that actual evapotranspiration be estimated through the concept of atmospheric demand-soil water supply. For this purpose, a daily time step is required in the calculation of water balance variables relevant to groundwater recharge to account for daily actual evapotranspiration and rainfall distribution. Improved recharge estimates are possible with the combination of atmospheric factors (PET and ET), vegetation (plant response to water stress, root system), soil and lithology (water storage, flow direction) and geology (texture, porosity, conductivity, fractures).

2.4 Preferential flow

2.4.1 Preferential flow processes

Much work was done on preferential flow in the past decades and comprehensive documents are available. For example, Bosch and King (2001) edited proceedings of an international symposium on preferential flow, water movement and chemical transport in the environment, published by the American Society of Agricultural Engineers (ASAE).

Preferential flow is defined as those phenomena where water and solutes move along certain pathways, while by-passing other volume fractions of the porous soil matrix (Gerke, 2006 in Coppola *et al*., 2009). From this definition, the concept of mobile/immobile water (Gaudet *et al*., 1977) and dual porosity flow (Moench, 1984; Arbogast, 1987) was deduced. Fetter (1993) classified preferential flow as i) short-circuiting, ii) fingering and iii) funnelling. Short-circuiting occurs due to movement of infiltrating water along preferential paths (e.g. rock fractures and fissures). Fingering occurs due to pore-scale variations in permeability and instability of the wetting front, especially at boundaries where finer sediment overlies coarser sediment. The wetting front is the zone that water (and contaminants) invades advancing into an initially dry medium, with matric potentials typically just below saturation (between 0 and –2 J kg^{-1} or 2 kPa suction). Wang and Wang (2001) differentiated between finger flows of type I – preferential flows in homogeneous continuum media with randomness in initial conditions – and finger flows of type II – preferential flows in heterogeneous ontinuum media. They indicated that Darcy’s law is applicable to both cases, as well as to the case of discontinuous media, with the concept of random potential equally applicable. Funnelling occurs whenever water is funnelled on sloping impermeable layers, and concentrated at the end of these layers where it percolates vertically. Nieber (2001) classified preferential flow as i) macropore flow, ii) gravity-driven unstable flow, iii) heterogeneity-driven flow, iv) oscillatory flow, and v) depression-focused recharge. Nieber

(2001) also discussed spatial scales at which each of these preferential flow processes occurs.

It should be noted that there is a need to clearly differentiate between the concept of preferential flow occurring in soils and sub-soils, and the different scales at which it occurs. In soils, preferential flow is generally referred to fingering and water movement through macropores formed by root systems, animal burrows, or swelling and shrinking clay. The most common mechanisms of preferential flow in sub-soils are through rock fractures and fissures as well as through funnelling. Preferential flows occur at a small scale, but the effects (e.g. groundwater contamination) are often visible at a large scale (Fluhler *et al*., 2001). In some cases, modelling random transmissivity variability and detailed preferential flow paths lead to small differences in predictions of contaminant spreading (Simic and Destouni, 2001). Gee and Hillel (1988 in De Vries and Simmers, 2002) differentiated three scales of localized recharge through preferential flow: i) micro-scale pathways (shrinkage cracks, roots and burrowing animals); ii) meso-scale flow paths (due to local topographic or lithological variations); and iii) macro-scale flow paths (karst sinks or playa basins). McCarthy and Angier (2001) differentiated flow pathways through open channels (small scale) and layers of soil with high hydraulic conductivity (large scale) in riparian wetlands.

Besides spatial scales, preferential flow may also vary with time. For example, McIntosh and Sharratt (2001) found that soil macropores change over time as a result of biological and physical processes (e.g. wetting/drying or freezing/thawing). On the other hand, preferential flow paths were shown to be stable for decades in a study conducted in structured forest soils (Hagedorn and Bundt, 2002). Zhou *et al*. (2001) found, using soil water content tomography, that preferential flow is dominant in short-duration rainfall and at the beginning of rainfall events, whilst infiltration is more homogeneous as the rainfall event proceeds and in long-duration rainfall events.

An important mechanism, especially in hillslope hydrological studies, is also lateral preferential flow (Weiler and McDonnell, 2007). This is particularly relevant in studies related to land use change, contaminant transport and water quality, where the quantification of flow amount and components of flow are relevant.

2.4.2 Measurement or estimation

An overview of measurement, interpretation, modelling and upscaling of preferential flow can be found in a Special Issue of the Journal of Contaminant Hydrology (Coppola *et al*., 2009).

Luxmoore (1992) summarized methodologies for the measurement and estimation of preferential flow in soils. Methodologies were classified into:

- Direct measurements consisting in digging pits and collecting water from the bottom.
- Subsurface water collectors to measure throughflow.
- Drainage systems and drain tiles buried at shallow depths in the soil.
- Breakthrough curves of chemicals by: i) soil column (ideally undisturbed) laboratory experiments, with associated difficulties of extrapolation to field conditions; ii) field lysimeters; iii) ponding the soil surface, thereafter soil sampling and analyses; or iv) analysis of isotopic signature in waters and hydrograph separation.

Luxmoore (1992) also summarized methods to determine the volumes of macropores (preferential flow paths), including tension infiltrometers, tomography and air permeametry.

Methods discussed by Nieber (2001) included the tension infiltrometer, time domain reflectometry, chemical tracing, and geophysical methods such as ground penetrating radar and electrical resistance tomography. Nieber (2001) also indicated that the application of theoretical methods like Darcy's law and Richards' equation may not be valid for some types of preferential flow.

Several methods for estimating preferential flow were applied in practice to specific problems. For example, Fuchs *et al*. (2009) used trenches to measure flow and transport of phosphorus. Preferential flow channels can also be identified by applying dyes to the soil surface (Janssen and Lennartz, 2009) and digging a soil profile thereafter. Some comparative assessment of preferential flow between sites was also obtained with double ring infiltrometers, in combination with soil water content measurements and tomography (Nimmo *et al*., 2009). Perret *et al*. (2001), and Luo and Lin (2009) used X-ray scanning to follow tracers released in undisturbed column experiments. Rates of preferential flow can be estimated from soil moisture readings with specialized equipment, for example time-domain-reflectometry sensors (Germann, 2001) or capacitance probes (Starr, 2001).

Mohnaty *et al*. (2001) indicated that conceptual models for preferential flow exist (e.g. based on equivalent continuum, dual porosity and dual permeability approaches), but they are seldom verified through measurements. In particular, factors determining macropore flow and its intensity, like pore geometry and continuity, the nature of top and bottom boundary conditions, and textural layering are not always easy to measure. Preferential flow is commonly modeled using dual flow models (Akay *et al*., 2009; Dusek *et al*., 2009). However, the volumes of porous material to attribute to either micro- or macropore flow and to be used as model input are often unknown. Wu (2005) attempted to determine the ratio of volume of fractures to matrix in order to quantify recharge in the TMG aquifer. Rawls *et al*. (2001) attempted to determine hydraulic conductivity in macropores as a function of fractal geometry and radius of macropores. Changes in hydraulic conductivity and solute diffusivity at the matrix/macropore interface may cause additional mechanisms of dual flow and solute transport (Gerke *et al*., 2001). In modeling dual porosity, double soil physical, hydraulic and chemical properties are required as well as the ratio of micro- and macropores. Examples of dual porosity flow process models are MACRO (Jarvis, 1994), RZWQM (De Coursey *et al*., 1992) and SWAP (Kroes and van Dam, 2003). Stochastic modeling of preferential flow also proved successful in some instances (Shirmohammadi *et al*., 2001).

It should be noted that tracer experiments are often the preferred method for estimating groundwater recharge, provided positions of sampling/coring are selected appropriately. Tyner *et al*. (2001) indicated that the coring scale for chloride mass balance analysis may not always be sufficient to determine large scale preferential flow paths. De Vries and Simmers (2002) suggested a combination of time-domain reflectometry and point scale Cl mass balance in the estimate of preferential flow (localized recharge).

It was recommended that, for the purpose of this research project, a combination of tomography during rainfall events, tracers, as well as groundwater level monitoring be adopted. The adoption of these and other techniques depends, however, on the characteristics of specific sites where preferential flow is measured.

2.5 Estimation of uncertainties

Many methods are available to estimate uncertainties in natural systems. The adoption of a specific method, or combination thereof, depends on the number and type of variables, the spatial and temporal scales as well as the objectives that one wants to achieve. Large uncertainties are generally associated with i) variables that are difficult to measure and that display large spatial variability (e.g. hydraulic conductivity, in particular under unsaturated conditions), ii) error propagation (e.g. errors in each water balance term), and/or iii) unknown variables. For example, rooting depth of vegetation is often a key variable for accurate estimates of recharge (De Vries and Simmers, 2002; Schenk and Jackson, 2005; Tietjen *et al*., 2009), but it is seldom measured. Uncertainties also materialize when long-term estimates of recharge are required, but historic information on land use and vegetation is not available.

Mishra (2009) reviewed a number of uncertainty analysis techniques that are used in hydrological modeling, namely Monte Carlo simulation, first-order second-moment analysis, point estimate method, logic tree analysis and first-order reliability method. Mishra (2009) also reviewed sensitivity analyses techniques like stepwise regression, mutual information (entropy) analysis and classification tree analysis. A simple estimation of groundwater recharge uncertainties (Giambelluca *et al*., 1996), using first-order uncertainty analysis and sensitivity analysis, resulted in large calculated uncertainties of recharge from agricultural fields in Hawaii (49% of the mean for sugarcane and 58% of the mean for pineapple). Diodato and Ceccarelli (2009) used log-normal kriging to produce maps of probability of recharge. Van der Brink *et al*. (2008) used a Monte Carlo simulation and a Latin hypercube sampling procedure to quantify uncertainty of a regional-scale transport model of nitrate in groundwater. Statistical tools like spectral (Fourier) analysis, or harmonic series, were also used to evaluate variations in groundwater time series (e.g. seasonal variations due to rainfall or abstraction) (Del Rosario *et al*., 2005). This methodology involves the determination of periodicity (occurrence of an event at regular intervals) and forecast (extrapolation of certain parameters to predict future values based on observed time series). Both periodicity and forecast imply a certain degree of uncertainty. Factor analyses can also be used to determine the most important variables to consider in natural systems, i.e. those that may have the greatest effects on uncertainties, whilst cluster analyses are used to indicate variables with similar characteristics (Del Rosario *et al*., 2005). Both factor and cluster analyses can be used to determine target zones for intensive monitoring.

Other examples of uncertainty studies related atmospheric variables and evapotranspiration to hydrological processes. Betts *et al*. (2007) used the perturbed-physics ensemble technique to predict continental runoff as a function of plant physiological responses subject to uncertainties in future precipitation, by performing a large number of simulations with climate models. Kay and Davies (2008) compared the effects of potential evaporation calculated with global circulation models and Penman-Monteith-based formulae (Allen *et al*., 1998) on runoff simulated with the PDM hydrological model (Moore, 2007). They concluded that the uncertainty introduced with the Penman-Monteith formulae is less than that due to the climate models. Destouni *et al*. (2009) calculated uncertainties in runoff predictions of Swedish catchments using different evapotranspiration estimates based on precipitation, temperature, soil and land cover data, under current and projected conditions of climate change. Similar work was done by Rawlins *et al*. (2006), who highlighted the high degree of uncertainty present in climate data and the range of water fluxes generated from model drivers. Or and Hanks (1992) used the Kalman filter, commonly used in geophysics as part of ensemble forecasting, to estimate uncertainties due to spatial and temporal variations in soil water and evapotranspiration.

Scanlon *et al*. (2002) stressed the need for using multiple techniques in the estimation of recharge in order to account for uncertainty. Ye *et al*. (2006) used five different recharge models with different levels of complexity to assess groundwater recharge uncertainty a priori, based on expert judgment, and a posteriori, based on calibration of a regional flow model against observations. The statistical method used was the maximum likelihood Bayesian model averaging. Alley *et al*. (2002) recommended the use of several techniques at once, in combination with data collection and research. They highlighted more research is required to account for heterogeneities determining preferential flow, and on climate being the driver of evapotranspiration and groundwater recharge.

In many hydrological studies, uncertainties are determined by lumping processes into hydrological models. In this way, uncertainty depends on a large number of temporal and spatial variables, but it is assigned to a unique output variable (e.g. drawdown of groundwater table, baseflow and similar). However, the increased complexity of hydrological models leads to a larger number of parameters, more spatial interactions, more complex responses and more modelling uncertainty. This is even more evident in coupled hydrological modelling systems. The most common sources of errors and uncertainty are i) the model structure, ii) parameters iii) data and iv) forecast of future conditions.

Methodologies for parameter optimization, uncertainty and sensitivity analyses are often incorporated into hydrological models (Leavesley *et al*., 1983), and they are used in combination to improve model's performance. Parameter optimization is used to determine the optimal combination of input parameters that yields the least error in the objective function (difference between observed and simulated data). This optimization process is essential for spatial parameters (e.g. soil properties) that are otherwise impossible to delineate with accuracy over large areas. The sensitivity analysis is the quantification of the effects of changing input(s) on the output result(s). The uncertainty analysis is the quantification of the effects of lack of knowledge or potential errors on the output result(s).

Uncertainties in modelling can be determined in three steps:

1) The first assessment of uncertainty can be done visually. For this purpose, visualization tools for measurements, model outputs and uncertainties are crucial as part of an improved representation of hydrological processes.

2) The second step in assessing uncertainties is through simple statistical indicators, used also as model's performance measure. Commonly used statistical indicators are:
   - Mean error between observed and simulated data
   - Standard deviation
   - Root Mean Square Error (RMSE)
   - Mean Absolute Error (MAE)
   - Coefficient of determination R^2
   - Coefficient of efficiency E (Nash and Sutcliffe, 1970)
   - Index of agreement d (Willmott, 1981)

   It should be noted that these statistical indicators are not always suitable for all applications and the values may be misleading. Different indicators have different sensitivity to data and it is difficult to define what values of these indicators are acceptable in terms of model's performance.
3) Thirdly, uncertainties can be quantified using complex tools. Examples of these tools that are incorporated in the PRMS model (Leavesley *et al*., 1983) are:
   - Rosenbrock parameter optimization
   - Troutman sensitivity analysis
   - Shuffle complex evolution optimization
   - Multi-Objective Generalized Sensitivity Analysis (MOGSA)
   - Multi-Objective COMplex Evolution Algorithm (MOCOM)
   - Generalized Likelihood Uncertainty Estimation (GLUE)
   - Relative sensitivity, correlation and hat matrix
   - Error propagation table
   - Joint and individual standard errors in parameters
   - Correlation and hat
   - Let Us Calibrate (LUCA)
   - Ensemble streamflow prediction

It should be noted that no single approach for quantification of uncertainties and error analyses is suitable for all applications, and universal guidelines for uncertainty analysis do not exist. Rather, a combination of tools should be used depending on the model structure, the objectives, data constraints, spatial and temporal scales of application. International groups are currently collaborating to assess existing methods and tools for uncertainty analysis and to explore potential avenues for improvement in this area (http://www.es.lancs.ac.uk/hfdg/uncertainty_workshop/uncert_intro.htm, accessed on 25

February 2010). Some rule-of-thumb conditions are that the model outputs should behave consistently and realistically, they should match observations and yield small uncertainties.

2.6 Research gap analysis and recommendation

From the critical review of methods for determining uncertainties in the estimation of groundwater recharge, evapotranspiration and preferential flow, the following recommendations are made:

- For the estimates of groundwater recharge, a combination of techniques (physical methods, tracers and numerical models) needs to be adopted.
- The concept of atmospheric demand-soil water supply should be employed in the quantification of actual evapotranspiration. A daily time step is recommended in the calculation of water balance variables relevant to groundwater recharge to account for daily actual evapotranspiration and rainfall distribution. Improved recharge estimates are possible with the combination of atmospheric factors (PET and ET), vegetation (plant response to water stress, root system), soil and lithology (water storage, flow direction) and geology (texture, porosity, conductivity, fractures).
- For the estimates of preferential flows, a combination of tomography during rainfall events, tracer studies and groundwater level monitoring are recommended. The adoption of these and other techniques, however, depends on the characteristics of specific sites where preferential flow is measured.
- No single approach can be recommended for quantification of uncertainties. It depends on the objectives, data constraints, spatial and temporal scales of application.

In selecting methods for the estimation of groundwater recharge, it is firstly essential to clearly define the purpose of the study. Secondly, a conceptual model of the area of interest needs to be designed in order to understand the mechanisms of groundwater recharge (how, where, when and why does recharge occur). The conceptual model should provide the information on the mode of groundwater recharge (e.g. diffuse or focused), the occurrence of groundwater recharge (e.g. event-based, seasonal, annual or steady), spatial scale of interest (e.g. field, watershed, regional), factors affecting groundwater recharge (e.g. climate, geology, topography, vegetation and land use) and, ideally, at least a rough indication of the water budgets.

A number of criteria need to be considered in the selection of methods:

- The methods need to match the spatial and temporal scales of the study objectives.

- The assumptions of the methods need to be consistent with the conceptual model.
- Budget and time frame of application need to be within certain limits for a specific study.
- Data availability is a major constraint for the application of specific methods, namely existing data and type of data to be collected (e.g. climate, surface water, unsaturated zone, groundwater).

3 EXPERIMENTAL

3.1 Site selection

The main criterion for selection of research sites was their representativity of the two main modes of groundwater recharge, namely diffuse and localized. The diffuse recharge mechanism occurs through vertical fluxes and it is typical of coastal plain sandy aquifers. For this recharge mechanism, a site was selected in the Riverlands Nature Reserve. The localized recharge mechanism occurs through restricted areas that can be represented by fractures and faults. For this recharge mechanism, the selected site was the Oudebosch catchment in the Kogelberg Nature Reserve, representing the TMG aquifer.

In addition, Riverlands was the research site in Water Research Commission (WRC) project No. K5/1696 on "Nitrate Leaching from Soil Cleared of Alien Vegetation" (Jovanovic *et al*., 2009a). Much of the baseline data information was available (topography, soil physical and chemical properties, etc.) and much of the equipment was installed and available for use (groundwater loggers and soil water sensors). The research at Oudebosch in the Kogelberg Nature Reserve gave the opportunity to build on the project funded by the Water Research Commission on the potential environmental impacts of the proposed large-scale exploitation of the TMG aquifer (Colvin *et al*., 2009). The Kogelberg area was identified as one of a set of sites that was suitable for exploratory drilling aimed at gaining a deeper understanding of groundwater dynamics in the TMG aquifer and groundwater-surface water interactions. The groundwater exploration programme was run by the City of Cape Town, managed by Aurecon (Cape Town) with contributions by Geoss (Somerset West). Recent studies at this site also investigated groundwater flow and discharge points with the use of isotopic tracers. The site was also suitable to investigate the wetland and groundwater dependent ecosystems in the bottom part of the valley.

Both Riverlands and Oudebosch were partially equipped with instrumentation and the infrastructure for measurement of groundwater levels and quality was already in place.

Weather and groundwater monitoring was on-going for several years, so time series of monitored data could be built on.

A description of the monitoring programme designed and implemented during the course of this project at the two sites follows. It was retained that this set of monitored variables would be sufficient to generate data for estimating groundwater recharge with improved methods, for setting up and running hydrological and groundwater flow models, and ultimately to fulfil the objectives of the project.

3.2 Riverlands Nature Reserve

The focus of the monitoring programme at Riverlands was to improve estimates of evapotranspiration and reduce uncertainties in the estimation of groundwater recharge at this site characterized by pre-dominantly vertical fluxes in the unsaturated zone.

3.2.1 Location and site description

Riverlands Nature Reserve, managed by Cape Nature Conservation, is located about 10 km South of Malmesbury (Western Cape) (Figure 2). The experimental site was used in 2007 and 2008 for WRC project No. K5/1696 (Jovanovic *et al*., 2009a and b). The hydrological boundaries indicate that the experimental site gravitates towards quaternary catchment G21D, based also on the groundwater flow directions established in WRC project No. K5/1696 (Jovanovic *et al*., 2009a and b).

Riverlands Nature Reserve is situated on deep, well-leached, generally acidic and coarse sandy soils of marine and aeolian origin. The soils are classified as Vilafontes 1120/10 and Lamotte 1100 (Soil Classification Working Group, 1991) or Luvic Cambisol (FAO, 1998). The Reserve is situated on Cenozoic deposits with Cape granite outcrops occurring in the surroundings. Mean annual rainfall is about 450 mm, occurring mainly from May to August. Mean daily temperature varies from about 7.0°C in July to 27.9°C in February, and there are about 3 days of frost per year. Mean potential annual evaporation is about 2150 mm and daily evaporation exceeds rainfall for about 70% of the time.

The experimental site extends across the boundary between the Burgerpost Farm and the Riverlands Nature Reserve (Figure 3). In the previous WRC project No. K5/1696, monitoring plots were established in three treatments (Figure 3), namely: i) a bare soil plot cleared of alien invasives by the Working for Water Programme (Department of Water Affairs and Forestry) – ‘cleared’ treatment; ii) a plot invaded by alien species (*Acacia saligna* or Port

Jackson) on Burgerspost farm – ‘uncleared’ treatment; and iii) a plot with natural vegetation Atlantis Sand Plain Fynbos – ‘fynbos’ treatment. These plots were equipped with monitoring boreholes, including water level and temperature monitoring loggers (Leveloggers model 3001; Solinst Ltd., Georgetown, Canada). The positions of boreholes, surface topography and groundwater level contours are indicated in Figure 3. Daily weather records for the study period were available from the South African Weather Services for the Malmesbury station and from the Western Cape Department of Agriculture for the Langgewens holdings. Daily rainfall data collected with a rain gauge were available from Riverlands Nature Reserve. A complete description of topography, soil physical and chemical properties were done by Jovanovic *et al*. (2009a). An important recommendation from WRC project No. K5/1696 was to determine evapotranspiration from fynbos, as this was never measured/estimated before. In this project, we therefore focused mainly on intensive data collection within the fynbos vegetation. Both historic existing data and those collected during the course of this project are summarized in the next section.

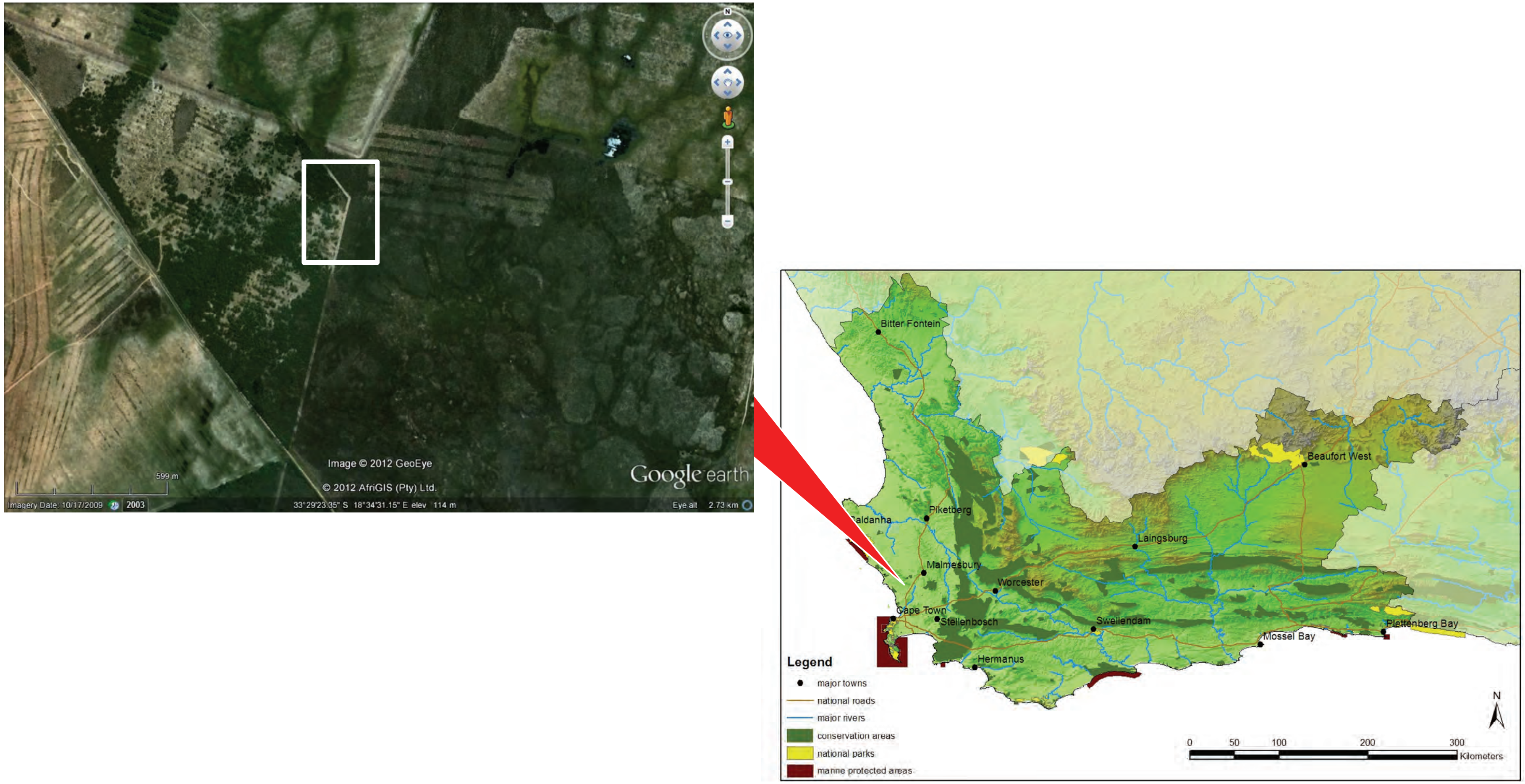

Figure 2

Location of the Riverlands Nature Reserve on the Western Cape map of conservation areas. The white square in Google Earth indicates the experimental area

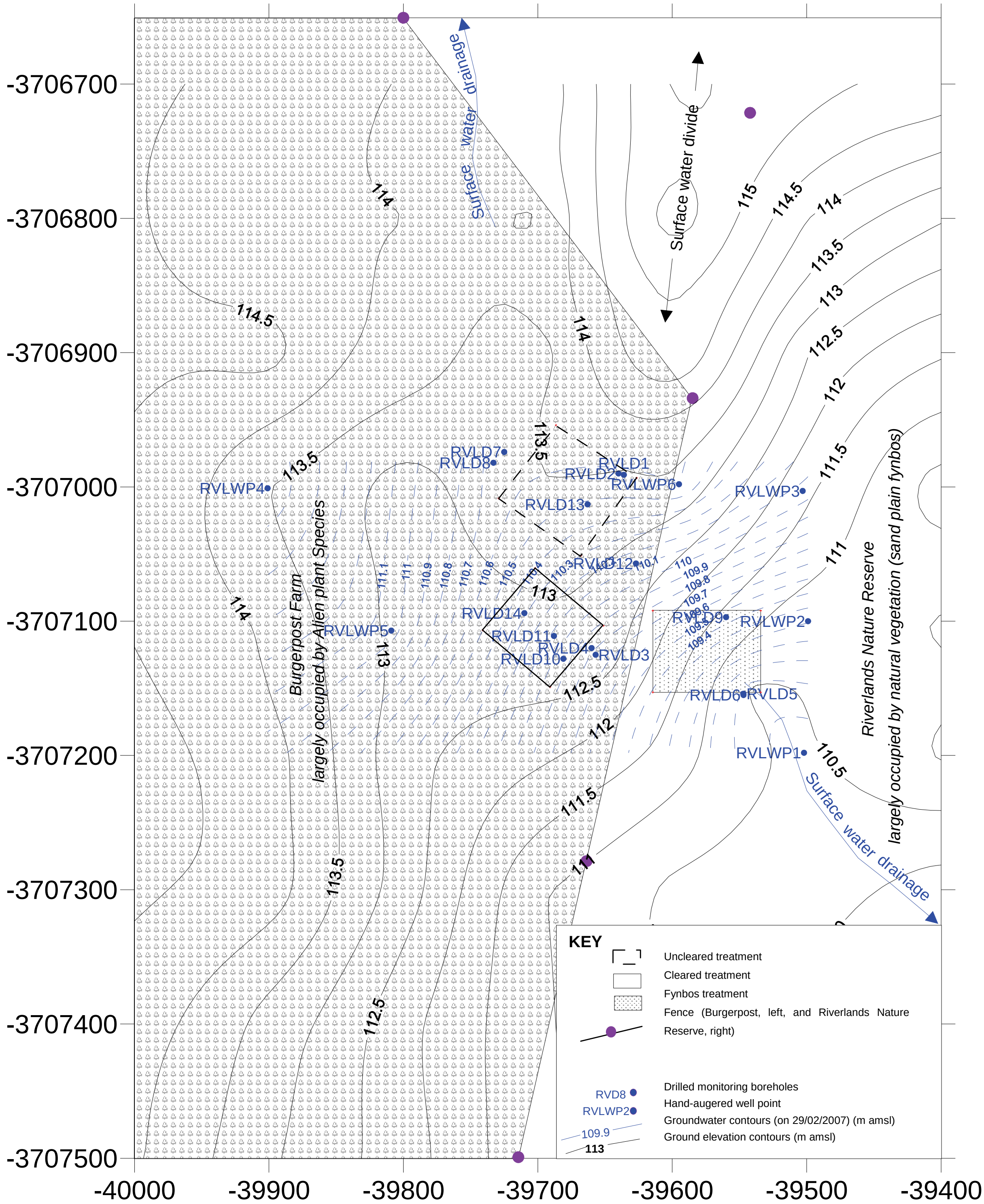

Figure 3

Map of experimental site (the coordinates are represented in the WGS 1984 reference positioning system, the projection is Transverse Mercator, the central meridian is 19.0, the linear units are expressed in m)

3.2.2 Data collection

Well-drained alluvial sandy soils are a typical example of a system where vertical water fluxes dominate. Rain water infiltrates in the unsaturated zone, it generates a wetting front and it refills soil layers from the surface towards the bottom of the soil profile. Infiltrating rain water is available for evapotranspiration. Excess water is drained into deeper soil layers and eventually recharges the unconfined aquifer. The amount of groundwater recharge is therefore dependent on initial soil water content, rainfall amounts and distribution, and evapotranspiration. The main purpose of the experiment at Riverlands was to quantify the various components of the one-dimensional soil water balance (rainfall, soil water storage, evapotranspiration and groundwater recharge) occurring in Atlantis Sand Plain Fynbos. Measurements of rainfall, soil water storage and evapotranspiration allowed to calculate recharge as the unknown component of the soil water balance. The monitoring programme included:

- ***Topography*** (Jovanovic *et al*., 2009a).
- ***Daily weather data*** from the nearby weather stations in Malmesbury (South African Weather Services) and Langgewens (Western Cape Department of Agriculture).
- ***Daily rainfall*** records collected by Riverlands Nature Reserve (from May 2007 to September 2011).
- ***Soil mapping and description of soil forms***.
- ***Soil physical and hydraulic properties*** (Jovanovic *et al*., 2009a).
- ***Soil infiltration*** with double ring infiltrometers and dye infiltration tests.
- ***Soil chemical properties*** were measured monthly during 2007 in particular to describe migration of N in the soil profile (Jovanovic *et al*., 2009a).
- ***Soil water content and temperature*** at different depths in the profile (10, 40 and 80 cm), at two locations (adjacent to trees/bushes and in open space areas) and on different vegetation stands (Sand Plain Fynbos, *Acacia saligna* and bare soil). Continuous hourly records were collected from May 2007 to February 2011. Data were collected with Echo-TE sensors and logged with Echo-loggers (Decagon Devices Inc., USA).
- ***Vegetation description*** with the purpose of spatially delineating groups of hydrologically homogeneous plant communities occurring in typical hydrological environments driven by elevation and water table depth (hydrological niche).
- ***Measurement of fynbos evapotranspiration with scintillometry*** in the period 14-27 October 2010.
- ***Measurements of canopy cover*** with an AccuPar light sensor in the range of photosynthetically active radiation in October 2010 (Decagon Devices Inc., USA).

- ***Root distribution*** measurements, in particular root density and depth (Jovanovic *et al*., 2009a).
- ***Canopy interception of rain water*** with rain gauges (Jovanovic *et al*., 2009a).
- ***Groundwater levels and temperature from 14 drilled and 6 manually augered boreholes*** (Figure 3). Hourly logged data of groundwater levels were available for 2007 and 2008 from WRC project No. K5/1696. Upon completion of WRC project No. K5/1696, the water level loggers were removed to prevent theft. The loggers (Leveloggers model 3001; Solinst Ltd., Georgetown, Canada) were again installed in April 2009 for hourly collection of groundwater levels and temperatures, and secured with locks. Correction of groundwater level data was done using hourly atmospheric pressure data collected with a barometer logger. Manual readings of groundwater level were taken during field visits.
- ***Groundwater quality*** was measured monthly during 2007 (Jovanovic *et al*., 2009a).

Surface water, with the exception of occasional ponding in the low-lying areas, did not occur in this section of the catchment due to the sandy nature of the soil and high infiltration rates.

3.3 Oudebosch catchment

The focus in the Oudebosch catchment was to improve estimates of both evapotranspiration and preferential flow to reduce uncertainties in the estimation of groundwater recharge at this site characterized by pre-dominantly preferential flow fluxes in the unsaturated zone.

3.3.1 Location and site description

The Kogelberg Biosphere Reserve is located East of Cape Town (Western Cape) (Figure 4). The Oudebosch catchment within the Palmiet river basin is located North-East of Betty's Bay. This catchment is used as part of the groundwater exploration programme of the City of Cape Town. The Oudebosch is a seasonal stream and the hydrological boundaries indicate that the site is located in quaternary catchment G40D.

Soils are shallow in the upper, steep parts, and deep, alluvial in the bottom parts of the catchment. The geology is classified in the Cape Supergroup and dominated by the TMG originated from deposition of sediments comprising quartz arenites and minor shale layers. Mean annual rainfall is approximately 800 mm (occurring mainly from May to October) and mean annual potential evapotranspiration > 1200 mm. The vegetation on steep slopes is dominated by Kogelberg Sandstone Fynbos. In the lowest part of the catchment, wetland species are present in the alluvial valley. Both historic existing data and those collected during the course of this project are summarized in the next section.

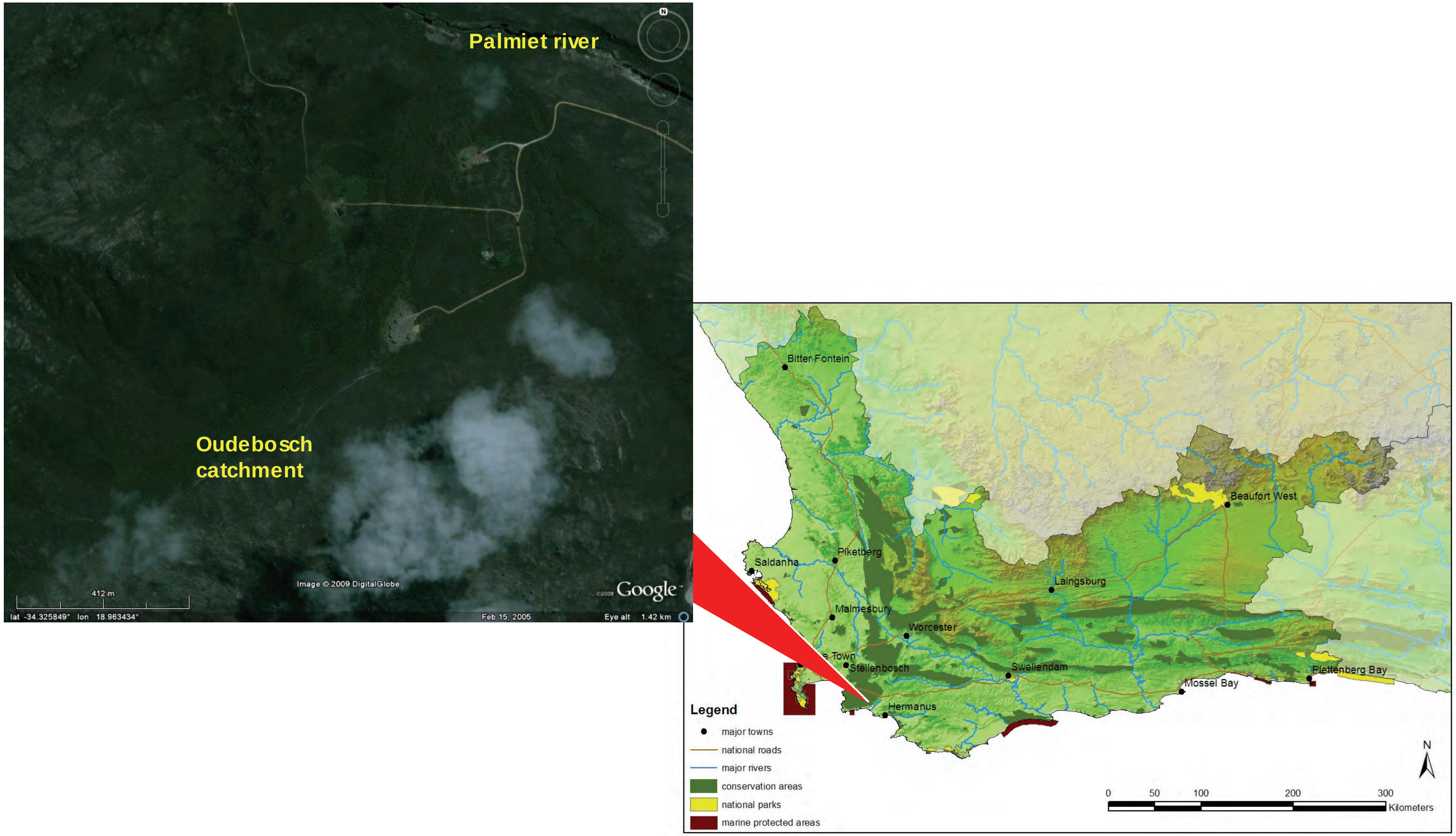

Figure 4

Location of the Oudebosch catchment in the Kogelberg Biosphere Reserve on the Western Cape map of conservation areas

3.3.2 Data collection

The Kogelberg Biosphere Reserve is located in geology typically characterized by the Table Mountain Group. Rain water infiltrates in the soil through the matrix as well as preferential flow pathways. Excess water is drained into deeper layers and eventually recharges the complex fractured aquifer system. The main purpose of the experiment at Oudebosch was to quantify the various components of the soil water balance (rainfall, soil water storage, evapotranspiration and groundwater recharge) as well as to generate data for application of numerical groundwater flow models and empirical models based on groundwater level fluctuations. The monitoring programme included:

- ***Topography*** (Surveyor General, Cape Town).
- ***Daily weather and rainfall data*** from July 2008 to July 2011 with an automatic weather station installed in the field (Campbell Scientific Inc., Logan, Utah, USA). The station was installed for the groundwater exploration programme of the City of Cape Town.
- ***Geology map*** (Council for Geoscience).
- ***Geophysical study*** with a resistivity tomography Lund imaging system. The purpose of resistivity measurements was to identify hydrological properties of the sub-soil and possible preferential flow paths of water. The resistivity readings were taken in transects at sites 1 and 2 (Figure 5).
- ***Soil mapping and description of soil forms*** once-off at the beginning of the experiment. The purpose of the mapping was to spatially delineate soil characteristics and set up hydrological models.
- ***Soil physical and hydraulic properties***.
- ***Soil infiltration*** with double ring infiltrometers and dye infiltration tests.
- ***Soil chemical properties***.
- ***Soil water content and temperature*** at different depths in deep alluvial soil at the bottom of the catchment (10, 40 and 80 cm; site 1, Figure 5) and in the shallow soil profile on a steep mountain slope (10 and 40 cm; site 2, Figure 5). Continuous hourly records were collected from September 2010. Data were collected with Echo-TE sensors and logged with Echo-loggers (Decagon Devices Inc., USA). Site 1 was destroyed by a fire in March 2011.
- ***Vegetation description*** with the purpose of spatially delineating groups of hydrologically homogeneous plant communities. It was observed that faults occurring in the catchment represent a favourable micro-environment for colonization, from which certain plant species draw water.
- ***Measurement of fynbos evapotranspiration with scintillometry*** in the period

8 April-8 June 2011 (mountain slope) and 3 September-19 October 2011 (alluvial area).

- ***Measurements of canopy cover*** with an AccuPAR light sensor in the range of photosynthetically active radiation in October 2010 (Decagon Devices Inc., USA).
- ***Groundwater levels and temperature*** logged data from 9 boreholes (Figure 5) from the beginning of 2007 until September 2011. The loggers were installed at different times, historic data were collated with data collected during the course of this project. Correction of groundwater level data was done using hourly atmospheric pressure data collected with a barometer logger. Data were obtained from the groundwater exploration programme of the City of Cape Town.
- ***Groundwater quality*** over time by sampling and laboratory analyses. Data were obtained from the groundwater exploration programme of the City of Cape Town. Data included complete inorganic analyses from 2005 until 2010.
- ***Piezometric level*** logged with loggers (Leveloggers model 3001; Solinst Ltd., Georgetown, Canada). Water level installed in the lowest part of the seasonal stream was measured with a piezometer.

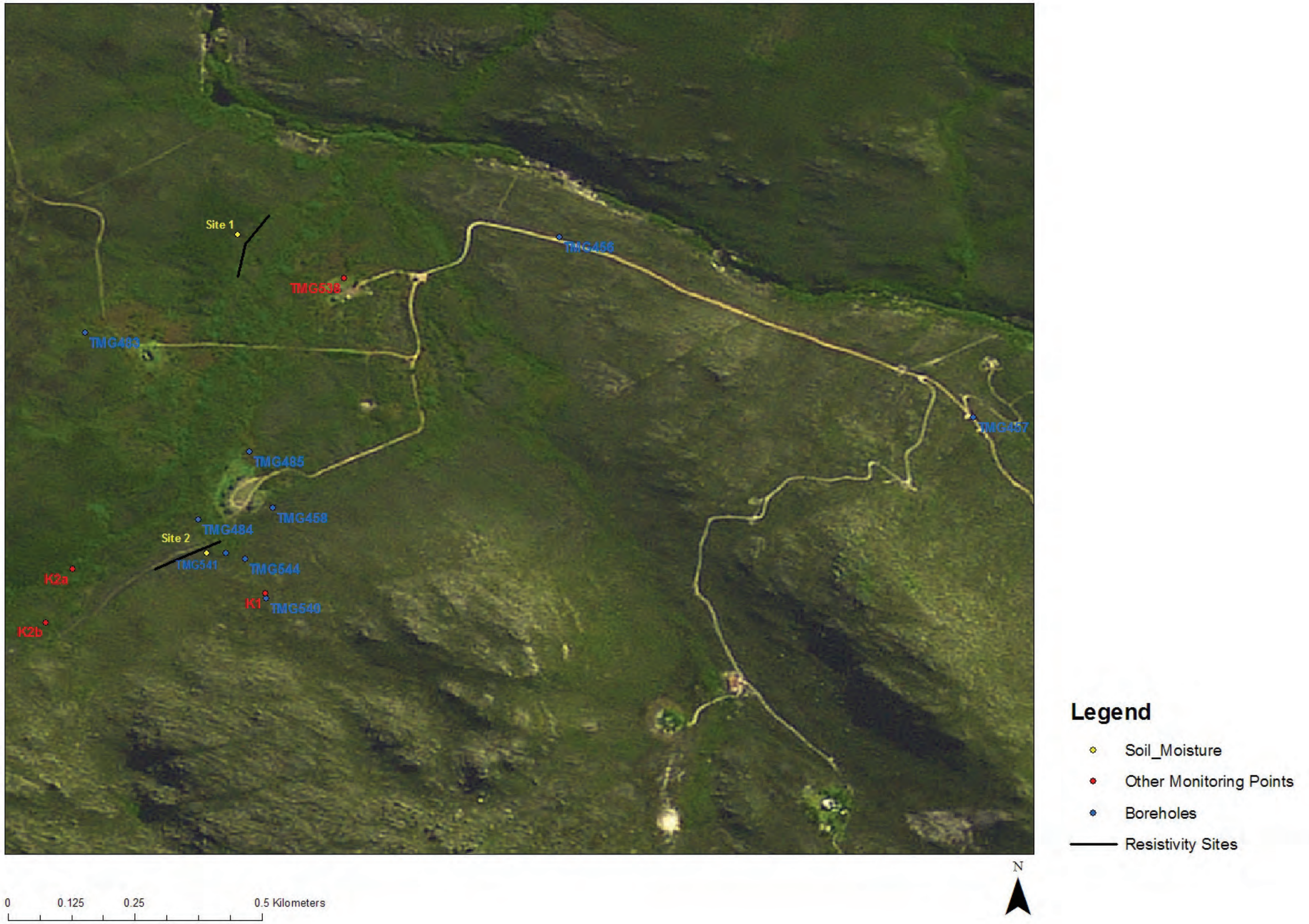

Figure 5

QuickBird view of the Oudebosch catchment in the Kogelberg Biosphere Reserve and monitoring points. Blue: Groundwater boreholes; Red: Piezometers and weather station (TMG538); Yellow: Soil water sensors; Black: Resistivity measurement transects

3.4 Presentation of results and selection of groundwater recharge methods

Intensive monitoring at the pilot sites in Riverlands and Oudebosch allowed the collection of data to be applied in different methods for estimation of groundwater recharge. All raw data are included in the CD attached to this report. Data collection, processing and interpretation are available in interim reports and Deliverables of this project. Deliverable 11 contains the most updated data collection report.

In this report, results that are directly relevant to evapotranspiration, preferential flow and recharge estimates are presented. In particular, evapotranspiration estimates with scintillometry, soil mapping and infiltration studies as well as the resistivity tomography study are discussed. These data were used to apply a selection of methods for estimation of groundwater recharge.

The groundwater recharge estimation methods used in this study and the reasons for their application are:

7) ***Coupled atmospheric-unsaturated-saturated zone model*** for the unconfined aquifer at Riverlands, mainly because this method implies the coupling of scientifically sound process-based models. In this instance, evapotranspiration estimated with an energy balance approach (scintillometry) was used as input into the HYDRUS-2D model (Simunek *et al*., 1999), which makes use of Richards' equation to calculate drainage from the unsaturated zone. The method was applied to determine one-dimensional water fluxes.
8) ***Groundwater flow model MODFLOW v. 2.8.2*** (McDonald and Harbaugh, 1988) for the TMG fractured rock aquifer at Oudebosch. Because of the complexity of the TMG aquifer and the larger spatial scale of application compared to Riverlands, it was not possible to capture the detail and spatial variability required in unsaturated zone models. MODFLOW simulations were therefore carried out at the scale of a small catchment. Groundwater recharge was estimated by calibration against observed groundwater levels.
9) Both unsaturated zone and groundwater flow models are highly data-intensive. A simpler method called ***Rainfall Infiltration Breakthrough (RIB)*** was then used in this study. It is based on historic fluctuations of groundwater tables and data analysis. The RIB software, written in Excel, was applied both at Riverlands and Oudebosch. This approach is less data-intensive but it requires long series of groundwater level and rainfall data, as well as a sound knowledge of aquifer characteristics.

4 EVAPOTRANSPIRATION STUDIES

4.1 Introduction

This Section discusses the results of three campaigns of ET measurements with scintillometry. The first campaign was carried out on Atlantis Sand Plain Fynbos in October 2010 in the Riverlands Nature Reserve. The other two campaigns were carried out in April-June 2011 and in September-October 2011 on Kogelberg Sandstone Fynbos in the Oudebosch catchment (Kogelberg Biosphere Reserve). It was the first time that evapotranspiration (ET) of these two types of endemic fynbos vegetation has been determined. The window period for the campaigns was chosen to be at season change in spring and autumn, at a time when both sunny days with high atmospheric evaporative demand and overcast days with low evapotranspiration can be expected. In this way, both high and low daily ET values were obtained and compared to reference evapotranspiration ETo (Allen *et al*., 1998). ***The overall aim of these measurements was to improve estimates of ET of fynbos and consequently estimates of groundwater recharge.***

4.2 Description of vegetation

4.2.1 Riverlands (Jovanovic *et al*., 2009a)

The background information for vegetation description was taken primarily from Rebelo *et al*. (2006), and supplemented from Yelenik *et al*. (2004). Botanical terminology follows Rebelo *et al*. (2006), and Manning and Goldblatt (1996).

The dominant vegetation type of the reserve is Atlantis Sand Plain Fynbos (FFd4, Rebelo *et al*., 2006), one of the 11 forms of sand plain fynbos that occurs on the coastal plains of the western and southern coast of the Western Cape Province. Figure 6 depicts Atlantis Sand Plain Fynbos showing the restio dominated community of the lower-lying areas in the foreground and the taller shrubs of the higher-lying community in the background. Atlantis Sand Plain Fynbos occurs as a series of islands in renosterveld, being confined to areas with deep sandy soils from about Kleindrif Station on the Berg River to Philadelphia in the South-West and Atlantis to Blouberg on the west coast. Riverlands is situated in the catchment of the Groen River, which drains into the Diep River. The vegetation type is classified as vulnerable with only about 6% conserved, mainly at Pella, Riverlands (1,111 ha) and Paardeberg. About 40% of the vegetation type has been transformed for agriculture, urban and industrial development, and plantations of eucalypts (for firewood and windbreaks) and pines (windbreaks). Large areas have been invaded by *Acacia saligna* and

A. cyclops which were used to control drift sands from the mid-1800s up to the 1950s, often in areas that were denuded of vegetation by grazing and excessive burning. Some 42 bird species have been recorded in the reserve but only four were recorded as breeding during two surveys (BIRP, 1999). The reserve has at least 400 plant species, a number of which are only known from the area.

Figure 6

A view of the Atlantis Sand Plain Fynbos in the Riverlands Nature Reserve

The vegetation is dominated by 1-1.5 m tall emergent shrubs with a dense mid-storey of other shrubs and Restionaceae and a ground layer of recumbent shrubs, herbaceous species, geophytes and grasses with occasional succulents. The vegetation structure is strongly controlled by the depth to the water table, both in areas where it is shallow and where it is deep (Rebelo *et al*., 2006). Where the water table is very deep, the community is dominated by drought-hardy Restionaceae and, as the depth decreases, the incidence and cover of shrubs of the Asteraceae increases. Where the water table is shallower, and shows little seasonal variation, the Proteaceae comprise the dominant shrubs and the canopy cover is higher. Where water tables become shallower, albeit seasonally, the community is dominated by Restionacaeae and Cyperaceae (sedges). This results in marked topographically-related patterning of the vegetation in line with the general trends described above (Figure 6).

The Atlantis Sand Fynbos at Riverlands is characterized by a relatively high cover of shrubs of the Proteaceae, Ericaceae and Rutaceae. Shrubs of *Euclea racemosa* and *Diospyros glabra* are also reasonably frequent. The vegetation of the fynbos site has two different communities that seem to be controlled by the micro-topography (Figure 6). Slightly higher-lying areas are dominated by *Protea scolymocephala*, *Leucadendron salignum, Leucadendron cinereum* and *Leucospermum calligerum* with *Erica mammosa*, *Erica* species, *Euclea*, *Diospyros, Phylica cephalantha, Staavia radiata* and shrubs in the Rutaceae. In the lower-lying areas the dominant species were from the Restionaceae – *Chondropetalum tectorum, Willdenowia incurvata, Staberoha distachyos, Thamnochortus spicigerus* – with *Diastella proteoides, Berzelia abrotanoides, Serruria decipiens* and *S. fasciflora*. The prostate, spreading shrub *Leucospermum hypophyllocarpodendron* (subspecies *canaliculatum*) occurred in both communities, but was more common in the higher-lying areas. The ground layer included a wide variety of geophytic species in the Liliaceae and Iridaceae, seasonal herbs and a few grass species.

Most of the reserve is young following fires in 2004 (53 ha, CWCFPA, 2005) and 2005 (206 ha) but the area of ET measurements is situated in a section shown as being 11-15 years old. This compared well with an estimated age of 12-13 years based on counts of shoot growth increments on *Protea scolymocephala* shrubs. The canopy cover measured with an AccuPAR (Decagon Inc., USA) in the range of photosynthetically active radiation was between 39.2 and 48.9 %. LAI calculated with the AccuPAR varied between 1.12 and 1.54. The difference in elevation in the area of ET measurement was of the order of 3 m, and the distribution of species is finely controlled by the depth to the water table.

4.2.2 Oudebosch catchment

The Kogelberg Biosphere Reserve is globally recognised as a core botanical conservation area with more than 1,400 plant species, a large number of which are endemic. The scientific names follow those used in Goldblatt and Manning (2000) and those from earlier sources have been updated where necessary.

The Oudebosch valley is oriented roughly southeast–northwest along an ancient fault line which defines the main valley axis (Boucher, 1978; Colvin *et al*., 2009). It is situated between the lower, south-facing slopes of Platberg on the northern side and the north-facing slopes of Elephant Rock mountain to the south (Figure 7). The valley marks a major vertical fault, with the Goudini formation and the Cedarberg shale formation exposed on the northern side and the Peninsula formation on the southern side.

Figure 7

View up Oudebosch valley looking west from the tourist housing. Note the Psoralea pinnata dominated wetland in the middle-ground (just below centre)

Both the Goudini and the Peninsula formations are hard sandstones which weather slowly and give rise to shallow, sandy soils. The shales of the Cedarberg formation and tillites of the Pakhuis formation give rise to finer textured soils with a greater moisture holding capacity and higher nutrient levels. In much of the study area, this valley bottom is formed by deep alluvial sands derived from the sandstone formations. In the lower-lying areas, near streamlines and in some of the wetlands there has been an accumulation of organic matter resulting in peaty soils. The vegetation characteristics are strongly influenced by the differences in soils. Some of the faults permit groundwater accumulation and flow along them, resulting in the formation of wetlands which were the focus of previous studies (Colvin *et al*. 2009).

Fynbos vegetation is subject to regular fires and the study area has experienced two fires in the last two years. Prior to this, the area was last burnt on 29/03/1991. The first fire began on 3 June 2010 and burnt the area to the south and east of the main reserve access road, including most of the wetland and slope of the scintillometer measurement area (Figure 8). The next fire was on 16 March 2011 and burnt the portion of the wetland transect between the Oudebosch offices and the main reserve access road (approximately the 1st 100 m). The differences between two post-fire ages vegetation were quite marked because sprouting plants can initiate growth soon after the fire but seed-regenerating species would only begin germinating in June-July. Thus seedlings are only a minor element in the younger vegetation compared to the older vegetation where fast growing, herbaceous species like *Othonna quinquedentata* and *Osmitopsis asteriscoides* have already reached the flowering stage.

The vegetation forms part of the Kogelberg Sandstone Fynbos which covers the mountain areas from Franschhoek to the Kogelberg (Rebelo *et al*., 2006). This vegetation type is characterised by a high diversity of plant species, a high proportion of which are endemic to this vegetation type. The structure ranges from a short (<0.6 m), open community (±50-60% cover) with a high proportion of fine-leaved (ericoid) shrubs with emergent Proteaceae (proteoid) to a dense (>90% cover), up to 4 m tall mixture of ericoids and proteoids. A low woodland to closed forest vegetation is found along streamlines and in river floodplains. The vegetation in the Kogelberg area was mapped in great detail by Boucher (1978) who identified two main plant communities in the study area: (a) Fynbos on yellow, plinthic soils and (b) Mixed ericoid-restioid fynbos of the xeric seaward slopes. The latter is found in relatively dry areas including the north-facing slopes of Elephant Rock mountain. The former was subdivided into two forms: *Protea-Tetraria* short fynbos and *Berzelia-Leucadendron* moist tall fynbos. A form of the *Protea-Tetraria* community is found in the dry parts of the alluvial soils and the *Berzelia-Leucadendron* occurs in the wetter areas and on the shale-derived soils of the lower slopes of Platberg. The wetlands on the slopes of Elephant Rock mountain have community similar to the *Berzelia-Leucadendron* community but much shorter. A low (<4 m) woodland vegetation occurs along the streamlines in the alluvium on the valley bottom.

One of the two ET measurement transects extended from the slope above the Kogelberg chalets to a point near the trail up to Oudebosch forest (Figure 8, slope transect). The total length of the transect was about 530 m. There were four main communities on this transect.

The dryer form of the *Protea-Tetraria* community (Figure 8 **A**) dominated the central ±190 m of the transect, with a total canopy cover of 10-30%. It was dominated by sedges, restioids (reeds), ericoid shrubs and proteoids. Common species included *Protea scabra*, *Tetraria* sp., *Peucedanum strictum*, *Brunia* sp., *Leucadendron salignum*, *Elegia stipularis*, *Erica* sp., *Phylica spicata*, *Cliffortia atrata*, and occasional *Protea lepidocarpodendron.* The wetter form (Figure 8 **B**) dominated ±70 m at the eastern end of the transect, had a greater canopy cover of 30-50%, and was characterised by a greater abundance of *Leucadendron xanthoconus,* Bruniaceae (including *Berzelia lanuginosa*) and *Psoralea pinnata* in the wettest parts.

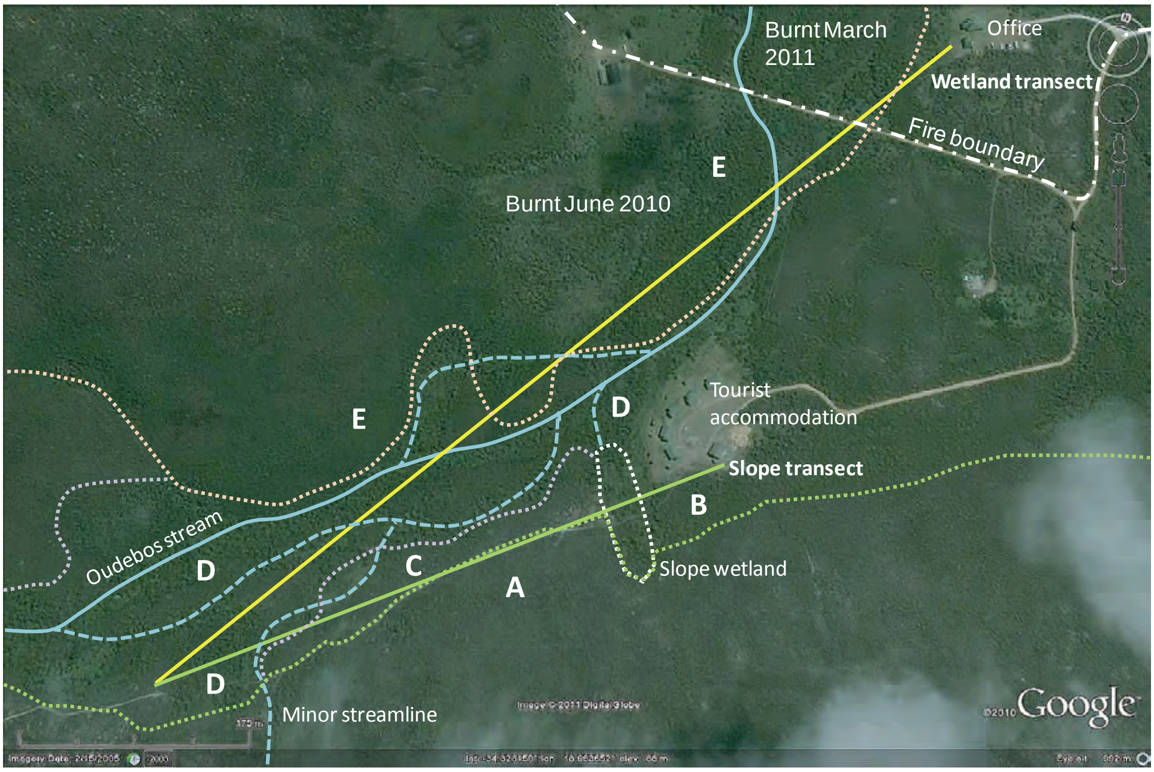

Figure 8

Google view of the study area in the Oudebosch valley showing the approximate location of the two scintillometer transects (wetland and slope), the extent of the fires, watercourses, boundaries of the main vegetation types, and the buildings and other infrastructure. For descriptions of the vegetation types (A, B, C, D, E) see the text

The eastern part of the transect included a section of the dry, short (<0.5 m tall) alluvial community (Figure 8 **C**) which was characterised by a low canopy cover (10-20%) and dominance by restioids, sedges and herbaceous species. The remainder of the transect was in the moist, mixed alluvial community (Figure 8 **D**) which was about 0.5-1.0 m tall, with a high percentage cover (50-70%) with a variable mixture of restioids (e.g. *Restio spp., Staberoha* sp., *Elegia* sp.), *Othonna* sp., *Osmitopsis asteriscoides,* ferns (e.g. *Pteridium aquilinum)* and sedges with occasional *Protea lepidocarpodendron* shrubs and patches dominated by *Psoralea pinnata* and *Berzelia lanuginosa*. Occasional forest trees (e.g. *Rapanea melanophloeos*) and occasional *Widdringtonia* clumps occurred throughout this community. The moist, mixed alluvial community was not necessarily noticeably lower-lying than the dry, short alluvial community. It is possible that the moist form was simply growing in situations where the soils were deeper, or there may have been greater access to groundwater or to the water table, or the soils may have contained more organic matter.

The main course of the Oudebosch River passes through the study area and had taller woodland vegetation which included species such as *Brabejum stellatifolium, Metrosideros angustifolia, Brachylaena neriifolia* and *Laurophyllus capensis*. These trees occasionally formed a closed-canopy community on the river banks, especially the north bank adjacent to the unburnt *Berzelia-Leucadendron* community. There was a narrow (±3 m across) riparian community along a fault-linked streamline that crossed the transect at about 50 m from its western end. This had a total canopy cover of 50-70%, dominated by restiods, sedges and ericoids with *Mimetes cucullatus* and a low cover of *Berzelia* species and *Psoralea pinnata*. The perennial spring upslope of this wetland supplies water to the labourer's houses that are being replaced by tourist accommodation at present. The more extensive, fault-linked wetland (slope wetland) at the eastern end of the transect is about 30 m across and had a high percentage cover of *Berzelia* sp., *Leucadendron salicifolium*, *Psoralea pinnata*, *Osmitopsis asteriscoides*, restioids, sedges and ericoids and some *L. xanthoconus*. This wetland was one of those studied by Aston (2007) in his comparison of the ecophysiology of wetland and dryland plant species. There was evidence that the change in communities between the eastern and western sides of the slope wetland is due to a vertical displacement along an underlying minor fault so that the shale band exposure is shifted upslope on the eastern side (Colvin *et al*. 2009).

The wetland transect extends from the back of the office area up the valley to essentially the same point as the slope transect and is about 950 m long. It was largely dominated by the moist, mixed alluvial community (Figure 8 **D**) described above which occupied about 692 m (73%) of the total length. This community was quite variable and graded into the *Berzelia-Leucadendron* community which was found on the southern slopes of Platberg (Figure 8 **E**). The *Berzelia-Leucadendron* community was generally taller than the mixed alluvial community, reaching 3.5-4.0 m in height, and had a higher percentage cover even at young age (>75%). It had a high percentage cover of *Berzelia lanuginosa, Leucadendron salicifolium, Protea lepidocarpodendron* and patches of *Psoralea pinnata*. It covered only a short section of the wetland transect (about 96 m) but it was located near the centre of the entire transect. There were also patches of the transition between the *Berzelia-Leucadendron* and the moist, mixed alluvial community (Figure 8 **D**) distributed throughout the latter. There was a section of the transect, about 50-100 m south of the road which was only partially burnt in the fire, leaving some surviving plants including *Berzelia lanuginosa*.

The last section of about 50 m at the eastern end of the wetland transect crossed a community which was dominated almost exclusively by *Pteridium aquilinum* (bracken) which may have been an indicator of disturbance in this area. The remaining part are the road, minor streamlines and the main Oudebosch stream crossing the transect (Figure 8) but they, and the associated woodland vegetation, occupy only a small percentage of the total length. Images of the vegetation at Kogelberg can be found in Deliverable 13 of this project.

4.3 Scintillometer description

Total evaporation (ET) can be defined as the algebraic sum of all processes of water movement into the atmosphere. Soil evaporation (E) and transpiration (T) occur simultaneously and are determined by the atmospheric evaporative demand (mainly the available energy and the vapour pressure deficit of the air), soil water availability and canopy characteristics (canopy resistances) (Rosenberg *et al*., 1983). Total evaporation is also referred to as evapotranspiration (Kite and Droogers, 2000). In this study, total evaporation refers to the sum of evaporation from the soil surface, transpiration by vegetation, and evaporation of water intercepted by vegetation, as estimated with large aperture scintillometers (Jarmain *et al*., 2009).

A Scintec boundary layer large aperture scintillometer system (BLS900, Scintec AG, Germany) was used to estimate total evaporation in all three campaigns. The BLS900 system measures the path-averaged structure parameter of the refractive index of air (C_N^2) over a horizontal path. Measurements of C_N^2 together with standard meteorological observations (air temperature, wind speed and air pressure) collected with an automatic weather station are used to derive the sensible heat flux density (H). The latent heat flux (and hence total evaporation) is subsequently calculated using the simplified surface energy balance equation, with measurements of net irradiance, soil heat flux and H (estimated with the large aperture scintillometer – Rosenberg *et al*., 1983). The net irradiance was measured using a North – facing net radiometer (CNR1, Kipp & Zonen, Delft, The Netherlands) installed in the middle of the transect over representative vegetation while the soil heat flux was measured at three different locations within the scintillometer transect using pairs of soil heat flux plates (Campbell Scientific. Ltd, USA) installed at depths of 3 and 8 cm, respectively.

The BLS900 system determines C_N^2 and total evaporation over distances of 500 m to 5 km. Estimates of total evaporation are spatially averaged over the area between the transmitter and receiver sensor with a larger proportion of the flux emanating from the middle of the transect. As such, the scintillometer transects were selected with dominant vegetation types, e.g. *Protea-Tetraria* on the North-oriented slope and the mixed alluvial community in the alluvial plane (Figure 8). Additional measurements included rainfall, air temperature and humidity, vertical temperature gradients, wind speed and direction as well as the volumetric soil water content with the CS616 time domain reflectometers (Campbell Scientific Ltd, USA). The energy balance theory and methods for measurement of ET were extensively discussed by Savage *et al*. (2004) and Jarmain *et al*. (2009). Figure 9 shows the equipment, including the transmitter and receiver of the scintillometer, and the weather station. All data were collected and stored in CR23X data loggers (Campbell Scientific Ltd, USA) for the weather and available energy data and in the Signal Processing Unit of the scintillometer.

Figure 9

Scintillometer set-up: transmitter (bottom) and receiver (top left) of the scintillometer; and weather station and energy balance system (top right)

4.4 Scintillometer measurements

Table 3 summarizes measurement periods, the coordinates of the scintillometer transects (positions of receiver and transmitter), as well as ranges of canopy height, canopy cover and leaf area index of the vegetation measured with an AccuPAR sensor (Decagon Inc., USA), the length of the measurement transects and the description of the vegetation. Measurements of total evaporation were made during selected window periods (representative of transition periods between seasons).

TABLE 3
LOCATION OF SCINTILLOMETER MEASUREMENTS, DURATION AND VEGETATION CHARACTERISTICS

Location	Period of measurements	Coordinates Latitude (S) Longitude (E) Elevation (m)	Canopy height range (m)	Canopy cover[1] range (%)	Leaf area index[1] range (-)	Transect length (m)	Description of vegetation
Riverlands Nature Reserve	14-27 October 2010	Transmitter: 33.49665 S; 18.57265 E; 114 m Receiver: 33.50103 S; 18.58454 E; 111 m	0.1-2.8	29.0-48.9	1.12-1.54	1,160	Atlantis Sand Plain Fynbos
Oudebosch catchment	8 April-8 June 2011	Transmitter: 34.329314 S; 18.960728 E; 117 m Receiver: 33.326342 S; 18.945333 E; 82 m	0.3-2.0	4.1-23.3	0.15-0.43	530	Kogelberg Sandstone Fynbos (North-oriented slope)
Oudebosch catchment	3 September-19 October 2011	Transmitter: 34.32877 S; 18.96030 E; 109 m Receiver: 34.32266 S; 18.96620 E; 53 m	0.75-1.8	32.7-85.9	0.54-3.32	950	Kogelberg Sandstone Fynbos (alluvial valley)

[1]Average of 10 readings

Figure 10 shows the positions of the measurement transects at the study sites. One transect was measured on Atlantis Sand Plain Fynbos in Riverlands (Table 3 and Figure 10). Two transects were measured in the Oudebosch catchment with marked differences in vegetation (see section 4.2.2 on vegetation description). The one transect was on the North-oriented slope characterized by dry conditions, shallow soils and sparse vegetation (Table 3 and

Figure 10, slope transect). The other transect was taken in the alluvial plane on closed canopy and characterized by deep alluvial soils and wet conditions along the Oudebosch stream valley (Table 3 and Figure 10, wetland transect). A third transect on the South-oriented slope was considered. This is characterized by long-standing vegetation that did not burn recently and by moister conditions than on the North-oriented slope. However, it was difficult to access the South-oriented slope and scintillometer measurements were therefore not feasible.

The BLS900 and the weather and available energy monitoring systems were used to determine the components of the surface energy balance:

$$Rn = H + LE + G$$

Rn – Net radiation (W m^{-2})
H – Sensible heat flux (W m^{-2})
LE – Latent flux of vapourization (W m^{-2})
G – Soil heat flux (W m^{-2})

Rn was measured with the net radiometer, G was measured with soil heat flux plates and H was calculated from measurements of C_N^2 together with standard meteorological observations (air temperature, wind speed and air pressure) collected with the weather station. LE was then calculated as residual of the energy balance equation assuming: 1) closure of the surface energy balance, and 2) that the energy used for processes like photosynthesis was negligible. The components of the energy balance were measured every half hour at Riverlands and every 5 and 10 min at Kogelberg. The calculated LE values in W m^{-2} (energy used to evaporate water) were converted into the equivalent water depth units cumulated over the day in mm d^{-1}.

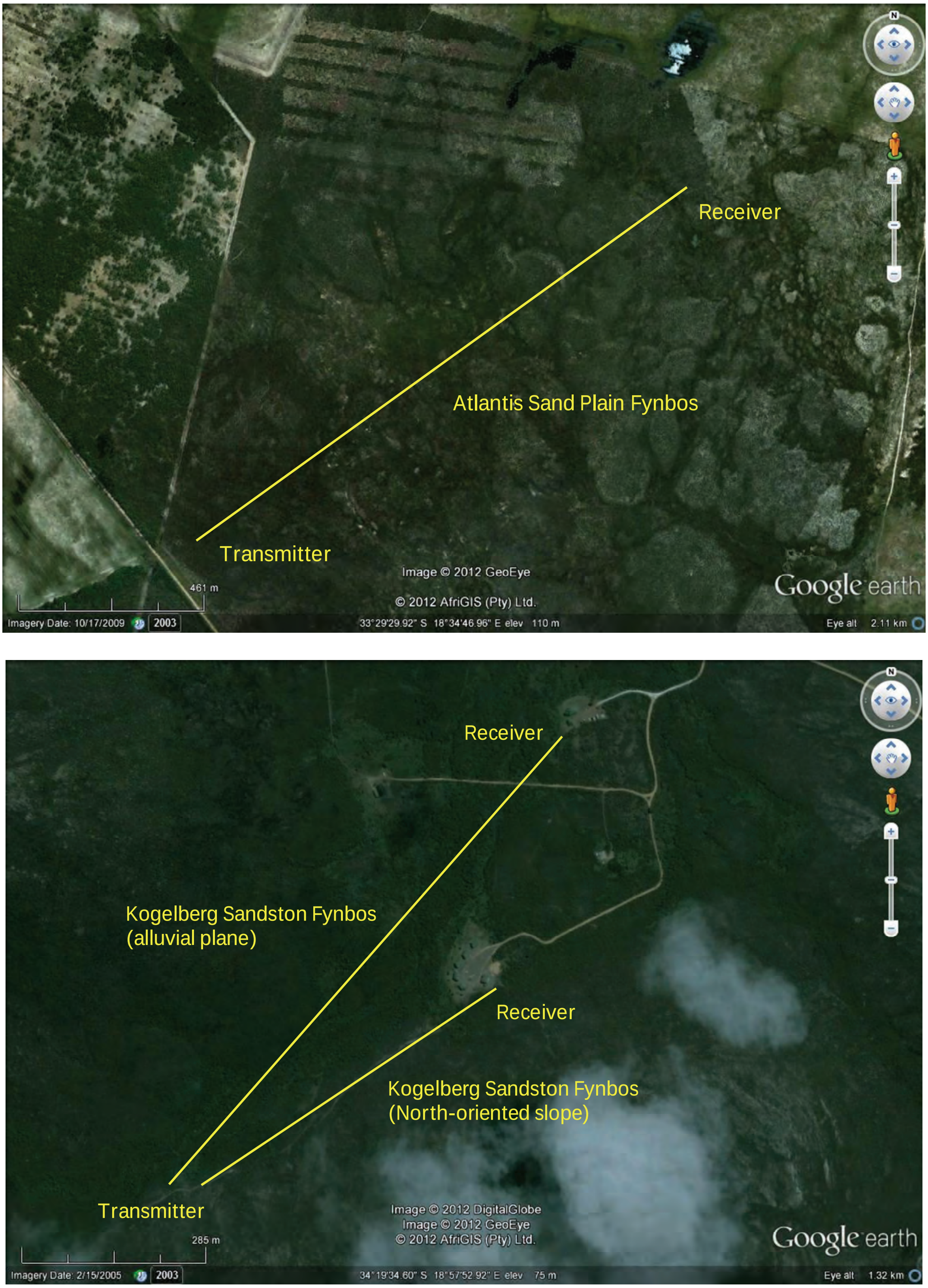

Figure 10
Google view of positions of scintillometer transects at Riverlands (top) and Kogelberg (bottom)

4.5 Results

4.5.1 Atlantis Sand Plain Fynbos (Riverlands)

Daily weather data collected with the weather station from 14 to 27 October 2010 are shown in Figure 11, in particular solar radiation, wind speed, maximum and minimum air temperature and relative humidity, rainfall and vapour pressure deficit. Both sunny and cloudy days occurred during this period, as evident from the daily solar radiation values ranging from 9.4 to 28.2 MJ m^{-2} d^{-1}. High air temperatures generally matched high solar radiation levels and vice versa. Daily average temperatures ranged between 13.0 and 19.8°C. Low radiation levels occurred especially on rainy days (21-24 October 2010). Average daily wind speed ranged from 1.5 to 4.4 m s^{-1}. Vapour pressure deficit was between 0.43 and 1.13 kPa, depending mainly on temperature and minimum relative humidity.

Total evaporation values for the measurement period are shown in Figure 11. These ET values represent the actual evapotranspiration from an Atlantis Sand Plain Fynbos surface and they ranged between 0.8 mm d^{-1} on 21 October 2010 (rainy day) and 5.3 mm d^{-1} on 26 October 2010 (sunny day). For comparative purposes, grass reference evapotranspiration calculated with the Penman-Monteith equation (ETo; Allen *et al*., 1998) was also plotted alongside the actual ET in Figure 11. Values of ETo ranged between 2.6 mm d^{-1} (21 October 2010) and 6.8 mm d^{-1} (27 October 2010). The average ratio of ET/ETo for the measurement period was 0.69 with a standard deviation of 0.18. It should be noted that the root system of this vegetation taps into the shallow groundwater table (about 1 m depth) (Jovanovic *et al*., 2009a) and water stress conditions seldom occur. The ET values measured in this study could therefore represent the potential evapotranspiration of this vegetation. It should also be considered that this ratio integrates vegetation and large patches of land not covered by the vegetation and the limited direct evaporation from the soil.

Figure 12 represents the components of the energy balance determined every 30 min. It is noticeable that the main driver is the net radiation (Rn). High Rn values were recorded under clear sky conditions, and low values on cloudy days when rain occurred, as expected. Positive values of Rn were recorded during the day-time when the sum of the incoming solar and downward long wave radiation from the sky exceeded the sum of the reflected solar (upward) and emitted terrestrial long wave radiation. Negative values were recorded at night when the converse situation prevailed. Positive values of H indicate convective heat fluxes, whilst negative values indicate thermal inversion conditions. Positive LE values indicate evaporative fluxes, whilst negative values indicate condensation. Soil heat flux was a minor component of the surface energy balance throughout the measurement period. Values of G were positive during the day due to surface heating and negative during the night due to emission of the terrestrial radiation (surface cooling).

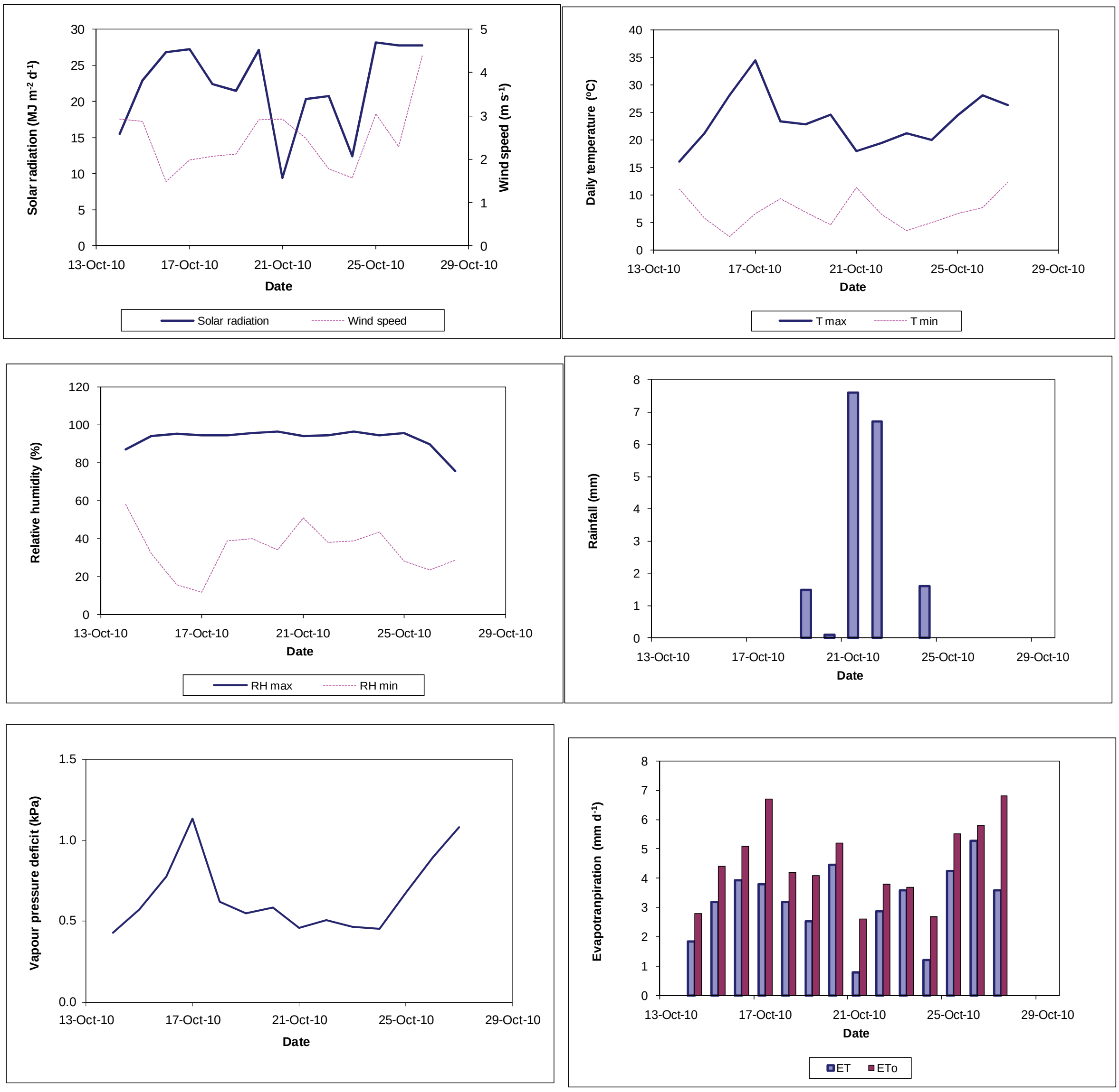

Figure 11

Daily solar radiation, wind speed, maximum and minimum daily temperature, maximum and minimum relative humidity, rainfall and vapour pressure deficit measured with the automatic weather station, evapotranspiration (ET) measured with the scintillometer and reference evapotranspiration (ETo) calculated with the Penman-Monteith equation 14-27 October 2010 at Riverlands on Atlantis Sand Plain Fynbos

High evaporation values were measured between 14 and 27 October 2010. A considerable amount of water is stored in the soil for ET at the end of the rainy season, a shallow water table occurs (~1 m) and well-established fynbos species are able to tap into the groundwater as the root systems are developed deeper than 1 m (Jovanovic *et al*., 2009a). This resulted in relatively high ET values. The sensible heat flux component was also considerably high during the measurement period. The average canopy cover along the measurement transect was 39.2%. The average ratio H/LE was 0.80 for the whole measurement period, ranging between 0.34 on 26 October 2010 (sunny day) and 3.79 on 21 October 2010 (rainy day). G was 18% of Rn on average.

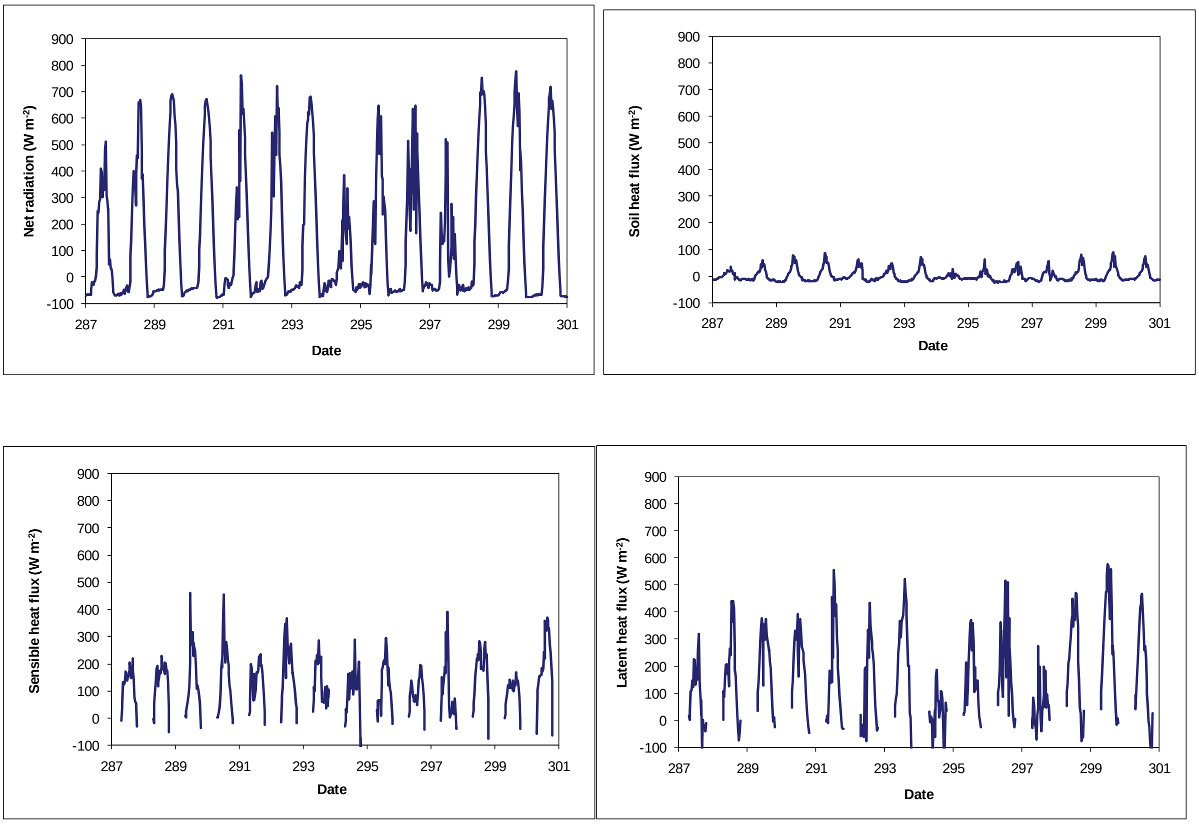

Figure 12

Energy balance measured with the BLS9000 and the weather monitoring systems at Riverlands (14-27 October 2010, Days of Year 287-301) on Atlantis Sand Plain Fynbos

4.5.2 Kogelberg Sandstone Fynbos (slope transect)

Daily weather data collected with the weather station from 8 April to 8 June 2011 are shown in Figure 13. Daily solar radiation values ranged from 2.3 to 18.1 MJ m^{-2} d^{-1}. High air temperatures generally matched high solar radiation levels and vice versa. Low radiation levels usually matched rainy days (e.g. 23 April, 22 May 2011). Minimum recorded air temperature was 7.5°C and maximum was 31.3°C. Average daily wind speed ranged from 0.7 to 5.4 m s^{-1}. Average vapour pressure deficit was 0.67 kPa, ranging from 0.33 to 1.51 kPa. Data recording was interrupted between 29 April and 4 May 2011 due to malfunction of the instrumentation.

Total evaporation values for the measurement period are shown in Figure 13. These ET values represent the actual evapotranspiration from an approximately one-year old Kogelberg Sandstone Fynbos on a North-oriented slope surface after a fire in June 2011. ET ranged between 0.17 mm d^{-1} on 21 May 2011 (day with low wind speed and radiation) and 1.40 mm d^{-1} on 9 April 2011 (sunny day with high solar radiation and air temperature). Daily ETo values are also plotted alongside the actual ET values. Values of ETo ranged between 1.0 mm d^{-1} (8 June 2011) and 5.3 mm d^{-1} (22 May 2011, a rainy day with extremely high wind speed, moderately high maximum temperature and low minimum relative humidity). The average ratio of ET/ETo for the measurement period was 0.34. Such low value was mainly due to sparse vegetation (average canopy cover was 15.5%) and the poor water storage capacity of shallow soils on the sandstone slope. Maximum ET/ETo ratio was 0.64 on 6 June 2011 (day with low solar radiation, air temperature and ETo) and the minimum was 0.06 on 21 May 2011 (two weeks after the previous rain event). It was interesting to note that the ratios ET/ETo usually increased following rainfall events and dropped during periods without rain. Water stress conditions occurred relatively soon after rainfall events because of the low soil water storage capacity.

Figure 14 represents the components of the energy balance determined every 10 min. Sensible heat flux and latent heat flux fluctuated depending on rainfall and availability of soil water for evaporation. The average ratio H/LE was 1.49 for the whole measurement period, ranging between 0.32 on 7 May 2011 (occurring after a few wet days) and 6.55 on 21 May 2011. G was 24% of Rn on average. Extremely low values of LE were calculated on certain rainy days (e.g. 12 April and 8 June 2011), possibly due to condensation and rain drops on the scintillometer receiver surface distorting the signal on the instrumentation. These days were discarded from the calculations of ET/ETo and H/LE.

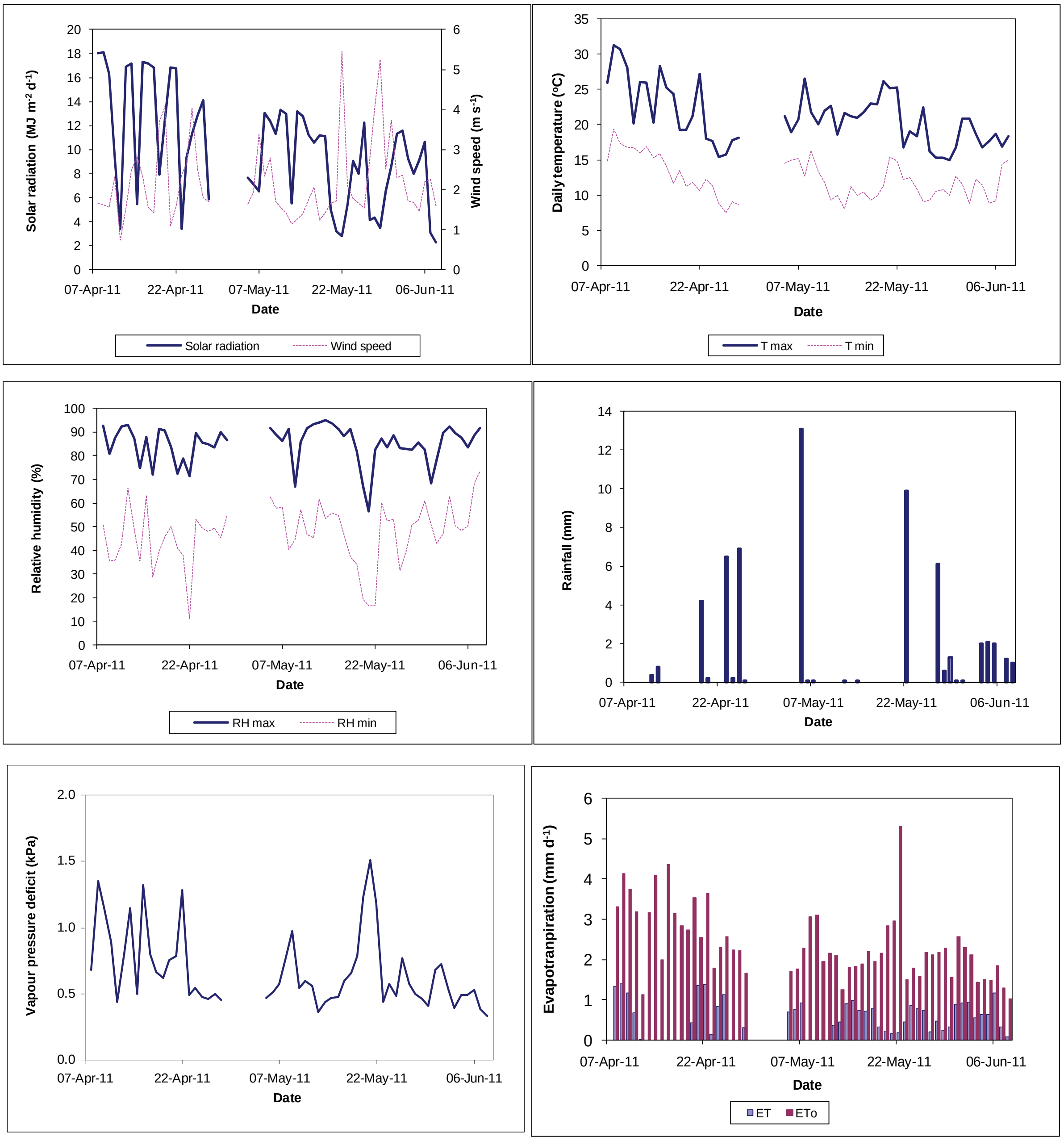

Figure 13

Daily solar radiation, wind speed, maximum and minimum daily temperature, maximum and minimum relative humidity, rainfall and vapour prressure deficit measured with the automatic weather station, evapotranspiration (ET) measured with the scintillometer and reference evapotranspiration (ETo) calculated with the Penman-Monteith equation for the period 8 April-8 June 2011 at Kogelberg om Kogelberg Sandstone Fynbos (North-oriented slope)

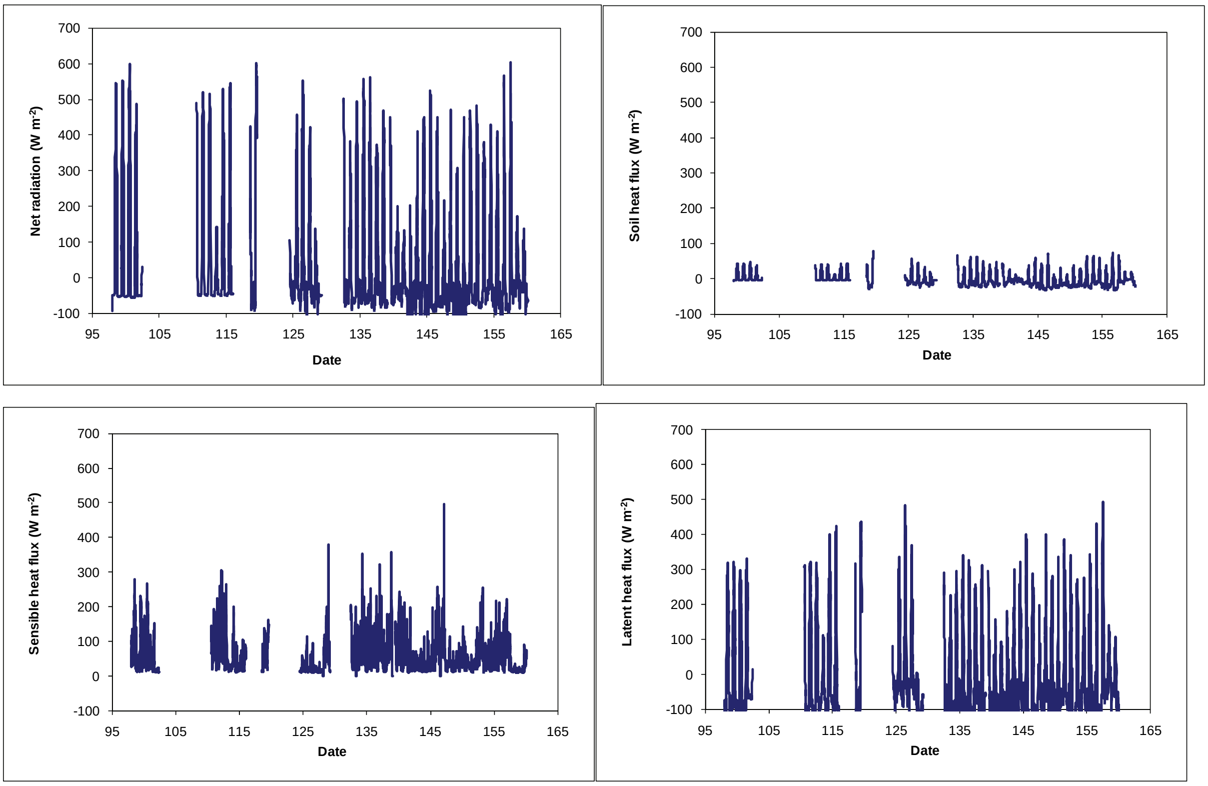

Figure 14

Energy balance measured with the BLS9000 and the weather monitoring systems at Kogelberg (8 April-8 June 2011) on Kogelberg Sandstone Fynbos (North-oriented slope)

4.5.3 Kogelberg Sandstone Fynbos (wetland transect)

Daily weather data collected with the weather station from 3 September to 19 October 2011 are shown in Figure 15. Daily solar radiation values were higher than during the April-June 2011 campaign and they ranged from 4.9 to 26.1 MJ m^{-2} d^{-1}. Low radiation levels usually matched rainy days (e.g. 17, 22 September 2011), as expected. Minimum recorded air temperature was 4.4°C and maximum was 28.2°C. Minimum recorded relative humidity was 29.1% and maximum was 94.7%. Average daily wind speed ranged from 1.1 to 5.6 m s^{-1}. Average vapour pressure deficit was 0.61 kPa, ranging from 0.36 to 1.09 kPa. Data recording was interrupted between 30 September and 12 October 2011 due to malfunction of the instrumentation. The air temperature sensor was also not operating from 3 to 17 September 2011.

Total evaporation values for the measurement period were plotted on the graph in Figure 15. These ET values represent predominantly the actual evapotranspiration from a well established wetland and riparian zone of the Oudebosch stream. ET values were higher than those recorded in the April-June 2011 campaign because of denser vegetation and more soil water available to the vegetation. ET ranged between 1.3 mm d^{-1} on 18 September 2011 (rainy day with moderately low temperature and high humidity) and 5.6 mm d^{-1} on 15 October 2011 (sunny day with high solar radiation and wind speed, following a rainy day). ETo ranged from 1.8 mm d^{-1} (4 October 2011, low radiation, wind and temperature) and 5.2 mm d^{-1} (17 October 2011). The average ratio of ET/ETo for the measurement period was 1.0. This means that the average ET of this vegetation was comparable to the reference evapotranspiration of a well-watered grass. The highest value of the ET/ETo ratio was 1.52 calculated on 24 September 2011 and the minimum of 0.41 was calculated on 18 September 2011. The ET/ETo ratios usually increased following rainfall events and dropped during periods without rain. Water stress conditions therefore occurred relatively soon after rainfall events because of the high transpiration rates of the vegetation and soil water depletion.

Figure 16 represents the components of the energy balance determined at 5 min intervals. Sensible heat flux and latent heat flux fluctuated depending on rainfall and availability of soil water for evaporation. The average ratio H/LE was 1.91 for the whole measurement period, ranging between 0.72 on 15 October 2011 (occurring after rainfall) and 5.26 on 28 September 2011 (following two dry weeks). G was 13% of Rn on average.

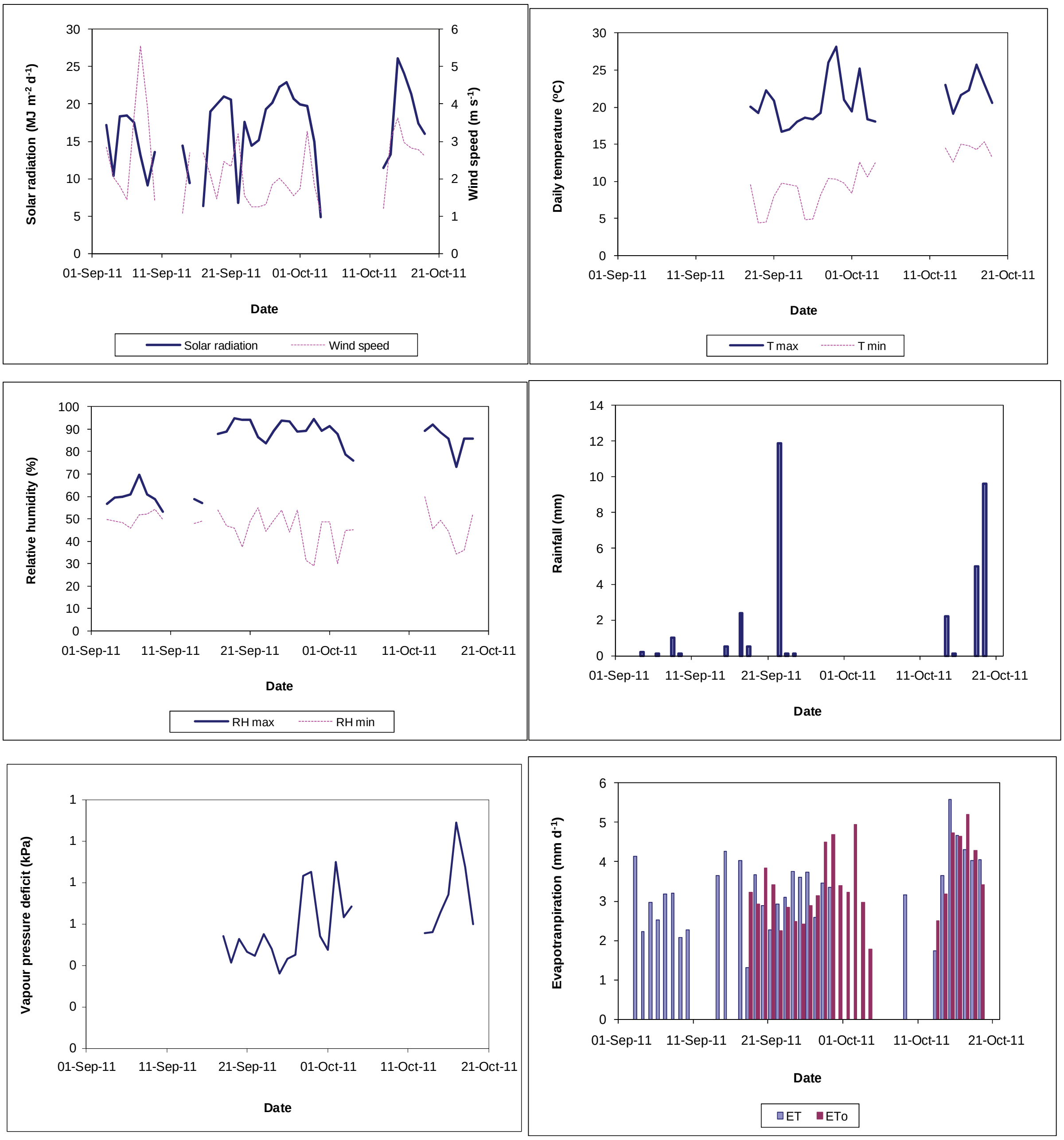

Figure 15

Daily solar radiation, wind speed, maximum and minimum daily temperature, maximum and minimum relative humidity, rainfall and vapour pressure deficit measured with the automatic weather station, evapotranspiration (ET) measured with the scintillometer and reference evapotranspiration (ETo) calculated with the Penman-Monteith equation for the period 3 September-19 October 2011 at Kogelberg om Kogelberg Sandstone Fynbos (alluvial plane)

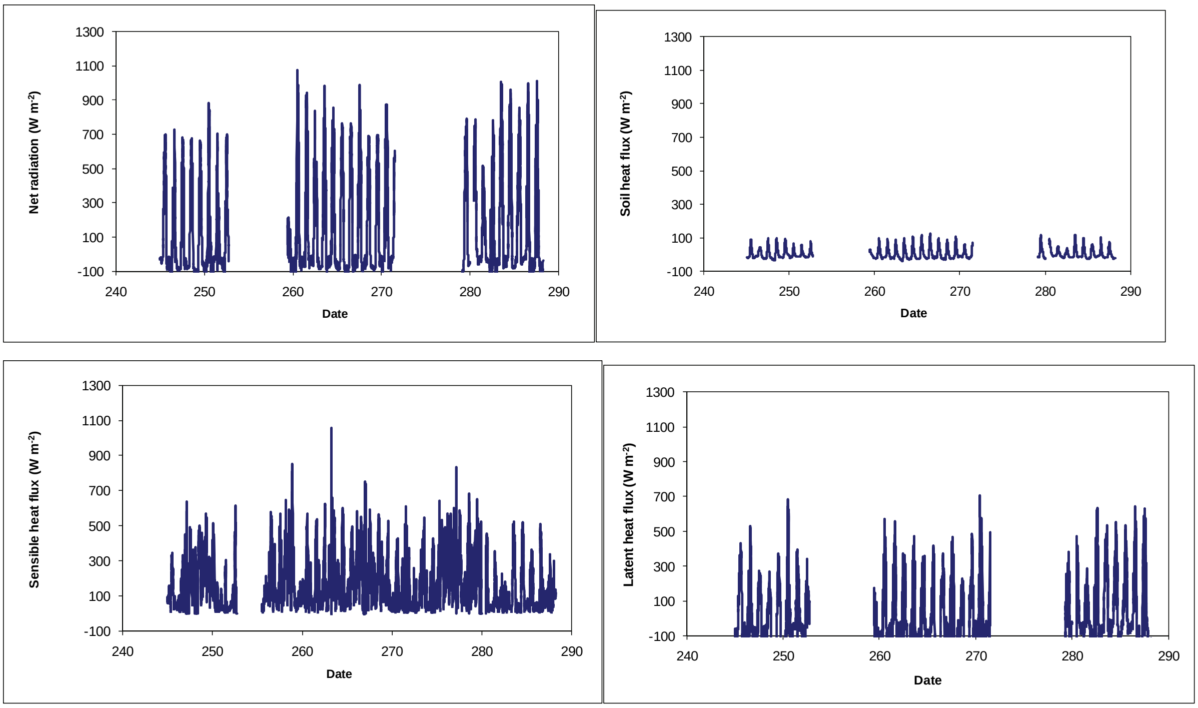

Figure 16

Energy balance measured with the BLS9000 and the weather monitoring systems at Kogelberg (3 September-19 October 2011) on Kogelberg Sandstone Fynbos (alluvial plane)

4.6 Conclusions

The BLS900 scintillometer, available energy and a weather monitoring system were used to determine actual evapotranspiration from Atlantis Sand Plain Fynbos and Kogelberg Sandstone Fynbos. It was the first time that ET from these types of vegetation was determined. The following was found:

- Atlantis Sand Plain Fynbos (Riverlands)

  High LE values were measured as a considerable amount of water is stored in the soil for ET at the end of the rainy season (14-27 October 2010), a shallow water table occurs (~1 m) and well-established fynbos species have root systems deeper than 1 m.

  The H component was also considerably high during the measurement period, probably due to direct evaporation from the sandy soil being limited, and heat fluxes occurring from empty patches of land as fynbos does not fully cover the ground (average canopy cover was 39.1%).

The average ratio H/LE was 0.80 for the whole measurement period, ranging between 0.34 and 3.79.

ET values ranged between 0.8 mm d^{-1} and 5.3 mm d^{-1}.

ETo ranged between 2.6 mm d^{-1} and 6.8 mm d^{-1}.

The average ratio of ET/ETo for the measurement period was 0.69 with a standard deviation of 0.18.

G was 18% of Rn on average.

- Kogelberg Sandstone Fynbos (North-oriented slope transect)

LE and H fluctuated depending on rainfall and availability of soil water for evaporation (8 April-8 June 2011).

The average ratio H/LE was 1.49, ranging between 0.32 and 6.55.

ET ranged between 0.17 mm d^{-1} and 1.40 mm d^{-1}.

Values of ETo ranged between 1.0 mm d^{-1} and 5.3 mm d^{-1}.

The average ratio of ET/ETo for the measurement period was 0.34, ranging between 0.06 and 0.64. Such low value was mainly due to sparse vegetation (average canopy cover was 15.5%) and the poor water storage capacity of shallow soils on the sandstone slope. ET/ETo usually increased following rainfall events and dropped during periods without rain.

G was 24% of Rn on average.

- Kogelberg Sandstone Fynbos (wetland transect)

LE and H fluctuated depending on rainfall and availability of soil water for evaporation (3 September-19 October 2011).

The average ratio H/LE was 1.91 ranging between 0.72 and 5.26.

ET values were higher than those recorded in the April-June 2011 on the slope transect because of denser vegetation and wetter conditions.

ET ranged between 1.3 mm d^{-1} and 5.6 mm d^{-1}.

ETo ranged from 1.8 mm d^{-1} and 5.2 mm d^{-1}.

The average ratio of ET/ETo for the measurement period was 1.0, ranging between 0.41 and 1.52. The ET/ETo ratios usually increased following rainfall events and dropped during periods without rain.

G was 13% of Rn on average.

The results of these measurements were used in the next Chapters to inform hydrological models and improve estimates of groundwater recharge.

5 PREFERENTIAL FLOW STUDIES

In previous work, Le Roux et al. (2011) demonstrated that hydrological soil types are topographically linked in a soilscape (hydrosequence, catena or toposequence). Water redistribution and the hydrological nature of soils are interrelated to soil morphological and hydraulic properties. Mapping soil properties can therefore be used for setting up hydrological models for prediction of hydrological behaviour in catchments.

In order to estimate the effects of preferential flow on groundwater recharge, investigations were carried out on soil and sub-soil. The soil studies included soil description at the two study sites as well as an investigation on soil properties, in particular hydraulic conductivity, in the spatial context. The soil studies also included dye experiments to identify and quantify preferential flow paths. The investigation in the sub-soil included acquisition and processing of resistivity tomography images during and following rainfall events in order to identify any changes in resistivity due to infiltration of water through preferential pathways in the TMG fractured rock system. Results emanating from these studies were also used to spatially delineate soil characteristics, to generate input data and set up hydrological models.

5.1 Soil patterns study

5.1.1 Introduction and rationale

In this Section, it is demonstrated that the application of soil surveying methods can facilitate the spatial conceptualization of catchment hydrology (Lin *et al*.; 1999; Sivapalan, 2003a and b). Survey information that can be used includes in-field observations such as soil depth (Asano *et al*., 2002; Gleeson *et al*., 2009), soil diagnostic horizon (Van Huyssteen *et al*., 2005) and colour (van Huyssteen, 1995) and laboratory determinations such as texture, particle size distribution, organic matter (OM) content (Lin *et al*., 1999) and bulk density (Pachepsky *et al*., 2006).

The validity of using soil survey information in hydrological models was addressed in this study. Two contrasting aquifer systems, the one a fractured aquifer system and the other a primary aquifer, were surveyed during which soils were classified according to the South African Soil Classification system (Soil Classification Working Group, 1991) and samples were taken at representative observation points. Hydrological properties were then estimated from texture and OM content, as well as determined from the soil samples of the various representative soil forms. The estimated hydrological data were then statistically compared in order to assess whether there are significant hydrological differences between the different soil classifications.

The two sites used in the study (Kogelberg and Riverlands) have two very different landscapes. This afforded the opportunity to also experiment with different soil surveying methods including a grid, transect and the reference group based approach. A binary decision tree was also defined as a set of rules to interpolate hydrological data.

Kogelberg predominantly has a mountainous landscape, with the Oudebosch catchment being characterised by deep valleys and high peaks. The geology of the catchment is dominated by Table Mountain Group (TMG) sandstones, quartzites and shales. Rocky outcrops are commonly visible on the surface of higher-lying areas. These rocky outcrops also commonly occur on steep slopes. The sediments are deposited at the footslopes by colluviation. In areas with steep slopes and high rainfall, soils are poorly developed. Alternatively, in the lower-lying and flat areas slope wash accumulation commonly occurs which shows deeper soil development (Boucher, 1978). The Riverlands Nature Reserve is characterised by an extensive and deep sand cover. The sandy soil plains in the reserve are of aeolian and marine origin and are coarse textured, generally acidic, deep and well leached.

5.1.2 Material and methods

A desktop study was firstly done to plan the field and laboratory work. Useful parameters from survey point observations were identified: soil form and family, soil depth, particle size distribution (texture), organic matter content (OM), electrical conductivity (EC), and pH of water and KCl.

Areas of variation, and so too representative sampling sites, were identified using an innovative approach. Conducting a detailed grid soil survey in a catchment with limited accessibility, as is the case in Kogelberg, would have been very time and labour intensive. A simplified, less field-intensive approach was thus required for the Kogelberg survey. Favrot (1981) recommended grouping areas on an aerial photo that present similar geological and topographical patterns into reference groups (RGs). These RGs would indicate areas of variation which need to be studied during the soil survey as these sites most likely present different soil types. This method limits the number of observation sites to areas of predicted variation.

As the terrain soil map had to be used for hydropedological purposes, the RGs in Kogelberg were classed based on expected wetness as this indicated areas of variation requiring investigation. The RGs were identified after two site visits and thorough aerial photo examination. ArcGIS software was used to delineate RGs from aerial photographs according to four factors: topography, aspect, surface vegetation/rock cover and expected wetness.

The survey of Riverlands was less complicated as there were fewer limitations in terms of vegetation and terrain. The greatest limitation was the imposed restriction on digging profile pits. Due to this limitation, only a small detailed survey was allowed in two areas of the reserve whereas a reconnaissance survey was done in the remainder of the reserve to look for deviation from the findings of the detailed survey. The detailed survey was conducted as:

i. A grid survey on the western boundary of the reserve where groundwater monitoring points are situated. This allowed for the understanding of the short-distance variation of soil properties.
ii. A transect survey along the northern boundary of the reserve. This transect encompassed most of the expected long-distance variation in the reserve from the laterite-rich heights in the north-eastern corner to the deep sandy low-lying areas further west.

Soil surveys were conducted in Kogelberg and Riverlands to determine soil form and family according to the South African Soil Classification system (Soil Classification Working Group, 1991). Some RGs could not be surveyed due to dense vegetation or steep slope. Point observations that were made in the field included soil form and family, depth (where digging stopped) and position in the landscape. Digital photographs were taken of each soil observation point. Soil samples were taken from each diagnostic horizon at all observations in Riverlands but only at representative profiles in Kogelberg. A *Garmin* GPS was used to determine the exact position of each observation point, accurate to ±5 m.

The laboratory analyses were conducted according to the procedures outlined in *Methods of Soil Analysis*, *Parts 1* (Klute, 1986) and *3* (Sparks, 1996). Analyses that were performed include: determination of pH(KCl) and pH(H_2O), EC, particle size distribution and identification of podzolic character [pH(NaF)]. Determination of pH in KCl and distilled water were done according to Thomas (1996). These results were reported as pH(KCl) and pH(H_2O) respectively. The EC (µS/cm) was measured using a calibrated Microprocessor Capacitance Meter, RE 387 Tx, Series 3, instead of the laborious saturated paste extract method (Rhoades, 1996). A simple laboratory method to determine podzolic character in soils is to measure the pH of a 1:2.5 soil to 1M NaF solution (Brydon and Day, 1970). This procedure was performed on those samples suspected to have podzolic character. A pH in 1 M NaF solution above 10.5 indicates convincingly that the soil has podzolic character. The results are reported as pH(NaF). Particle size distribution was done on an 80 g sub-sample of dried soil which had the coarse fraction removed already. The textural analysis was done according to Gee and Bauder (1986).

The texture, OM and coarse fraction content were used to estimate plant available water (PAW) and saturated hydraulic conductivity (K_{sat}) using the model of Saxton and Rawls (2006) that was described in detail in Deliverable 9 of this project. A one-way ANOVA without replication was done to investigate whether a significant difference exists between hydrological properties of different soil classifications. The investigation was performed on PAW and soil form, and K_{sat} and soil form. The "F-", "p-" and Kruskal-Wallis p-tests were interpreted as indicating significant difference between the groups if the $F > F_{critical}$ and if $p < 0.05$.

The point observations from both surveys were plotted in ArcMap. A terrain-soil map was compiled based on the RGs discussed above and the soil forms identified during the survey. The terrain-soil map is comprised of polygons that have a specific terrain unit and an association of soil forms. These polygons are termed hydrologically similar units (HSUs).

Interpolation of hydrological properties between observation points by kriging or the "nearest neighbour" method was not possible due to the limited number and sparse distribution of observations in Kogelberg. An alternative method of allocating these properties was thus developed. The interpolation by soil classification method of Voltz and Goulard (1994) and the binary decision tree (BDT) approach of Hansen *et al*. (2009) were combined to develop a BDT for interpolating hydrological properties. A BDT uses a series of "yes / no" questions to assign a value to an observation that lacks data.

5.1.3 Results of soil patterns study

A total of 108 observations were made during the Kogelberg survey. The RG-map was used to select areas for soil observation. The 10 different soil forms that were identified during the survey are shown in Table 4. From the 108 observations, 12 representative observation sites were selected where sampling from each diagnostic horizon was done for laboratory analysis.

The Riverlands survey consisted of five observation points from the transect survey, nine from the grid survey and numerous from the reconnaissance survey. The survey identified four different soil forms in total which are shown in Table 5. Samples were collected for each diagnostic horizon at all 14 sites for laboratory analysis.

Table 6 summarizes the statistical analysis of PAW against soil form for each site separately. There is no significant difference between the PAW of the soil forms in Riverlands. The Kruskall-Wallis p-test however found a significant difference between the PAW of the soil forms in Kogelberg.

The boxplot in Figure 17 shows that the PAW of the Cartref and Pinegrove soil forms differ significantly. The "whiskers" of the boxplot also illustrates the variation of PAW in Kogelberg.

Table 7 summarizes the statistical analysis of K_{sat} against soil form for each site separately. It shows that there is no significant difference between the K_{sat} of the soil forms in Riverlands ($F < F_{crit}$ and $p > 0.05$). The K_{sat} however differed significantly between the soil forms in Kogelberg ($p < 0.05$ and $F > F_{crit}$). The LSD test (Table 8) shows that the K_{sat} of the Cartref soil form differed most significantly from that of the Witfontein form ($p = 0.00839$), then the Fernwood form ($p = 0.00919$) and finally the Pinegrove form ($p = 0.01756$).

TABLE 4
SOIL FORMS OBSERVED DURING THE SURVEY OF THE OUDEBOSCH CATCHMENT, KOGELBERG

Soil Form (Abbreviation)	Number of Observations	Average Maximum Observed Depth (mm)
Cartref (Cf)	47	426
Pinegrove (Pg)	18	548
Fernwood (Fw)	11	700
Witfontein (Wf)	9	761
Glenrosa (Gs)	6	210
Concordia (Cc)	5	762
Groenkop (Gk)	4	715
Lamotte (Lt)	4	787
Houwhoek (Hh)	3	650
Katspruit (Ka)	1	550

TABLE 5 SOIL FORMS OBSERVED DURING THE SURVEY OF THE RIVERLANDS NATURE RESERVE		
Soil Form (Abbreviation)	Number of Observations	Average Maximum Observed Depth (mm)
Lamotte (Lt)	9	1153
Witfontein (Wf)	3	1454
Concordia (Cc)	2	1700
Fernwood (Fw)	Observed during reconnaissance survey without detailed notation	

TABLE 6 SUMMARY OF STATISTICAL ANALYSIS OF PROFILE AVAILABLE WATER (PAW) AND SOIL FORM					
Site	Independent Variable	Dependent Variable	F	P	Kruskal-Wallis (p)
Riverlands	Soil form	PAW	0.1111	0.90	0.92
Kogelberg	Soil form	PAW	1.8570	0.13	0.04

TABLE 7 SUMMARY OF STATISTICAL ANALYSIS OF K_{sat} AND SOIL FORM					
Site	Independent Variable	Dependent Variable	F	P	Kruskal-Wallis (p)
Riverlands	Soil form	K_{sat}	1.6902	0.20	0.42
Kogelberg	Soil form	K_{sat}	2.7284	0.03	0.04

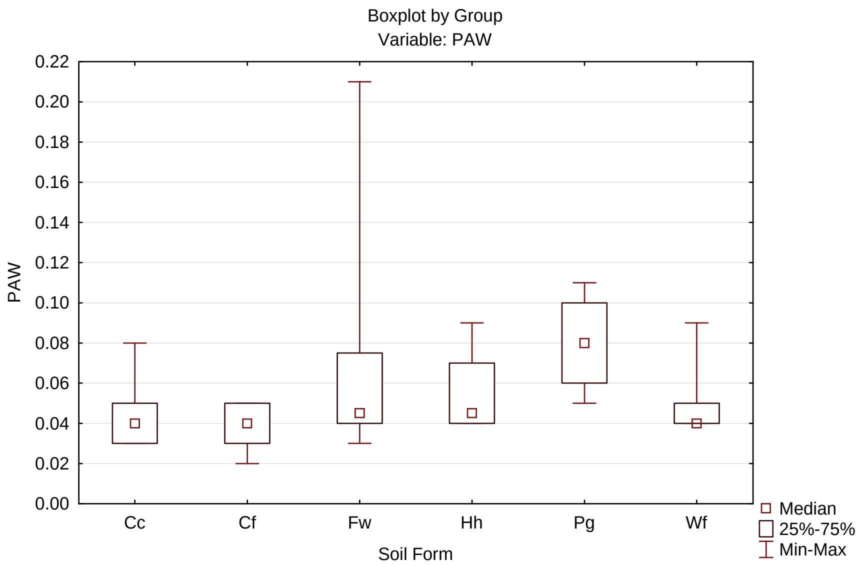

Figure 17

Boxplot of plant available water against soil form in Oudebosch catchment

TABLE 8
LSD TEST FOR SIGNIFICANT DIFFERENCE OF SATURATED HYDRAULIC CONDUCTIVITY (K_{sat}) BETWEEN THE SOIL FORMS FOR KOGELBERG

Cell No.	Probabilities for post-hoc test Error: between MS = 923.55; df = 35.000 Numbers in bold indicate significant difference – P < 0.05						
	Soil form	Average K_{sat}					
		117.93	100.78	141.50	113.39	140.70	148.14
1	Cc		0.239	0.119	0.805	0.164	0.083
2	Cf	0.239		**0.009**	0.495	**0.018**	**0.008**
3	Fw	0.119	**0.009**		0.140	0.961	0.704
4	Hh	0.805	0.495	0.140		0.173	0.097
5	Pg	0.164	**0.018**	0.961	0.173		0.689
6	Wf	0.083	**0.008**	0.704	0.097	0.689	

The terrain-soil map in Figure 18 shows the HSUs in Kogelberg delineated based on the position in the landscape and the soil forms present therein. The soil forms in Kogelberg were grouped into hydrological similar soil classes based on the results from the statistical analysis (Table 9). The HSUs in Figure 18 were grouped into correlating HSUs if their slope and soil types were similar yet their aspects and vegetative cover differed (Table 10) for use in the BDT.

The complexity of the Kogelberg catchment provided the opportunity to experiment with different methods of mapping and interpolation of hydrological properties. The terrain-soil map (Figure 18) shows an ensemble of different HSUs, each with a unique combination of soil forms and terrain units. The conventional interpolation of hydrological properties was however not possible due to the limited number of observations and the large degree of variation. The combined approach of using the “soil classification” and “binary decision tree” (BDT) methods was used to allocate the most accurate hydrological property to unsampled observation points using data from sampled observation points.

The BDT that was compiled for interpolation in Kogelberg is shown in Figure 19. It is non-parametric and simple to train and interpret. Tables 9 and 10 accompanying the BDT show the correlating HSUs, that have similar terrain characteristics but vary in their aspect or vegetative cover, and hydrological similar soil classes (the hydrologically similar soil classes are soil forms that were shown to have similar infiltration patterns during recharge) respectively. Table 9 is used in level 3 and 5 of the BDT and Table 10 in level 4 and 5 of the BDT. The coarse fraction content of the soil and the position in the landscape were however also taken into account when dividing the soils into groups as these factors were found to influence flow (Saxton and Rawls, 2006; Ticehurst *et al.*, 2007).

TABLE 9 GROUPINGS OF HYDROLOGICALLY SIMILAR UNITS
R1 + R2
Mw + Mn
T1 + T2 + T3
Ba + Bb + Bc + Bd + Be
Fs + Fn + La
Lb + Lc

TABLE 10 HYDROLOGICALLY SIMILAR SOIL CLASSES	
Description	Abbreviated Soil Forms
Deep sandy soils / Located on level or moderately sloping terrain	Fw, Cc, Ka, Lt, Pg, Wf
Shallow soil with a high coarse fraction / Grades to bedrock / Commonly occurring on high-lying or sloping terrain	Cf, Gk, Gs, Hh

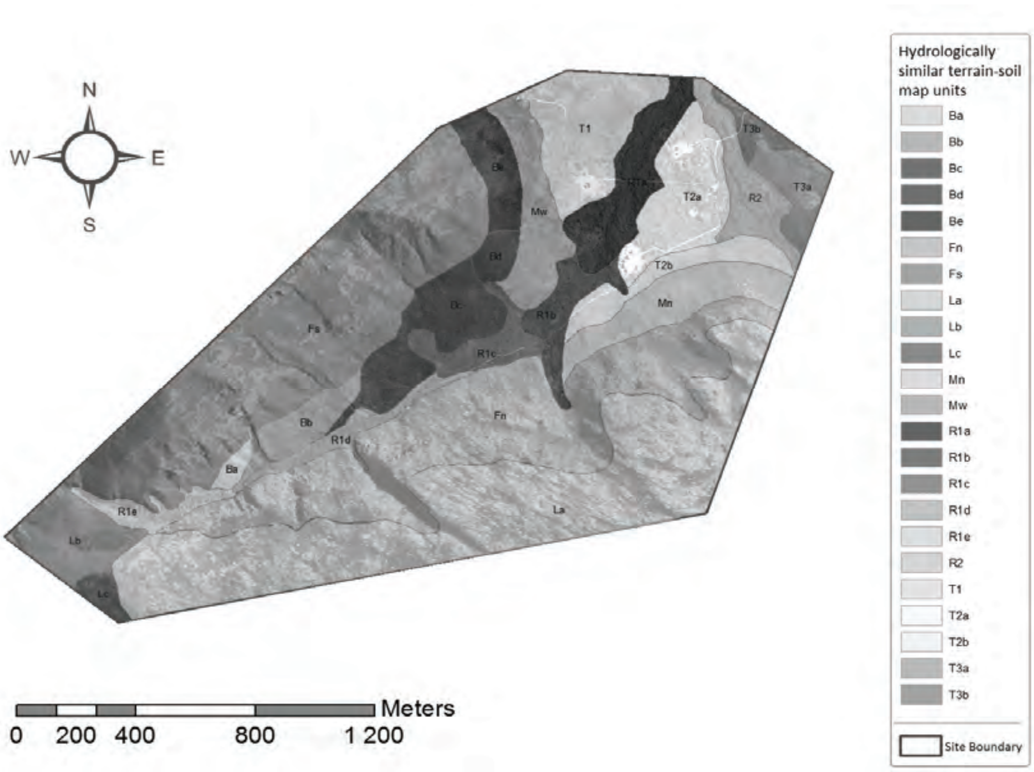

Figure 18

Hydrologically similar units based on terrain and hydrologically similar soil classes at Kogelberg

The soils in Kogelberg however, can roughly be grouped into one of two classes which were used as “hydrological similar soil classes” (Table 4):

i. Deep, macroscopically homogenous, sandy textured soils, with small coarse fraction content, predominantly occurring on moderately sloping or level terrain on foothills and valley floors. Examples of such deep sandy soil forms are Fernwood, Witfontein, Pinegrove, Lamotte, Katspruit and Concordia.
ii. Shallower soils with very high coarse fraction content, that gradually grade into bedrock. These soils are dominant on high-lying level terrain and steep slopes. Shallow rocky soil forms (and exposed bedrock) include Cartref, Glenrosa, Houwhoek and Groenkop.

The observation that the hydrological properties differ significantly between contrasting soil forms is a development in hydropedology as it ties in with the findings of Van Huyssteen *et al.* (2005) who argued that the annual duration of saturation differs between diagnostic horizons according to the South African Soil Classification system. These conclusions can aid in the upscaling of hydrological maps by providing grounds for grouping HSUs.

The data in this study showed that there are grounds for grouping soil forms based on their hydrological properties. For the purpose of hydrological modelling, the area of the Oudebosch catchment was divided into three parts:

- North-oriented slope characterized by large slope (>10%), shallow soils and 1-2 years old vegetation after fire
- South-oriented slope characterized by large slope (>10%) and well-established vegetation as no fire occurred recently
- Alluvial plane characterized by variable slope usually <10%, deep soils, moist conditions and well-established vegetation

It is indicative that the type of vegetation is usually associated with the soil morphology and hydrologic conditions.

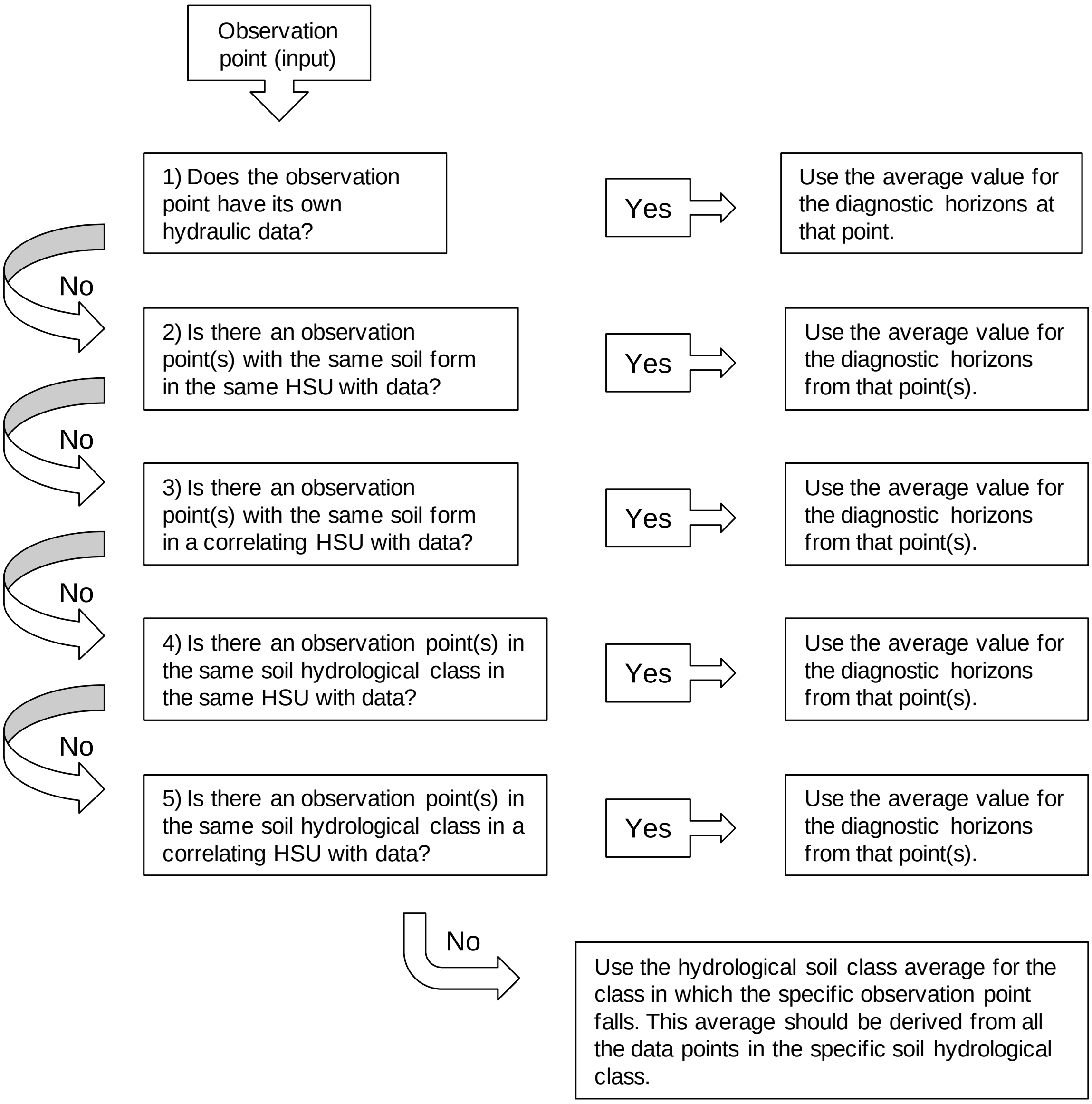

Figure 19

Binary Decision Tree (BDT) for interpolating hydrological properties to unsampled observation points

The soil spatial pattern in Riverlands was less complex compared to Kogelberg. The soil types were interpolated with reference to the observations made in the reconnaissance survey as well as the observed soil forms to produce an interpolated soil map of the entire reserve (Figure 20). The observed soil types were compared according to their position in the landscape, lithology, slope, position relative to the tributaries and surface soil colour during interpolation. Such mapping by interpolation techniques have been proven useful in local studies by Hensley *et al*. (2007) and Lorentz (2007).

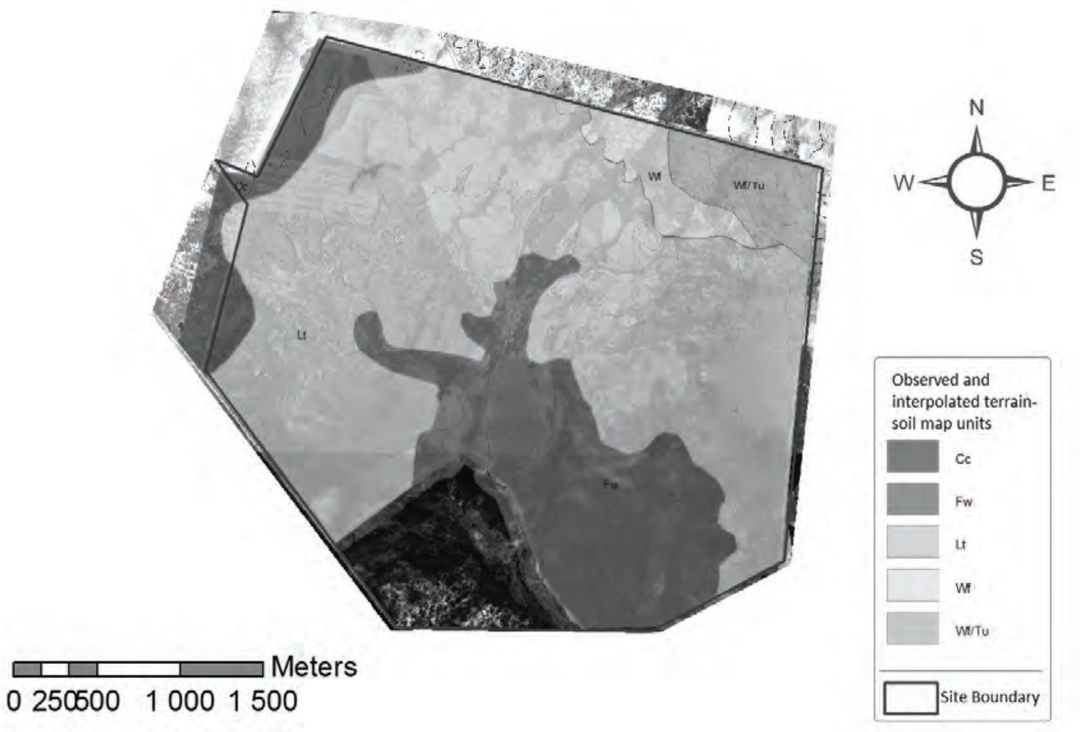

Figure 20

Interpolated terrain-soil map of Riverlands Nature Reserve

The soils in Riverlands have formed from aeolian material (Jovanovic *et al*., 2009a), however there is an area in the north-eastern corner of the reserve where relict laterite is abundant. The soils in the reserve are however macroscopically homogenous and uniformly deep. The survey identified that the texture becomes finer closer to the confluence of the flow paths into the stream, a pattern which is common in landscapes (Ticehurst *et al*., 2007). Humic acids leached from fynbos vegetation usually form organo-metal compounds in the soil, the accumulation of which gives rise to podzolic character (Midgley and Schafer, 1992). The soils in the laterite-rich terrain were classified as Witfontein and Lamotte, with the possibility of also being a Tukulu or Vilafontes forms. The soils outside the laterite zone were classified as Lamotte, Witfontein, Concordia and Fernwood.

The statistical analysis revealed that the soils in Riverlands were fairly uniform regarding their PAW and K_{sat} as no significant differences were observed. These soils would thus be regarded as having a similar hydrological response. This is in line with the low degree of expressed soil form variation relative to that of Kogelberg.

The Riverlands catchment was fairly homogenous in terms of relief, soil forms and soil depth. The observed soil forms and their relative position in the landscape could thus be used to predict a soil distribution map of the entire reserve, a method previously used by Browning and Duniway (2011) in New Mexico, USA. A reconnaissance survey was done to observe the soils outside the grid and transect boundaries in order to identify anomalies in the remainder of the reserve. The interpolation process took into account the expected degree of wetness, the abundance of vegetation, the relief and the lithology. Thus by incorporating the results of grid and transect surveys one can use ArcGIS software to interpolate the soil distribution if the correct input data is available (Hensley *et al*., 2007; Lorentz, 2007). The available data include soil point observations, an accurate geo-referenced orthophoto and contour lines.

5.1.4 Conclusions of soil patterns study

Two sites, characterised by different aquifer systems. were surveyed to investigate the effect of soil pattern on groundwater recharge. These findings were then graphically presented using different mapping techniques. The Oudebosch catchment in the Kogelberg Nature Reserve is a fractured bedrock aquifer, whereas the Riverlands Nature Reserve is a cover sands aquifer. The concluding results are as follows:

- Use of GIS and remote sensing techniques can help delineate reference groups in a sloping landscape, based on surface features and terrain morphology, to identify areas of expected variation which may aid to reduce the number of field observations required to conduct a comprehensive soil survey.
- Pedo-transfer functions can effectively be used to predict hydrological properties, K_{sat} and PAW, from soil texture, gravel and OM content determined in a laboratory from soil samples.
- There is a statistically significant difference between the estimated K_{sat} of the deep sandy Fernwood, Witfontein and Pinegrove soil forms and shallow rocky Cartref soil forms in the Kogelberg Nature Reserve.
- There is a statistically significant difference between the estimated PAW of the deep Pinegrove soil form and shallow rocky Cartref soil form in the Kogelberg Nature Reserve.

- There is no statistically significant difference between either the K_{sat} or PAW of any of the soil forms sampled in the Riverlands Nature Reserve.
- GIS can be used to graphically delineate HSUs in a catchment based on terrain morphology and soil pattern distribution on grounds of statistical differences.
- A combination of the soil classification method and the rules defined by the binary decision tree can be used to interpolate hydrological properties in unsampled observation sites.

5.2 Soil hydraulic conductivity study

5.2.1 Introduction and rationale

Water infiltration occurs in soils according to one of two flow patterns: uniform or non-uniform. Uniform flow occurs as a more or less horizontal wetting front, usually parallel to the soil surface. Non-uniform flow, referred to here as preferential flow, occurs as an irregular wetting front in which water or solutes will move faster in certain areas of the vadose zone than in others (Hendrickx and Flury, 2001).

Many different causes of preferential flow have been suggested. However, estimating whether preferential flow will occur in soil cover and the degree to which the preferential flow affects the rate of infiltration and recharge is not well understood. Thus research that aims to investigate which soil systems give rise to preferential flow, and describe the effect of preferential flow on recharge, can significantly reduce uncertainties in groundwater recharge estimation models.

Traditional methods of investigating the effects of soil type/characteristics on groundwater dynamics include the use of hydraulic head data, temperature profiles, streamflow, stable isotope and dye tracers, drip infiltrometers, double ring infiltrometers and mini-disc permeameters. Modelling flow in fractured bedrock aquifers poses a unique challenge as using hydraulic information alone is not passable and temperature profiles are difficult to attain due to the rock content (Praasma *et al*., 2009).

The comparison was done on a quantitative and qualitative basis. The quantitative comparison was done using numeric data in the form of volumetric water measurements and hydraulic conductivity measurements, whereas the qualitative comparison was done based on photographic support of water flow paths using a staining dye and digital image classification. ***This study illustrates flow patterns specific to certain soil types which may improve the accuracy of groundwater recharge estimation.***

5.2.2 Material and methods

Two infiltration sites were selected at each study location. The aim was to conduct the infiltration experiments at contrasting soil observation points. The variation of soils in the study area can be broadly summarized into two groups: (1) shallow soils with high coarse fraction, grading into bedrock, mostly found on sloping terrain (site K1 at Kogelberg) or (2) deep sandy soils, with low coarse fraction, predominantly on level valley floors (sites K2 at Kogelberg, R1 and R2 at Riverlands).

Kogelberg presented a large degree of soil variation as reported in the survey. A shallow rocky Cartref (K1) and deep sandy Fernwood (K2) soil forms were selected for the infiltration tests as these represent the most divergent soil forms in terms of depth, coarse material content, expected moisture and position in the landscape. Both these sites were also easily accessible with all the required equipment. All the soils found in the reserve were slightly acidic with pH (H_2O) generally less than 6. Both sites had a coarse sand texture and low clay contents of less than 2.75% and 3.95% for K1 and K2 respectively. The coarse fraction however differed greatly as K1 exhibited as much as 32% and K2 less than 1%. The vegetation at K1 was generally 0.5-1 m high grass with scattered fynbos. The lush riparian vegetation found at K2 is common for areas close to a stream.

The soil survey of Riverlands revealed much less heterogeneity in terms of soil form and soil depth than in Kogelberg. The infiltration investigation was thus performed on two common soil forms found on different landscape positions. R1 is a Lamotte soil form with a medium sand texture and no coarse fragments found on a low-lying concave slope. The vegetation is 0.2 high grass with scattered burnt remnants of fynbos. R2 is a Vilafontes (transition to Lamotte) soil form with a medium sand texture on a high-lying convex slope. The coarse fraction and clay content increase with depth where the texture eventually grades to loamy sand. The vegetation is similar to the grass found in R1 but with scattered restioid reeds. The soils in the reserve are generally acidic, i.e. pH (H_2O) below 7.

Saturated hydraulic conductivity was determined in the field using the constant head method in a large double ring infiltrometer. The rates of infiltration at both Riverlands and Kogelberg were very rapid which made it difficult to maintain a strictly constant water head using the available equipment. A potassium iodide (KI) solution was used instead of water to combine the infiltrometer and flowpath visualization experiments for convenience. Saturated hydraulic conductivity was calculated using Darcy's law and input parameters: double-ring inner surface area (A), time (t), volume of water applied (V), the difference between the initial and final height of the water level in the specific time interval (ΔH) (taken as 1 cm in each case as time was taken as the dependent variable in this experiment) and the change in height of the water head with the soil surface as reference level (L). The equation used was:

$$K_{sat} = \frac{V\,L}{\Delta H\,A t}$$

The visualization of water flow paths experiment was conducted as proposed by Hangena *et al*. (2003). The method is based on the colour change reaction between potassium-iodide (KI) and starch. Hangena *et. al*. (2003) used a 12% KI solution but a 7% solution is efficient to cause a colour change in the light coloured soils of the selected sites in this study. The KI solution was allowed to infiltrate the soil using the double ring infiltrometer as described above.

The infiltration site was then left undisturbed for 24 h. After the waiting period a vertical soil section was carefully excavated through the zone where infiltration occurred. The exposed surface was thoroughly wetted with household starch spray from an aerosol canister. A 12% hydrogen-peroxide solution was then applied onto the surface using a spray bottle to facilitate the release of I_2 and favour the blue colour formation. A 10 min waiting period was allowed for effective colour change to occur after which digital photographs were taken in "RAW format" for digital image processing. Adobe Photoshop Version 8.0 was used to convert the images from a RAW to a jpeg format as negative colour projections using a standardized filter.

The photo was cropped to ensure that only the area of infiltration was analysed. The negative colour image was further contrasted by reduced all the pixels in the image to either blue, indicating flow paths, or red, indicating areas that were by-passed during infiltration. The classification of pixels was done using the maximum likelihood classification tool in ESRI ArcGIS 9. The number of pixels in each class was then presented as a percentage relative to the total number of pixels in the image. These images are referred to as preferential flow visualisations.

Soil samples were collected in 10 cm depth intervals from the area of infiltration. The samples were sealed in air tight plastic bags and weighed in the laboratory. These initial masses were noted as wet mass. The samples were then air dried in a force draft room and weighed again. This time the mass was noted as dry mass. The change in mass was used to calculate the gravimetric water content (GWC).

Bulk density (BD) was not determined in the field and a rapid assessment was thus done in the laboratory. A 20 g sample was weighed off to three decimal places and placed into a measuring cylinder accurate to 1 cm^3. The cylinder was gently tapped on the worktable twenty times to allow partial consolidation to occur. The volume was recorded in cm^3 and is reported as measured bulk density. An estimated bulk density was also calculated in the SPAW software using texture and OM as input variables (Saxton and Rawls, 2006). Both the measured and estimated bulk densities were used to calculate volumetric water content (VWC).

Particle density (PD) was calculated using the volumetric flask method as outlined by Blake and Hartge (1986). Porosity was then calculated from PD and measured BD as:

Porosity = (PD – BD) / PD

The texture, OM and coarse fraction content were used to estimate PAW and saturated K_{sat} using the model of Saxton and Rawls (2006). These calculations were done on SPAW software version 6.02.74.

ArcMap GIS software was used to compile a map to indicate areas of differing recharge estimation accuracy. The map was used to group areas where “accurate estimation is possible”, “moderately accurate estimation is possible”, and “accurate estimation is unlikely”. These groupings were done based on the position of a map unit in the landscape, the soil forms present in the map unit, and thus the degree of expected preferential flow.

5.2.3 Results of hydraulic conductivity study

Table 11 summarizes the results of hydraulic properties of soil samples at different depths, diagnostic horizons and sites. Plant available water was estimated with the method of Saxton and Rawls (2006). Volumetric soil water content was determined from GWC and BD estimated with Saxton and Rawls (2006) and with the rapid assessment method in the laboratory. Saturated hydraulic conductivity was determined with the method of Saxton and Rawls (2006) and from constant head infiltration measurements with the double ring infiltrometer.

At Kogelberg site K1, on a Cartref 1200 soil (K1 – Cf1200) (Soil Classification Working Group, 1991), VWC using measured and estimated BD were not statistically different ($p = 0.277$; $F < F_{crit}$) (Table 11). The cumulative GWC for the stones subjected to KI infiltration was 22% higher than that of the stone samples containing only antecedent moisture. Only the stone samples subjected to KI infiltration presented the blue colour formation after starch and peroxide treatment, thus confirming that the water was not antecedent but rather infiltrated over night. The rock fraction, estimated at around 20 to 30%, is expected to increase with depth as the lithocutanic B horizon, starting at 30 cm, is expected to grade into bedrock according to the definition by the Soil Classification Working Group (1991). The inconsistent variation in VWC is thought to be due to the channelling of water into paths of least resistance between the coarse fractions. The volume of soil by-passed by preferential flow does not contribute to the total VWC and thus PAW. Thus preferential flow is seen to increase with depth, the profile is well drained and less water is retained in the profile (Petersen*, et al*. 2001). Estimated K_{sat} was fairly uniform throughout the profile, ranging from a minimum of 99.4 to a maximum of 139.9 mm h^{-1}. K_{sat} measured with the double ring infiltrometer a few centimeters below the soil surface was 492.3 mm h^{-1} (Table 11). The vast difference between the values may be explained by the presence of preferential flow paths in this profile as water that is funnelled between the coarse fragments. This type of flow, known as funnel flow, occurs on a Darcian scale in macroscopically heterogeneous soils as discussed by Kung (1990) and Hendrickx and Flury (2001). Figure 21 (left) shows the route of preferential flow where water converges into channels of least resistance between the coarse fragments. This pattern is not limited to one depth interval only; instead, it is continuous throughout the profile.

For Kogelberg site K2, on a Fernwood 1110 soil (K2 – Fw1110) (Soil Classification Working Group, 1991), VWC with estimated and measured BD did not differ significantly ($p = 0.081$; $F < F_{critical}$) (Table 11). VWC gradually increased and then declined with depth. The horizon where higher VWC was observed coincided with the horizons that had minimal preferential flow. Estimated K_{sat} values were fairly consistent, ranging from 102.3 to 148.1 mm h^{-1}, and did not differ greatly from the measured K_{sat} of 117.7 mm h^{-1} (Table 11). It would thus seem that the estimates were fairly accurate in predicting K_{sat} at site K2. The infiltration of KI solution indicates a uniform wetting front in Figure 22 (left). This is supported by the image analysis (right), which shows that flow paths covered 82% of the total area. The 18% which was by-passed can be a result of dissimilarities in hydraulic properties and particle size distribution. This is a minor case of unstable flow which has limited impact, a feature commonly found in macroscopically homogenous soils (Kung, 1990; Hendrickx and Flury, 2001). These preferential flow paths were thus not as dominant as at site K1 and K_{sat} could thus accurately be estimated in this deep sandy soil profile in Kogelberg.

TABLE 11
MEASURED AND ESTIMATED SOIL PHYSICAL AND HYDRAULIC PROPERTIES FOR THE FOUR INFILTRATION SITES IN KOGELBERG AND RIVERLANDS

Site[1]	Sample	Diagnostic Horizon	Estimated PAW[2] (%)	Porosity (%)	VWC[3] using estimated BD (%)	VWC[4] using measured BD (%)	Estimated[5] K_{sat} (mm h^{-1})	Measured[6] K_{sat} (mm h^{-1})
K1 (Cf1200)	0-10	Orthic A	6	38.5	-	-	139.9	492.3
	10-20	Orthic A / E1	5	30.9	17.63	20.72	122.2	
	20-30	E1	5	38.3	18.00	19.04	99.4	
	30-40	Lithocutanic B1	5	32.5	16.98	19.88	118.2	
	40-50	Lithocutanic B1	4	38.3	13.40	14.61	121.3	
K2 (Fw1110)	0-10	Orthic A	4	57.3	14.73	10.78	148.1	117.7
	10-20	Orthic A / E1	4	56.7	15.15	11.12	135.3	
	20-30	E2	5	51.7	19.29	15.75	102.3	
	30-40	E2	5	52.4	20.86	17.07	128.6	
	40-50	E3	4	49.3	16.22	14.22	135.3	
R1 (Lt1100)	0-10	Orthic A	5	41.5	7.10	6.99	157.3	182.6
	10-20	E1	4	44.6	6.52	6.16	168.9	
	20-30	E1	4	59.7	5.56	3.86	184.1	
	30-40	E2	4	58.1	5.50	3.96	184.1	
	40-50	E3 / Podzol	4	52.9	5.69	4.59	184.1	
	50-70	E3 / Podzol	4	53.4	6.22	4.99	175.3	
R2 (Vf2110)	0-10	Orthic A	3	47.9	6.62	5.77	152.6	148.2
	10-20	E1	4	47.7	7.67	6.65	102.4	
	20-30	E1	4	41.7	9.29	9.21	112.7	
	30-40	Neocutanic B1	4	45.1	10.73	9.68	88.0	
	40-50	Neocutanic B1	4	37.8	11.52	11.78	77.9	
	50-70	Neocutanic B2	4	40.9	12.63	11.89	54.8	

[1] K1 and K2 – Sites at Kogelberg; R1 and R2 – Sites at Riverlands. Cf – Cartref; Fw – Fernwood; Lt – Lamotte; Vf – Vilafontes soil forms (Soil Classification Working Group, 1991)
[2] Plant available water estimated with Saxton and Rawls (2006)
[3] Volumetric soil water content (VWC) calculated from gravimetric and bulk density (BD) estimated from Saxton and Rawls (2006)
[4] Volumetric soil water content (VWC) calculated from gravimetric and bulk density (BD) measured with the rapid assessment method in the laboratory
[5] Saturated hydraulic conductivity estimated from Saxton and Rawls (2006)
[6] Saturated hydraulic conductivity measured with the double ring infiltrometer

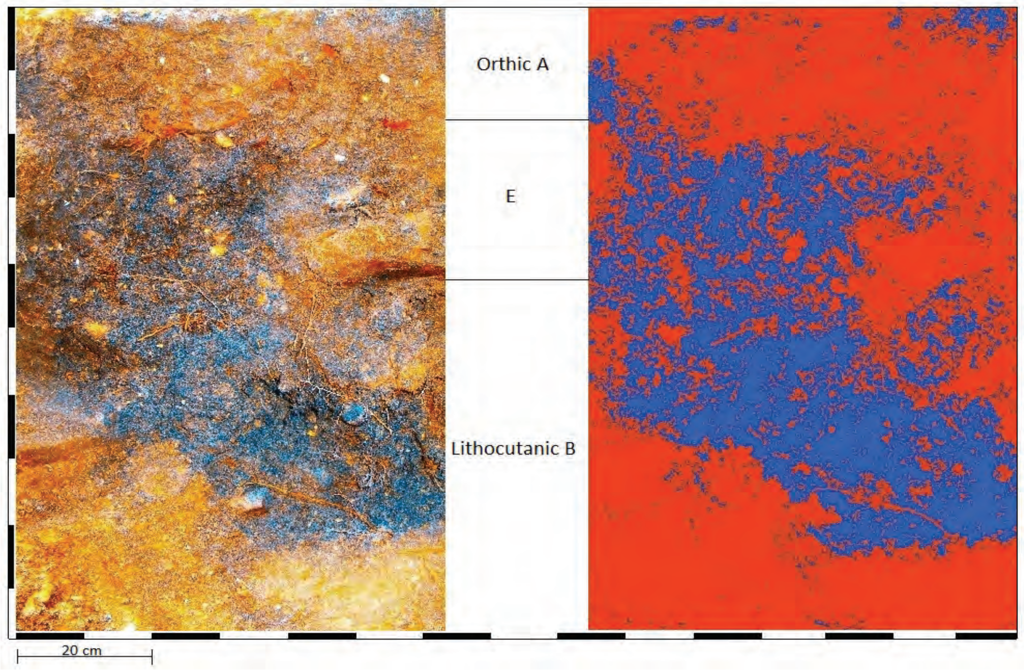

Figure 21

Left: Negative colour image of flowpath visualization for site K1. Right: ArcGIS maximum likelihood colour analysis for site K1 (Blue = Flow path / Red = By-passed)

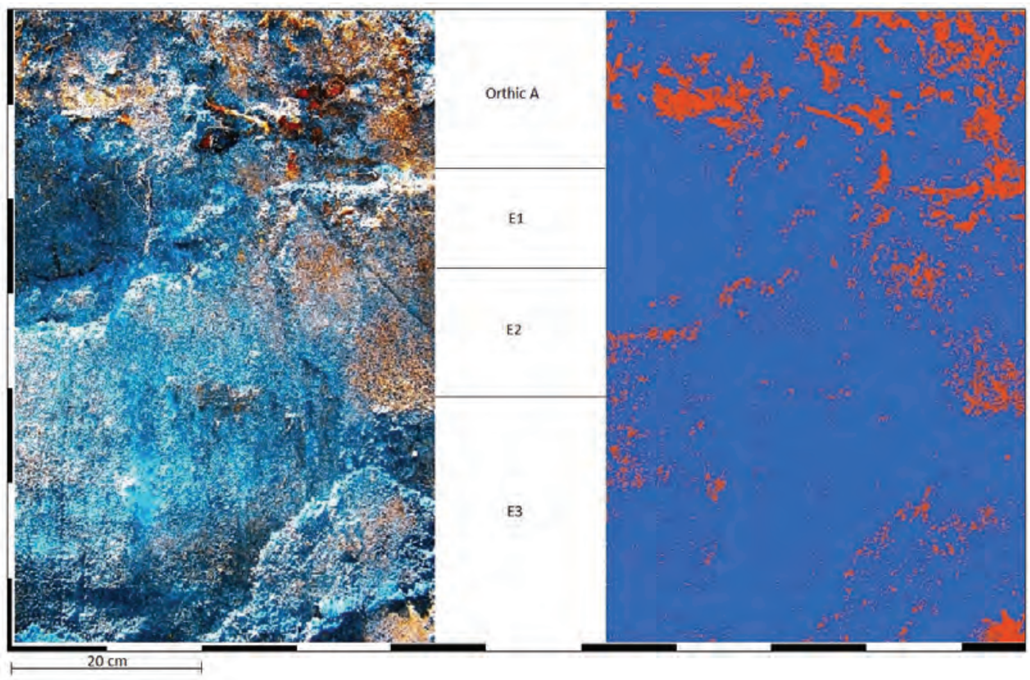

Figure 22

Left: Negative colour image of flowpath visualization for site K2. Right: ArcGIS maximum likelihood colour analysis for site K2 (Blue = Flow path / Red = By-passed)

For Riverlands site R1, on a Lamotte 1100 soil (R1 – Lt1100) (Soil Classification Working Group, 1991), VWC calculated from estimated and measured BD differed from a depth of 20 cm onwards, although these differences were not statistically significant ($p = 0.108739$; $F < F_{critical}$) (Table 11). The VWC declined from the surface to the 20 to 30 cm layer, but steadily increased again from 30 to 70 cm. This is explained through preferential flow paths occurring at depths between 20 and 50 cm, caused by coarser sand fractions at these depths (12.1%) compared to the surface layer (9.5%) and textural discontinuities. Joel and Messing (2001), and Weiler and Naef (2002) have reported that a change in macropore density and configuration may cause preferential flow. A divergence layer is present at 40-50 cm. This could be due to the lower coarse sand fraction of 8.8% and thus another change in macropore density and configuration. This trend of preferential flow diverging into uniform flow was also reported by Hendrickx and Flury (2001). From this depth on, the water was evenly distributed and infiltration occurred more or less uniformly. Estimated K_{sat} was fairly consistent throughout the profile, ranging from 157.3 to 184.1 mm h^{-1}. Measured K_{sat} of 182.6 mm h^{-1} is similar to the maximum estimated K_{sat} at soil depths of 20 to 50 cm (Table 11). Measured K_{sat} values were up to 20% higher than estimated K_{sat}, which indicates that recharge estimations should be done with care in this soil type in Riverlands as textural discontinuities in the vertical plane may affect the predictability of recharge estimation. Figure 23 shows continuous zones of preferential flow in the top 20 cm of the profile. This could explain why the measured K_{sat} is higher than the estimated K_{sat} for this layer. Flow through the layers from 20 to 40 cm was limited to two isolated preferential paths. The decline in VWC at depths 20-50 cm corresponded to layers where only preferential flow occurred. The image analysis reported that 62% of the image consisted of flow paths. The preferential flow in the 20-40 cm layer comprised the majority of the by-passed 38%. The increase in VWC towards the bottom of the soil profile was possibly due to capillary rise from shallow groundwater.

For Riverlands site R2, on a Vilafontes 2110 soil form (Vf – 2110 transition to Lamotte) (Soil Classification Working Group, 1991), there was no significant difference in VWC, calculated with estimated or measured BD ($p = 0.688$; $F < F_{critcal}$) (Table 11). VWC increased gradually with depth corresponding to an increase in clay content from 4.3 to 9.9%. The coarse sand fraction also increased with depth from 5.7 to 12.3%. In this instance, the ability of clay to increase water holding capacity outweighs the effect of coarse material. The decline of estimated K_{sat} with depth corresponds to the increase in coarse fraction and clay content. Measured K_{sat} of 148.7 mm h^{-1} corresponded to the K_{sat} estimated value of 152.6 mm h^{-1} observed in the 0-10 cm layer (Table 11). The flow paths comprised 72% of the image shown in Figure 24, indicating predominant uniform flow. The flow pattern changed below 40 cm and the estimated K_{sat} dropped below 80 mm h^{-1}. The presence of an E horizon above the Neocutanic B horizon (Figure 24) indicates that the subsoil presents a limitation to infiltration. Water may either dam up, forming a perched water table, or flow laterally when it reaches this point (Lin *et al*., 2006; Asano *et al*., 2002). The continual lateral redistribution facilitates infiltration of surface water at a higher rate than the limiting horizon(s) allows. Another theory is that preferential flow in the subsoil below 40 cm is rapid enough to drain the infiltrating volume of water, as supported by Glass *et al*. (2002). Everson *et al*. (1998) also reported that the flux between the B horizon and the groundwater zone is poorly understood.

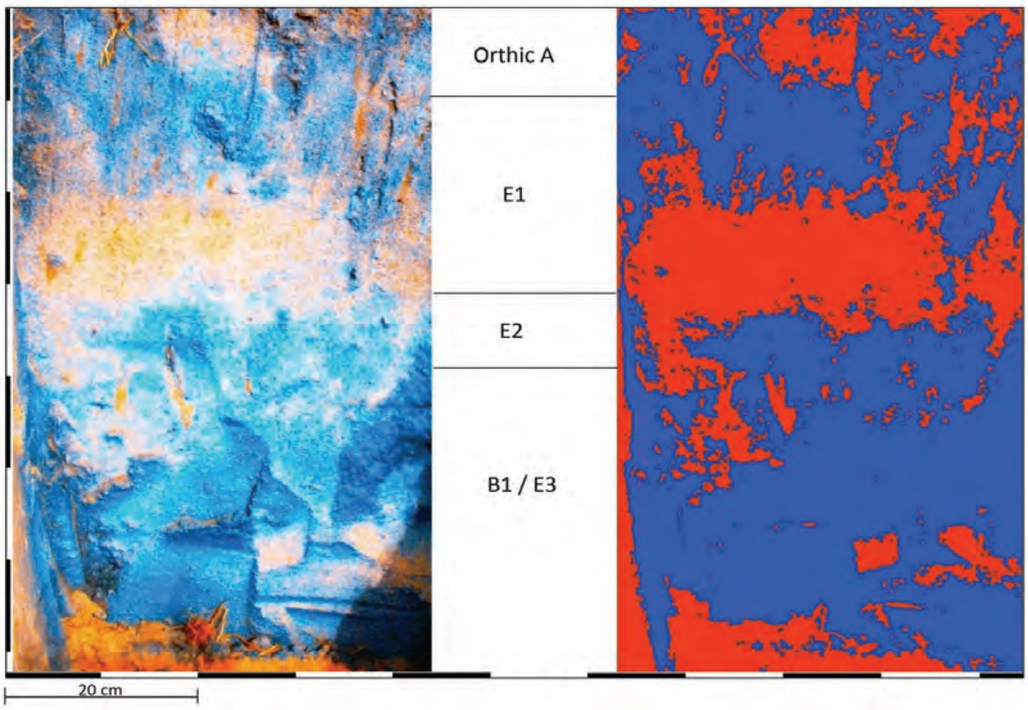

Figure 23

Left: Negative colour image of flowpath visualization for site R1. Right: ArcGIS maximum likelihood colour analysis for site R1 (Blue = Flow path / Red = By-passed)

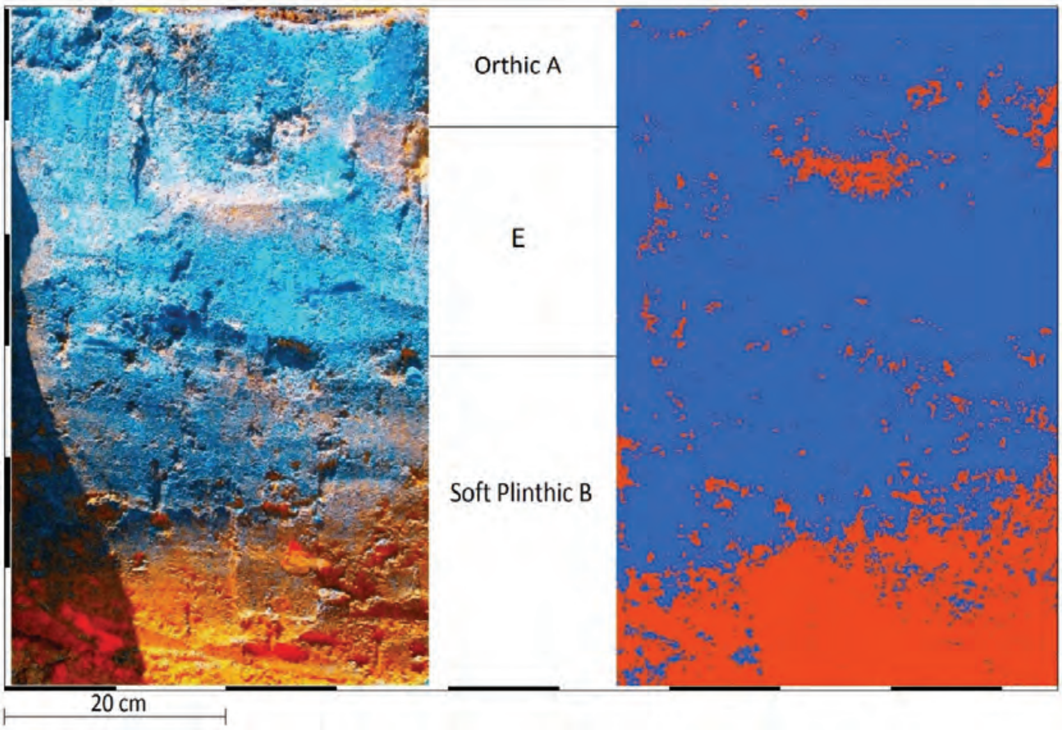

Figure 24

Left: Negative colour image of flowpath visualization for site R2. Right: ArcGIS maximum likelihood colour analysis for site R2 (Blue = Flow path / Red = By-passed)

5.2.4 Conclusions of hydraulic conductivity study

Hydraulic properties and the effects of preferential flow were investigated in four typical and contrasting soil profiles at Kogelberg and Riverlands. The study led to the following conclusions:

- A well-drained, shallow rocky soil type that grades into bedrock (site K1, soil form Cf 1200) contained large preferential flow paths between large stones, through channels of least resistance, throughout the depth of the profile. This form of preferential flow is commonly referred to as funnel flow and occurs in macroscopically heterogeneous soils. The flow volume of the profile amounted to 38% and consisted of both soil and coarse fraction. This is a substantial portion of the profile and the plant available water is thus expected to be low as the profile drains.
- Infiltration in the homogenous Fernwood soil form (Fw 1110 at site K2) occurred predominantly frontally. Infiltrating water by-passed only 18% of the profile. The soil's position at the foot of the mountain, next to the stream, suggests that the soil texture is well sorted and homogeneous.

- The soils in Riverlands (Lt 1100 at site R1 and Vf 2110 at site R2) were similar to site K2 in that they were deep, sandy and had a low coarse (gravel) fraction. The soils were better graded due to the level landscape compared to site K2. Estimated and measured K_{sat} matched at sites R1 and R2, in particular in the top soil. There were signs of preferential flow at both sites. Infiltrating water by-passed 38% of the profile at R1 and 28% of the profile at R2.
- Data on preferential flow obtained in this study were used to define hydraulic conductivities for hydrologically similar soils delineated on a map. Hydraulic conductivities are essential inputs in hydrological models and they need to account for preferential flow characteristics.
- As a conservative and mobile solute was used, the dye experiment also served the purpose of defining the possible fate of contaminants in the environment and impacts on groundwater quality.

5.3 Subsurface resistivity study

5.3.1 Introduction and rationale

Given prominent preferential flow paths were observed in the soils at Kogelberg, ***a subsurface resistivity study was conducted in order to investigate whether paths of rapid flow occur also in the sub-soil.*** This section summarizes the findings of the geophysical study conducted using resistivity tomography.

The aim of the investigation was to take snap shots of the subsurface by using resistivity tomography to identify preferential pathways. Resistivity changes in the subsurface are influenced by the movement of the wetting front during and after rainfall. Therefore, resistivity measurements were taken at short time intervals to produce profiles of the subsurface before, during and after rainfall events during the 2010 and 2011 rainy winter seasons (time-lapse analysis). It was envisaged that one would have been able to follow the water as it moved through the subsurface. This would have then allowed for differentiation of water movement through preferential pathways and matrix rock.

5.3.2 Material and methods

Electrical surveying is used to determine subsurface resistivity distribution in a non-invasive manner. This is a relatively inexpensive method used to provide a profile of different geological units due to changes in porosity and salinity of the pore fluids (Colvin *et al*., 2009; Binley *et al*., 1996). Resistivity is a common method used in various engineering and scientific research applications to identify water movement. Resistivity tomography was used at the Kogelberg Biosphere Reserve during a previous study to investigate the structural discharge regimes of the TMG and also in the Langebaan lagoon to define vegetation controls (Colvin *et al*., 2009; Saayman *et al*., 2007). The technique was used previously to identify water movement and quantify preferential flow on landfills (Perozzi and Holliger, 2008), soils (Samouelian *et al.*, 2003) and waste dumps (Grellier *et al*., 2005). Barker and Moore (1998) used resistivity tomography to study the flow of water through the vadose zone and flow changes due to water extractions.

The basic variable of electrical measurements is resistivity which is a physical property associated with the ability of a substance to conduct electricity (Loke, 2001). This is done by acquiring measurements on the ground surface and then using these measurements to estimate the true resistivity. Resistivity of the subsurface can be associated with various physical conditions of interest such as lithology, porosity, degree of water saturation, and presence or absence of voids in the rock (Loke, 2001).

Resistivity distribution of the subsurface is made by injecting current into the ground through two electrodes (C1 and C2 in the sketch in Figure 25). The resulting voltage difference is measured at two potential electrodes (P1 and P2 in Figure 25). By using the current (I) and voltage (Vt) values, an apparent resistivity (P_a) is calculated:

$$P_a = k\ Vt / I$$

where k is the geometric factor which is dependent on the arrangement of the four electrodes. In practice, apparent resistivity meters give a resistance (Res) value:

$$Res = V / I$$

which can be related to the current (I) and voltage (V) through Ohm’s Law (Loke, 2001), thus resulting in apparent resistivity being calculated by:

$$P_a = k\ Res$$

This means that the calculated resistivity value (measured by resistivity meters) is not the true resistivity of the subsurface, but an apparent resistivity. To calculate the true resistivity, a computer program Res2Dinv is used. The program generates 2D resistivity profiles of the subsurface which relates to the true resistivity measurements of the ground (Loke, 2001).

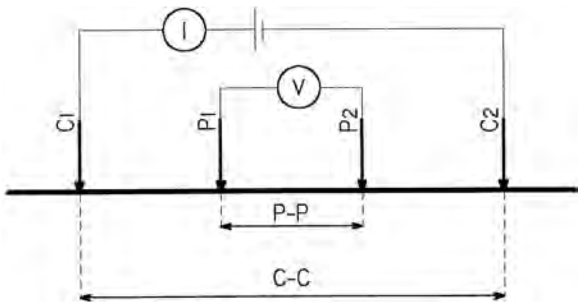

Figure 25

Sketch illustrating the principle of resistivity measurement: current (C) and potential (P) electrode set-up

For the resistivity tomography study, the Lund imaging system was used. The equipment comprises a resistivity unit, cables, electrodes, connecting cables with clamps, hammers, GPS, 12 volt batteries, multimeter, laptop and note book. The resistivity unit consists of two instruments, one is the Terrameter (Figure 26), which is the control unit, and the other is the Switcher Box (Figure 26), which connects the main cables (Figure 27) to the control unit. The main cables are used to connect the electrodes to the control panel. The connecting cables with clamps are used to connect the electrodes (Figure 27). For the purpose of this experiment, electrodes were steel rods (Figure 27), 60 cm long on average and approximately 2 cm in diameter. Hammers (Figure 27) are necessary (preferably 4 pound) to firmly hammer the electrodes into the ground. To power the system, a 12 volt battery (Figure 26) is needed and a multimeter (Figure 27) is required to check the voltage of the battery (if the voltage of the battery is too low, the resistivity meter is not accurate). It is recommend that two batteries are used, one to run the system and one as a back-up should failure occur.

Electrodes may be placed down boreholes (Daily *et al*., 1992) or along the surface (Barker, 1992) in the field. The "along the surface" method for geophysical exploration was applied at selected sites. The Standard Wenner Array (Loke) with 64 electrodes was used to cover the longest line possible with the equipment available. Electrodes were initially spaced 2 m apart corresponding to a signal depth of approximately 15 m. The laptop was used to download and view preliminary results in the field as well as to annotate any significant findings and field conditions. The GPS locations of the 1st, middle (34th electrode) and last (64th electrode)

electrode were acquired. This was done to mark the exact locations of the electrodes to facilitate repetitive measurements at the same site.

Three tasks were conducted in the resistivity study:

1. Testing various protocols (where a protocol defines the amount of sampling/data points to be used) to optimize the resolution vs. time constraint of the measurement, as well as spacing of electrodes vs. depth of profiling.
2. Obtaining background profiles at the end of the dry season, as well as information on geological controls driving preferential flow processes.
3. Collecting data during infiltration events.

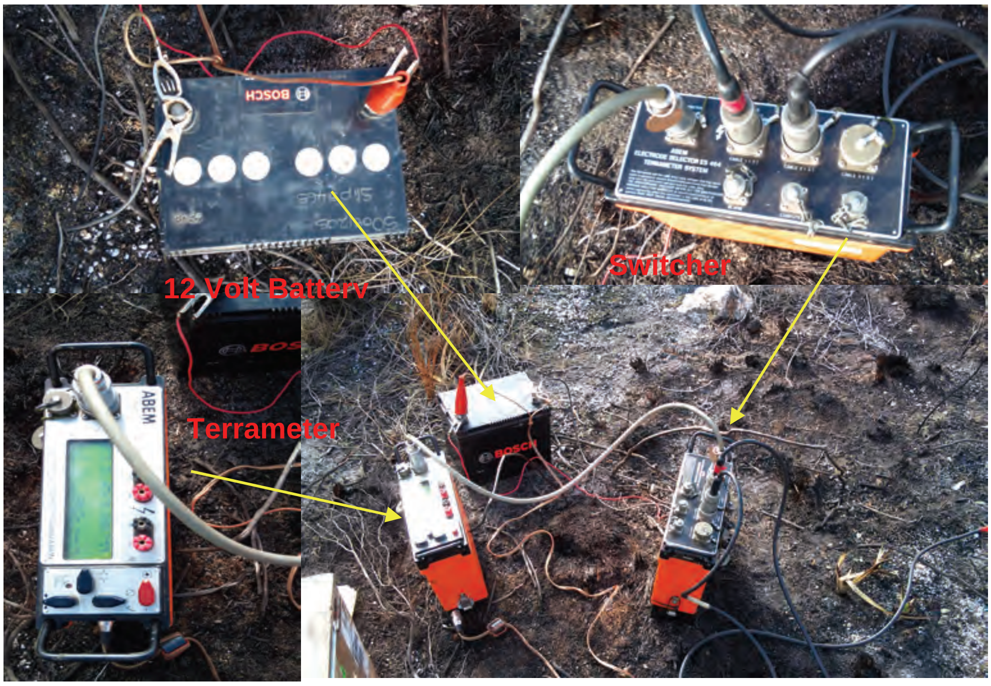

Figure 26

Resistivity tomography unit, showing 12 Volt battery, switcher unit and Terrameter

Figure 27

Electrodes, connecting cables and accessories (multimeter and hammer) required for resistivity tomography measurements

The main purpose of the resistivity measurements was tracking the movement of water through the subsurface. Several resistivity measurements were carried out during the 2010 and 2011 winter rainy seasons at two transects in the Oudebosch catchment (site 1 and site 2 in Figure 5). Site 1 was located on the alluvium (corresponding to site K2 of the soil infiltration study), whilst site 2 was located on the North-oriented slope (corresponding to site K1 of the soil infiltration study). Weather and daily rainfall data were also collected to correlate the amount of rainfall on the days of surveying with the amount of water infiltration. Borehole logs from boreholes available in the vicinity of the measurement sites were used to identify and correlate geological units associated with the profiles.

The initial idea was to take resistivity measurements in 2 hour sessions during rainfall events. However, due to the difficulties in predicting the timing of rainfall events of a sufficient magnitude, it was decided to take resistivity measurements immediately after rainfall events. Each measurement takes approximately 1.5 h. Several measurements were taken during one day.

5.3.3 Results of resistivity measurements

Selected results are reported in this section for Site 2 (Figure 5) as examples of applications of geophysical measurements. For additional information, the reader is referred to Deliverables 5 and 11 of this project. During 2011, numerous resistivity measurements were acquired and processed into profile images. Insight into potential geological controls and preferential flow processes were gained and some relevant results are presented in Figures 28 and 29.

Resisitivity contrasts identified in Figure 28 were interpreted to be associated with the occurrence of a fault along the measurement transect at Site 2. The fault occurs between the older Peninsula Formation and the younger Cederberg Formation. The different rock types were identified using published typical resistivity values associated with these rock types (Loke, 2001), as well as geological data available for the study area. Figure 28 also illustrates the increased vertical resolution achieved by reducing electrode spacing. The initial electrode spacing of 2 m resulted in a measured (horizontal) subsurface resistivity distribution of 128 m and a depth of about 15 m. After reducing the spacing to 1 m, the measured subsurface resistivity distribution was reduced to 64 m. The 1 m spacing increases the vertical resolution between 0 and 8 m depth. An increased vertical resolution allowed to zoom into the details of the profile and facilitated the identification of preferential flow paths. However, increased resolution reduced the sample size (length of the transect and depth of the profile).

Time lapse analysis was used on data acquired immediately after rainfall events and an example of the results is presented in Figure 29. The data represent consecutive profiles, acquired within hours (a and b), and the difference between the two (c). Clear finger-like patterns are evident in Figure 29 (c). Given that the survey line stayed constant and that ponding was observed on the surface of the soil, it was evident that this was associated with localized infiltration of water into the subsurface. The patterns are interpreted to be associated with preferential flow paths (fractures, joints, etc.) in the subsurface geology. The positive change in resistivity is due to the loss of water (e.g. drainage, evaporation) and the negative change in resistivity is due to the gain in water (infiltration).

It can be visually observed that the flow path volume of the profile in the top 2 m was about 40%, which is close to the value obtained for soils in the infiltration study in the vicinity of this site (38% of volume at site K1 in the soil infiltration study). These data were used to define hydraulic conductivities as inputs into hydrological models.

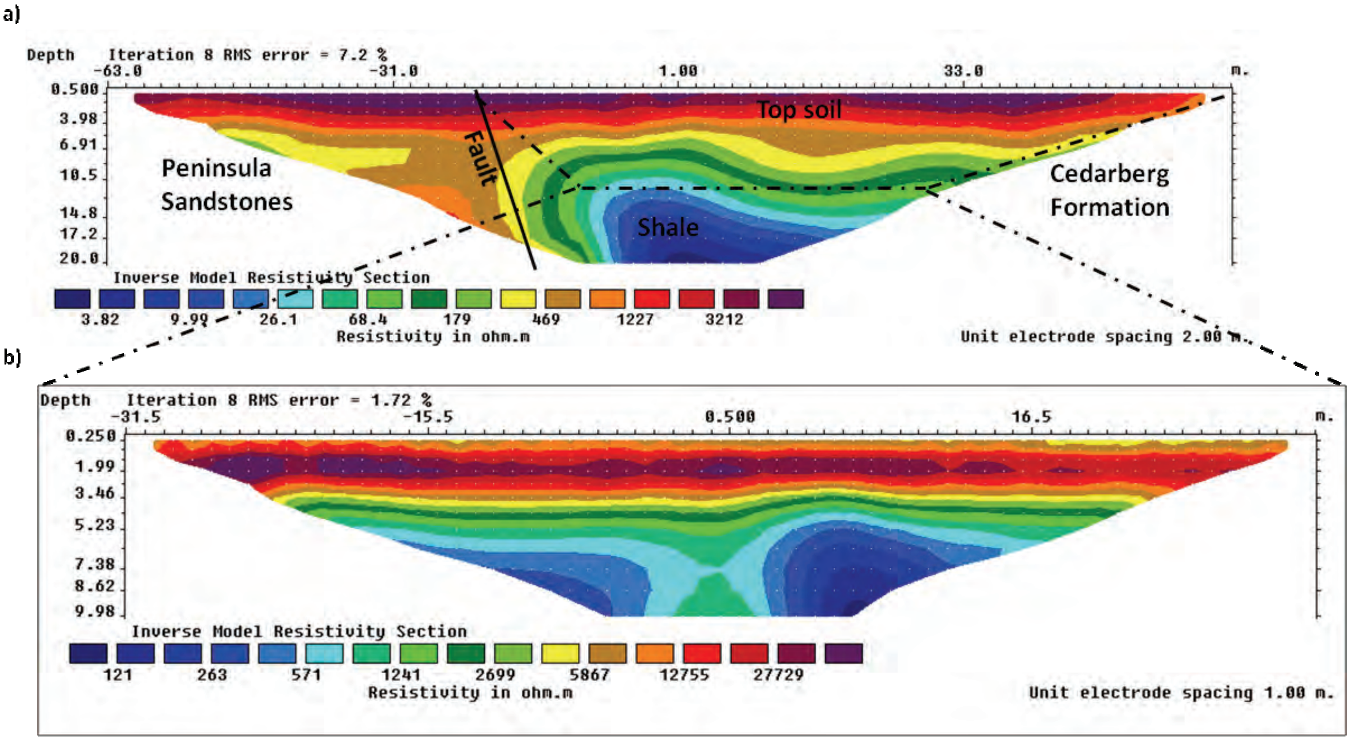

Figure 28

Geological characterisation of the resistivity transect with a 2 m electrode spacing (a) and subsurface resistivity profile using a 1 m electrode spacing (b) at Site 2 in the Oudebosch Catchment

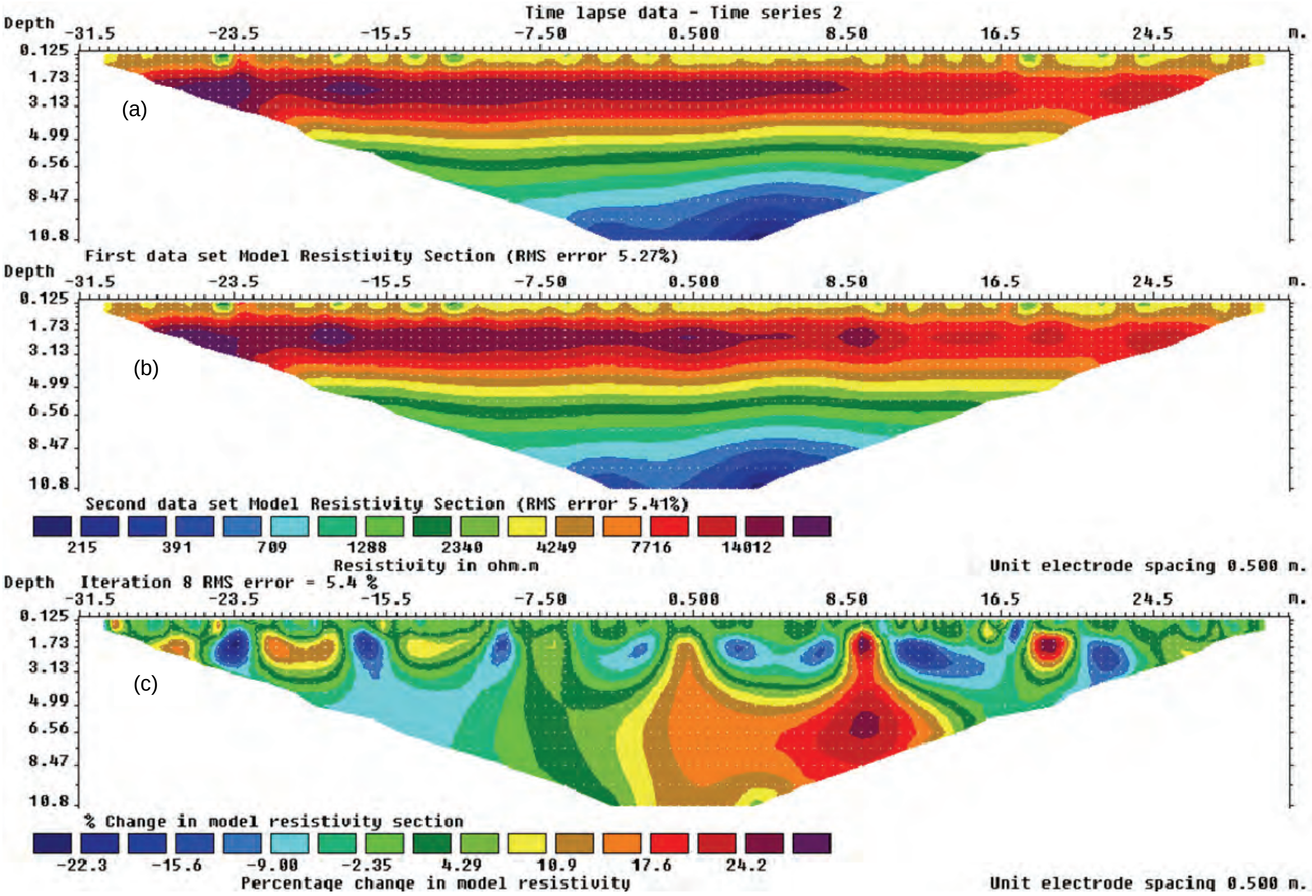

Figure 29

Change in subsurface resistivity over time after a rainfall event (a and b). The difference between these profiles is presented in (c)

6 CASE STUDY 1: COUPLED ATMOSPHERIC-UNSATURATED ZONE MODELLING (RIVERLANDS)

6.1 Introduction

***The purpose of modelling at Riverlands was to quantify evapotranspiration and recharge of an unconfined alluvial aquifer**.* Jovanovic *et al*. (2009a and b) developed a coupled atmospheric-unsaturated-saturated flow model for this site using HYDRUS-2D for the unsaturated zone and MODFLOW for the saturated zone. In this project, scintillometer measurements carried out in October 2010 represented the first estimates of evapotranspiration from Atlantis Sand Plain Fynbos. Evapotranspiration and weather measurements were used to estimate grass reference and potential evapotranspiration of the vegetation (Allen *et al*., 1998). Potential evapotranspiration was then used as input into HYDRUS-2D to calculate the soil water balance and recharge to the shallow groundwater table.

6.2 Coupled models

The first step in the coupling of models was to apply an atmospheric model to calculate potential evapotranspiration (PET) of Atlantis Sand Plain Fynbos. For this purpose, grass reference evapotranspiration (ETo) was first calculated from weather data with the Penman-Monteith formula and used to determine PET with the following equation:

$$PET = Kc_{max}\ ETo$$

Where Kc_{max} is a coefficient dependent on vegetation (i.e. height, morphology) and environmental conditions (i.e. weather variables), and PET represents the evapotranspiration immediately after a rainfall event (Allen *et al*., 1998). Daily PET was then used as input in HYDRUS-2D. Caution should be exercised in the use of this approach for natural vegetation that is usually heterogeneous.

HYDRUS-2D is computer software that can be used to simulate two-dimensional water flow, heat transport and movement of solutes in unsaturated, partially saturated and fully saturated porous media (Simunek *et al*., 1999). It uses Richards' equation for variably-saturated water flow and the convection-dispersion equations for heat and solute transport, which is based on Fick's Law. The water flow equation accounts for water uptake by plant roots through a sink term. The heat transport equation considers transport due to conduction and convection with flowing water, whilst the solute transport equation considers convectivedispersive transport in the liquid phase, as well as diffusion in gaseous phase. The solute flux equations account for non-linear, non-equilibrium reactions between the solid and liquid phases, linear equilibrium reactions between the liquid and gaseous phases, zero-order production and two first-order degradation reactions, the one independent of other solutes, the other providing sequential first-order decay reactions. A dual-porosity system can be set up for partitioning of the liquid phase into mobile and immobile regions and for physical non-equilibrium solute transport. A database of soil hydraulic properties is included in the model.

The HYDRUS-2D model does not account for the effect of air phase on water flow. Numerical instabilities may develop for convection-dominated transport problems when no stabilizing options are used, and the programme may crash when extremely non-linear flow and transport conditions occur.

The HYDRUS-2D model allows the user to set up the geometry of the system. The water flow region can be of more or less irregular shape and having non-uniform soil with a prescribed degree of anisotropy. Water flow and solute transport can occur in the vertical plane, horizontal plane or radially on both sides of a vertical axis of symmetry. The boundaries of the system can be set at constant or variable heads or fluxes, driven by atmospheric conditions, free drainage, deep drainage (governed by a prescribed water table depth) and seepage. The HYDRUS-2D version includes a CAD programme for drawing up general geometries and the MESHGEN-2D mesh generator that automatically generates a finite element unstructured mesh fitting the designed geometry.

The HYDRUS-2D software runs in Microsoft Windows 95, 98, and NT with an interactive graphics-based user interface (GUI) to facilitate data input and interpretation of model results. The code is written in FORTRAN, whilst the interface is in C++. The package requires a MS-DOS compatible system running Microsoft Windows 95 (or later), 16 Mb of RAM memory, VGA (SVGA is recommended), and at least 10 Mb of available disk space. Extensive on-line context-sensitive Help is available through the interface.

The HYDRUS-2D was used to calculate the soil water balance, in particular soil water fluxes towards the groundwater table (i.e. groundwater recharge) and from the shallow groundwater table upwards (i.e. capillary rise).

6.3 Input data

In a previous study on the soil water balance at Riverlands (Jovanovic *et al*., 2009a), simulations with HYDRUS-2D were run for the 2007 season. In this project, monitoring continued and a series of data was generated for 5 years. Simulations with HYDRUS-2D were therefore run on a daily time step from 1 May 2007 to 19 September 2011 (1602 days).

Input data used in the simulations are summarized in Table 12. The main processes simulated were water flow and root water uptake. A vertical plane in rectangular geometry was simulated with a homogeneous profile. The initial condition in water pressure head was established by setting pressure head = 0 at the bottom nodes with equilibrium from the bottom nodes upwards. The hydraulic properties model was van Genuchten-Mualem with no hysteresis. The hydraulic parameters (water flow parameters) were obtained from textural analyses, soil water retention properties and average bulk density (1.53 g cm^{-3}) (Jovanovic *et al*., 2009a).

The vertical rectangular dimension of the simulated geometry was 1.5 m, which corresponded approximately to the depth of water table at the beginning of the simulation. The boundary conditions were:

i) Atmospheric top boundary flux (rainfall, potential transpiration and potential evaporation). Potential transpiration and potential evaporation were calculated by splitting PET using average canopy cover (39%).
ii) Constant head = 0 at the bottom nodes to simulate a shallow groundwater table.
iii) No flux at all other boundaries.

Root distribution was set down to the water table, as such root densities in the soil profile were measured by Jovanovic *et al*. (2009a). The HYDRUS-2D model calculates actual evapotranspiration from PET and applies the method of Feddes to predict reduced transpiration due to water stress. The Feddes' water uptake reduction model incorporated in HYDRUS-2D was used with no solute stress, and parameters from the database of vegetation characteristics were chosen to be the closest possible to fynbos. Actual evaporation from the soil surface was calculated from soil water fluxes at the atmospheric boundary.

Observation nodes were set at 5 and 40 cm soil depth to write records of simulated soil water contents. These were also depths of installation of soil water sensors.

TABLE 12 SUMMARY OF INPUTS USED IN THE SIMULATION WITH HYDRUS-2D	
Parameters and variables	**Inputs**
Main processes	Water flow, root water uptake
Length units	cm
Type of flow	Vertical plane
Geometry	Rectangular
Number of materials and layers in the soil profile	1
Time units	Days
Initial time	0 (1 May 2007)
Final time	1602 (19 September 2011)
Initial time step	0.05 (default)
Minimum time step	1e-006 (default)
Maximum time step	0.5 (default)
Number of time-variable boundary records	1602
Maximum number of iterations	20 (default)
Water content tolerance	0.0005 (default)
Pressure head tolerance	0.05 (default)
Lower optimal iteration range	3 (default)
Upper optimal iteration range	7 (default)
Lower time step multiplication factor	1.3 (default)
Upper time step multiplication factor	0.3 (default)
Lower limit of the tension interval	1e-006 (default)
Upper limit of the tension interval	10000 (default)
Initial condition	In the pressure head
Hydraulic model	Van Genuchten-Mualem
Hysteresis	No
Residual water content (Qr)	0.02
Saturation water content (Qs)	0.35
α of the soil water retention function	0.036
n of the soil water retention function	1.56
Saturated hydraulic conductivity (cm d^{-1})	47.85
l of the soil water retention function	0.5
Water uptake reduction model	Feddes, default parameters for grass
Potential evaporation and transpiration	Daily values calculated from weather data and vegetation characteristics (Allen *et al.*, 1998)
Horizontal rectangular dimension (cm)	1
Vertical rectangular dimension (cm)	150
Slope of the base	0
Number of vertical columns	2
Number of horizontal columns	150
Mesh	Generated with MeshGen
Root distribution	Down to 1.5 m (bottom of geometry) with linear distribution with depth
Atmospheric boundary condition	Top nodes
Constant boundary condition	Pressure head = 0 at bottom nodes
Initial pressure head	Pressure head = 0 at bottom nodes with equilibrium from the bottom nodes
Depth of observation nodes (cm)	5 and 40 cm

6.4 Groundwater recharge simulations with HYDRUS-2D

The results of the simulation with HYDRUS-2D for fynbos vegetation are presented and discussed in this section. Figure 30 shows the daily rainfall data recorded at Riverlands with a manual rain gauge and the cumulative rainfall flux produced by HYDRUS-2D at the atmospheric boundary (input). Total rainfall for the period of simulation from 1 May 2007 to 19 September 2011 was 2778 mm. The flux units on the Y-axis of the HYDRUS-2D graph represent cm of rainfall. The flux is negative because the water is entering the system.

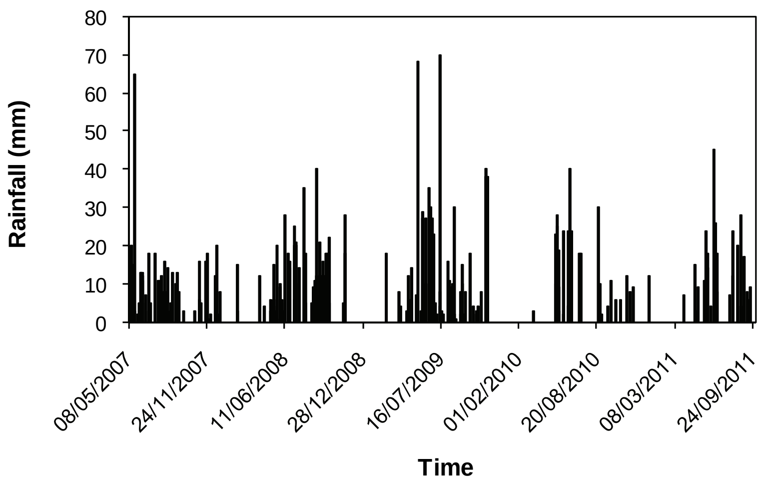

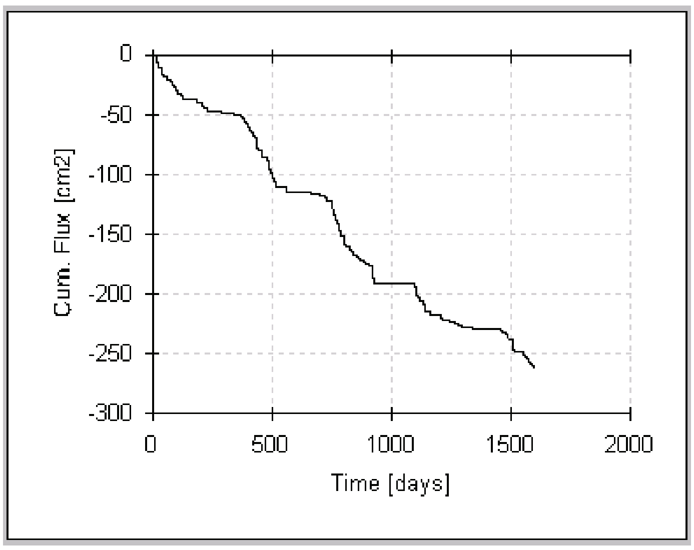

Figure 30

Daily rainfall data recorded at Riverlands with a manual rain gauge (top graph) and cumulative rainfall flux produced by HYDRUS-2D at the atmospheric boundary (bottom graph, screen printout)

Figure 31 represents measured and simulated volumetric soil water contents at 5 and 40 cm soil depth. Although no statistical analyses were performed between measurements and simulations, it can be visually observed that the trends and ranges of values obtained with HYDRUS-2D replicated measurements very well.

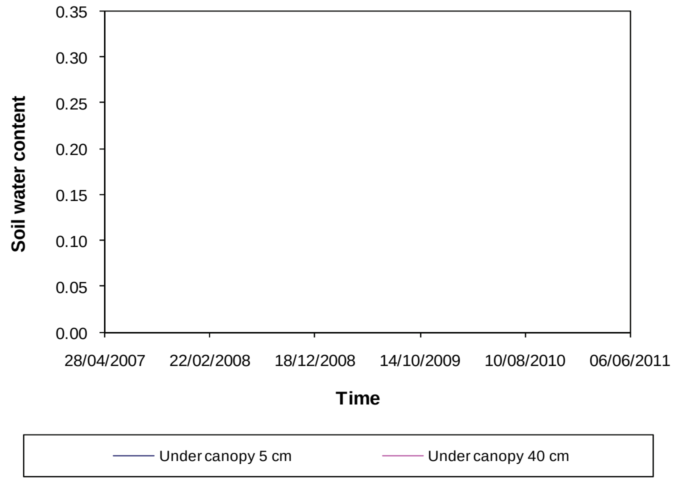

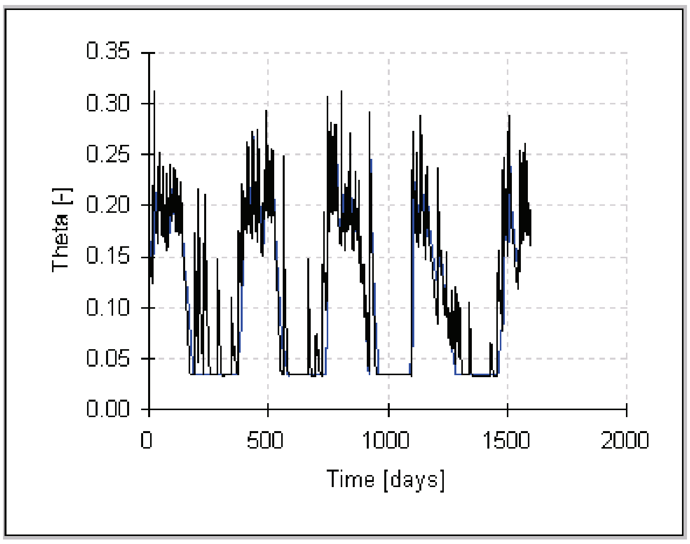

Figure 31

Hourly measurements of volumetric soil water content with Echo sensors (Decagon Inc., USA) (top graph) and volumetric soil water contents (Theta) simulated with HYDRUS-2D (bottom graph, screen printout) at 5 and 40 cm soil depth in fynbos at Riverlands

The HYDRUS-2D model calculates daily actual evapotranspiration from PET values by applying the method of Feddes to predict reduced evapotranspiration due to water stress. The model set-up allowed for root water uptake from the shallow water table by setting a constant pressure of 0 (groundwater table) at the bottom of the soil profile (1.5 m depth). Figure 32 represents HYDRUS-2D output graphs of cumulative potential root water uptake (input) and actual root water uptake calculated with Feddes' model. The fluxes are positive because water is leaving the system. The units on the Y-axes correspond to cm of root water uptake. Cumulative potential root water uptake for the simulation period was 6118 mm and actual root water uptake was 4183 mm (68%). In the two-weeks of scintillometer measurements done in October 2010 (Deliverable 13 of this project), the ratio of actual to grass reference evapotranspiration was found to be 69%.

Figure 33 represents the cumulative fluxes at the bottom boundary (groundwater table). Positive fluxes represent water leaving the system (groundwater recharge) and negative fluxes represent water entering the system (capillary rise from shallow groundwater). The units of the Y-axis correspond to cm. It can be noted that the cumulative flux increased on five occasions (five rainy seasons) and it decreased four times (four summers). The increases in flux corresponded to annual recharge that occurred during five rainy seasons. Net recharge was largely negative (1566 mm) because capillary rise from shallow groundwater was much larger than downward water fluxes. Lateral groundwater sources and sinks were not considered in the one-dimensional simulation.

Table 13 represents rainfall, recharge in mm (increases in cumulative flux in Figure 33) and expressed as % of rainfall (R^2 = 0.76 between annual recharge and rainfall). Comparatively, groundwater recharge in quaternary catchment G21D was estimated to be 81 mm a^{-1} by Vegter (1995). Bredenkamp and Vandoolaeghe (1982) estimated groundwater recharge to be 25% of annual rainfall using a mass balance approach at Atlantis (20 km South of Riverlands). Other estimates of groundwater recharge for catchment G21D included 15.4% of mean annual rainfall using a Cl mass balance approach (DWAF, 2006), 5% using a GIS-based groundwater recharge algorithm (DWAF, 2006) and 13% in the vicinity of Riverlands (Woodford, 2007).

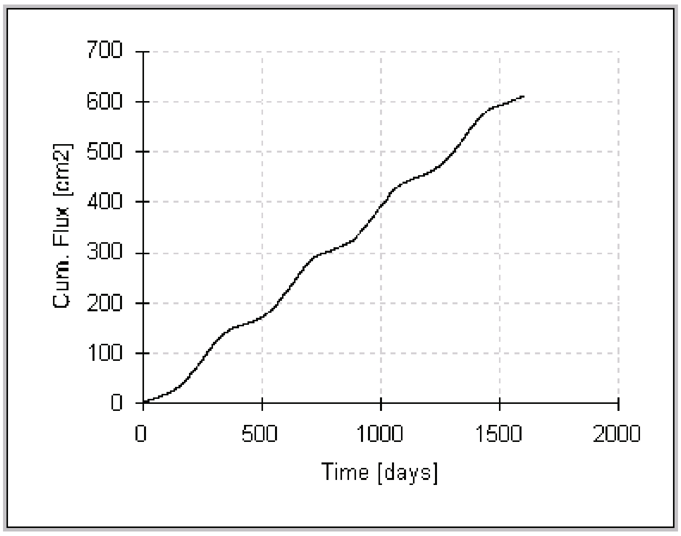

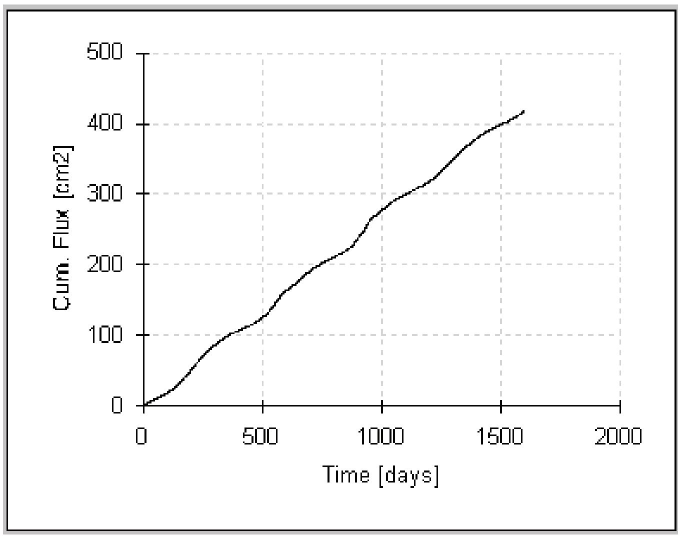

Figure 32

HYDRUS-2D simulations of cumulative potential root water uptake (top graph, input data) and actual root water uptake calculated with the Feddes' model (bottom graph) for fynbos at Riverlands

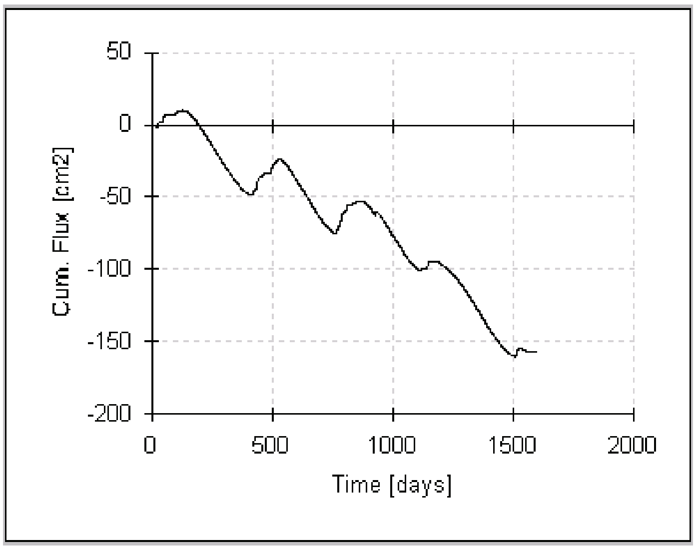

Figure 33

Cumulative bottom boundary flux simulated with HYDRUS-2D for fynbos vegetation at Riverlands

TABLE 13
ANNUAL RAINFALL AND GROUNDWATER RECHARGE AT RIVERLANDS

Year	Rainfall (mm)	Groundwater recharge (mm)	Groundwater recharge (% of rainfall)
2007	509	98	19
2008	718	253	35
2009	804	227	28
2010	390	65	17
2011	357	55	15
Total	2778	698	25

6.5 Conclusions

The following conclusions and recommendations can be drawn from the modelling at Riverlands with HYDRUS-2D:

- Continuous long term records (five years) of weather, soil water content, vegetation and groundwater were used to simulate the one-dimensional (vertical) soil water balance of fynbos at Riverlands.
- Measured and simulated volumetric soil water contents compared very well in terms of seasonal trends and ranges, as indication of model performance.

- The ratio of simulated actual to potential root water uptake was similar to the ratio of actual and grass reference evapotranspiration (ET/ETo) using scintillometer measurements.
- Simulated average groundwater recharge, as a % of rainfall, was 25% for the five years, ranging from 15 to 35%. Capillary rise from shallow groundwater was far higher than recharge during the rainy season.
- The uncertainty of these estimates of groundwater recharge depends on the accuracy of measured input data into the model (e.g. scintillometer measurements, weather instrumentation, etc.). The main uncertainties, however, are represented by spatial and temporal variability of inputs.

  For example, the average 25% of recharge is a figure that should be treated with caution because large variations in annual rainfall may result in large variations of recharge (15 to 35% in the five-year time series). It is therefore imperative to account for the seasonality and temporal distribution of rainfall and the other water balance components.

  Groundwater level fluctuations may result in changes of the capillary fringe and effects on the water balance in the unsaturated zone.

  Vegetation is spatially variable in terms of canopy cover, structure and speciation. This may have effects on the relation between ETo and PET, root depth and root water uptake and, ultimately, on the water balance.
- The study highlighted the following:

  The importance of monitoring all components of the water balance, in particular in the long term (it is an exceptional case that such a long time series of monitored data has been produced).

  The need to adopt daily time steps to describe temporal variabilities of the water balance (e.g. rainfall).

  The need to provide an accurate description of the spatial variability of environmental variables (e.g. variability in vegetation).

7 CASE STUDY 2: GROUNDWATER FLOW MODELLING (OUDEBOSCH)

7.1 Introduction

The purpose of modelling at Oudebosch was to quantify groundwater flow and to determine the effects of evapotranspiration and preferential flow on groundwater recharge using field data as inputs, and by calibration against observed groundwater levels. Given the objectives of modelling and the seasonal nature of the Oudebosch stream, MODFLOW was used to model the groundwater system.

7.2 Groundwater flow conceptualization

Groundwater flow was first investigated at a conceptual level using TopoDrive (Hsieh, 2001). TopoDrive is a two-dimensional model designed to simulate topography-driven groundwater flow. A topography-driven flow system is one in which groundwater flows from higher elevation recharge areas, where hydraulic head is higher, to lower elevation discharge areas, where hydraulic head is lower. This type of flow system is commonly encountered under natural conditions. The main factors that control groundwater flow are basin geometry, hydraulic head distribution and hydraulic properties (Domenico and Schwartz, 1990). TopoDrive enables users to investigate how these factors control groundwater flow. The user specifies the top boundary of the vertical flow section, as well as the hydraulic properties of the medium. The model computes hydraulic heads and groundwater flow paths under steady-state flow conditions. An interactive visual interface enables the user to easily and quickly explore model behaviour, and thereby better understand groundwater flow processes. TopoDrive is not intended to be a comprehensive modelling tool, but it is designed for modelling at the exploratory or conceptual level, for visual demonstration and for educational purposes. The model runs within a Java-enabled web browser on different computer operating systems (e.g. Microsoft Windows).

In this study, TopoDrive was used to conceptualize groundwater flow along a typical hillslope in the Oudebosch catchment. The model was used to draw hydraulic head contours and compute groundwater flow paths along this hillslope (Figure 34). The following input data were used:

- The length of the slope was 180 m with a water table fall of 35 m (this resembles the dimensions of the hillslope in the vicinity of boreholes TMG540/K1, TMG541, TMG544, and Site 2 for soil moisture and resistivity measurements, Figure 5).
- The mesh grid was generated with 40 columns x 40 rows.

- The hydraulic properties were:

  Hydraulic conductivity :

  - Case 1: 4.55 m d^{-1} or 0.0000527 m s^{-1} as an upper limit measured in the soil infiltration study (Box 2).
  - Case 2: 0.05 m d^{-1} or 0.00000057 m s^{-1} as a lower limit for the Skurweberg and Peninsula Formations (Seyler *et al*., 2011).

  Porosity:

  - Case 1: 44.3% as an upper limit determined in the soil study (Box 2).
  - Case 2: 2.5% as a lower limit for fractured sandstone (Xu *et al*., 2009).

As demonstrated in Figure 34, the travel time of groundwater from the highest to the lowest elevation along the hillslope ranged between 7.8 d (hydraulic conductivity = 4.55 m d^{-1} and porosity = 2.5%) and 13,200 d (hydraulic conductivity = 0.05 m d^{-1} and porosity 44.3%). It should be borne in mind that the low values of hydraulic conductivity and porosity refer to sandstone as porous matrix. These figures were valuable in order to get a feel of the orders of magnitude of hydraulic properties and groundwater flows to be simulated with the numerical groundwater flow model.

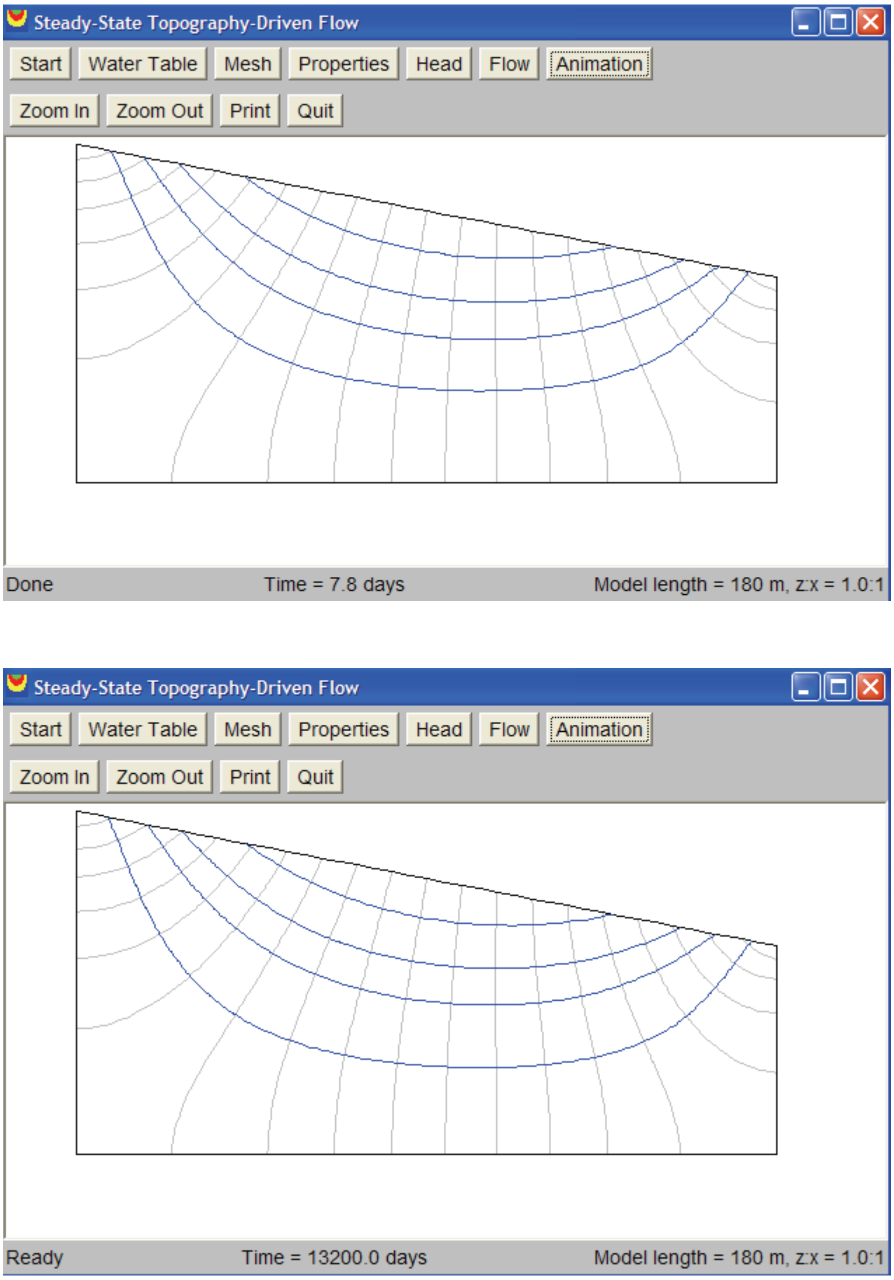

Figure 34

Output printouts of TopoDrive with graphical representation of hydraulic head contours (grey), flow lines (blue) and time of topographically driven groundwater flow (high elevation is to the left of the figure)

Box 2: Calculation of saturated hydraulic conductivity and porosity based on field measurements

Hydraulic conductivities and porosities were calculated based on measurements and estimations reported in Table 11 (soil infiltration study). On a shallow rocky Cartref 1200 soil typical of sandstone slopes (Soil Classification Working Group, 1991), constant head hydraulic conductivity was 492.3 mm h^{-1} or 11.8 m d^{-1} and flow routing was 38% of the sediment volume. The remaining 62% of the sediment volume was assumed to have a hydraulic conductivity of 0.05 m d^{-1} representing the lower limit for the Skurweberg and Peninsula Formations (Seyler *et al*., 2011). Total saturated hydraulic conductivity was then calculated by weighting the contributions to flow from preferential paths and matrix:

K_{sat} = (11.9*0.38+0.05*0.62) = 4.55 m d^{-1}

Water is funnelled between coarse fragments through preferential flow paths having a porosity of 35.7% (Table 11). The lower limit of porosity for fractured sandstone was found to be 2.5% (Xu *et al*., 2009). The total porosity for weathered material and coarse fragments was then calculated by weighting:

Porosity = (35.7*0.38+2.5*0.62) = 15.1%

A K_{sat} of 4.55 m d^{-1} and a porosity of 15.1% were therefore used as inputs for the slopes of the Oudebosch catchment.

Saturated hydraulic conductivity and porosity were calculated in a similar manner for the deep sandy Fernwood 1110 soil (Soil Classification Working Group, 1991), typical of the alluvial area in the Oudebosch catchment. The constant head hydraulic conductivity was measured to be 117.7 mm h^{-1} or 2.82 m d^{-1} (Table 11) occurring through 82% of the sediment volume. The total saturated hydraulic conductivity was calculated to be 2.31 m d^{-1}. Flow occurred through material with 53.5% porosity (Table 11) and the total combined porosity was 44.3%.

A K_{sat} of 2.31 m d^{-1} and a porosity of 44.3% were therefore used as inputs for the alluvial area of the Oudebosch catchment.

7.3 Numerical groundwater flow model description

Visual MODFLOW is a three-dimensional groundwater flow and contaminant transport model (Waterloo Hydrogeologic Inc., 1999). This integrated package combines MODFLOW and MT3D into a common graphical interface, whilst the CAD environment allows setting-up of complex spatial models and facilitates the visual control of input and output data.

The MODFLOW version included in Visual MODFLOW v. 2.8.2 is the USGS (U.S. Geological Survey) MODFLOW 96 (McDonald and Harbaugh, 1988), compiled for 32 bit applications in Windows 95/98/NT, whilst the contaminant transport numeric engines include several developments of the original MT3D v. 1.1 (DoD MT3D v. 1.5; MT3D 96; RT3D; DoD MT3DMS v. 3.00; MT3D 99) (Zheng and Wang, 1999; Zheng *et al*., 2001). The numeric engines are based on the theory of groundwater flow and mass transport (Freeze and Cherry, 1979; Domenico and Schwartz, 1990; Fetter, 1993; Zheng, 1993), finite-difference methods as well as explicit and implicit numerical methods. Minimum requirements to run Visual MODFLOW are a Pentium-based computer, 64 MB RAM, a CD ROM drive, a hard drive with at least 100 Mb free space and Windows 95/98/NT.

The MODFLOW model is used to simulate groundwater flow within a user-defined domain. It is a fully distributed model that calculates groundwater flow from aquifer characteristics. It solves the three-dimensional groundwater flow equation using finite-difference approximations. The finite-difference procedure requires that the aquifer be divided into cells, where aquifer properties are assumed to be uniform within each cell. MODFLOW is designed to simulate aquifer systems in which saturated flow conditions exist, Darcy's Law applies and the density of groundwater is constant. MT3DMS is a finite-difference model code for groundwater contaminant and solute transport that can simulate advection, dispersion, dual-domain mass transfer and chemical reactions of dissolved constituents in groundwater (Zheng and Wang, 1999; Zheng *et al*., 2001). MT3DMS uses the out-head and cell-by-cell flow data computed by MODFLOW to establish the groundwater flow field.

7.4 Spatial set-up and input data

For the purpose of setting up the catchment model, the following information was needed: geographical information, geological information, borehole construction data, groundwater level, as well as evapotranspiration and recharge. The main sources of information were:

1) Water Research Commission project No. 1327/1/08 on Ecological and Environmental Impacts of Large-Scale Groundwater Development in the Table Mountain Group

(TMG) Aquifer System (Colvin *et al*., 2009) for geographical, geological and borehole log information;

2) Groundwater recharge estimates from previous reports; and
3) Current project.

The groundwater flow model was prepared for the domain in Figure 35. The data were collated in Excel, processed into consistent formats, checked and used to prepare text files for input into the model. Visual MODFLOW version 2.8.2 was used to build the groundwater model on the densest allowable grid that resulted in grid cells of about 8.2 m x 10.4 m. Model domains were (309600; 6197700) and (314800; 6201800) in WGS84 UTM34 South. Following discussions within the research team, it was decided to develop a groundwater model that would include the area delineated in Figure 36. The area of interest was framed by inactivating cells in the grid (inactive cells are olive green in Figure 36).

The model consists of a one-layer system. One raster layer of elevation data (topography) was imported into MODFLOW. Interpolation of raster data using 5 nearest sample points was used. Figure 35 is a MODFLOW printout of the topographical map (coordinate units and contours are in m). The Oudebosch stream is visible in a direction from South-West to North-East, and its confluence into the Palmiet river, flowing in the eastern section of the domain (direction of flow North-South).

The following input data and boundary conditions were used in MODFLOW:

- The initial date (Day 1) of simulation was 30/10/2008, with head measurements at 5 boreholes on that day. An input data text file was therefore prepared for initial heads of these boreholes, and imported into MODFLOW.
- The final day of simulation was 25/08/2011 (Day 1030). Although modelling in daily time steps is encouraged in order to describe the variability of dynamic processes like rainfall and evapotranspiration, the model was run in transient mode in monthly time steps to reduce the simulation time. The stress periods were 36 (number of variable boundary conditions time series, i.e. inputs of evapotranspiration and recharge) with 10 time steps within each stress period. A default time step multiplier of 1.2 was used (ratio of the value of each time step to that of the preceding time step). A time step multiplier > 1 produces smaller time steps at the beginning of a stress period resulting in a better representation of the changes of the transient flow field.
- A K_{sat} of 4.55 m d^{-1} and a porosity of 15.1% was used as inputs for the slopes of the catchment (Box 2). The area is delineated in Figure 36 and it is based on the soil map in Figure 18 (map of hydrologically similar units of terrain and soil).

- A K_{sat} of 2.31 m d^{-1} and a porosity of 44.3% were used as inputs for the alluvial area of the catchment (Box 2). The area is delineated in Figure 36 and it is based on the soil map in Figure 18 (map of hydrologically similar units of terrain and soil).
- Storativity was assumed to be 0.0002 (Parsons, 2002) and specific yield for the fine fractured sandstone rock was given as 0.21 (Saayman *et al*., 2007).
- Observed daily groundwater heads were prepared in text files from logger readings. The Solinst loggers were set to record groundwater levels every half hour. The reading at 24:00 each day was used as daily reading. The data were then imported into MODFLOW. The network of 5 observational boreholes is shown in Figure 35.
- The Oudebosch river and Palmiet river represent well-defined boundaries of the groundwater model. River boundaries were therefore drawn into MODFLOW along the Oudebosch and Palmiet rivers (Figures 35 and 36). The elevation of the Oudebosch river bed was 340.8 mamsl down to 37.4 mamsl (from the boundary of the spatial model domain to the confluence into the Palmiet river), whilst the height of the river was 341.3 mamsl down to 37.9 mamsl (0.5 m higher than the river bed). The elevation of the Palmiet river bed was 20.3 mamsl down to 10.3 mamsl (boundaries of the spatial model domain), whilst the height of the river was 21.3 mamsl down to 11.3 mamsl (1.0 m higher than the river bed). The conductance of the river boundary was assumed to be:

$$C = K_{sat}\ L\ W\ /\ M$$

C – Conductance
K_{sat} – Hydraulic conductivity of the river bed material
L – Length of a reach through a cell
W – Width of the river in a cell
M – Thickness of the river bed

$$C = 0.91\ \text{m d}^{-1}\ \text{(for silt)} \times 10\ \text{m} \times 3\ \text{m} / 0.5\ \text{m} = 54.6\ \text{m}^2\ \text{d}^{-1}$$

for the Oudebosch river, and

$$C = 0.91\ \text{m d}^{-1}\ \text{(for silt)} \times 10\ \text{m} \times 10\ \text{m} / 0.5\ \text{m} = 182\ \text{m}^2\ \text{d}^{-1}$$

for the Palmiet river

The conductance for silt was obtained from Saayman *et al*. (2007).

- The effects of faults as boundary condition were debated, but they were not included in the current model.
- Total rainfall for the simulated period was 2391 mm. No rainfall data were available for the period 17/07/2010-24/08/2010 and 20/07/2011-24/08/2011. In Table 14, each stress period corresponds to approximately 30 d (monthly intervals).
- Reference evapotranspiration was calculated with the Penman-Monteith equation (Allen *et al*., 1998). Total ETo for the study period was 3530 mm. Reference evapotranspiration was multiplied by 0.34 to estimate actual evapotranspiration ET (Table 14), as the ratio ET/ETo was found to be approximately 0.34 on average (see Chapter 4 on scintillometer measurements). It should be borne in mind that this is an average value and the ratio depends on type of vegetation and soil water supply conditions. Extinction depth for evapotranspiration was 0.5 m. The vegetation types were not delineated spatially.
- Calibrated groundwater recharge for the simulated period was 470 mm, or 20% of total rainfall (Table 14).

TABLE 14
RAINFALL, EVAPOTRANSPIRATION AND CALIBRATED GROUNDWATER RECHARGE INPUTS IN THE MODFLOW SIMULATION OF THE OUDEBOSCH CATCHMENT

Stress period	Approximate month and year	Rainfall (mm)	Reference evapotranspiration (mm)	Actual evapotranspiration (mm)	Groundwater recharge (mm)
0-30	November 2008	30	147	50	0
30-60	December 2008	12	168	57	0
60-90	January 2009	25	168	57	0
90-120	February 2009	139	104	35	34
120-150	March 2009	176	106	36	52
150-180	April 2009	137	85	29	39
180-210	May 2009	124	70	24	38
210-240	June 2009	100	73	25	25
240-270	July 2009	131	83	28	37
270-300	August 2009	9	96	33	0
300-330	September 2009	12	108	37	0
330-360	October 2009	11	138	47	0
360-390	November 2009	50	145	49	0
390-420	December 2009	33	138	47	0
420-450	January 2010	148	130	44	30
450-480	February 2010	108	103	35	19
480-510	March 2010	93	102	35	12
510-540	April 2010	40	78	26	0
540-570	May 2010	149	68	23	45
570-600	June 2010	131	58	20	41
600-630	July 2010	93	73	25	18
630-660	August 2010	0	91	31	0
660-690	September 2010	25	95	32	0
690-720	October 2010	55	116	39	0
720-750	November 2010	83	131	45	0
750-780	December 2010	72	144	49	0
780-810	January 2011	31	148	50	0
810-804	February 2011	10	117	40	0
840-870	March 2011	35	119	40	0
870-900	April 2011	17	90	31	0
900-930	May 2011	69	74	25	7
930-960	June 2011	129	56	19	40
960-990	July 2011	113	59	20	32
990-1020	August 2011	0	48	16	0
1020-1030	-	0	16	5	0
Total		**2391**	**3530**	**1206**	**470**

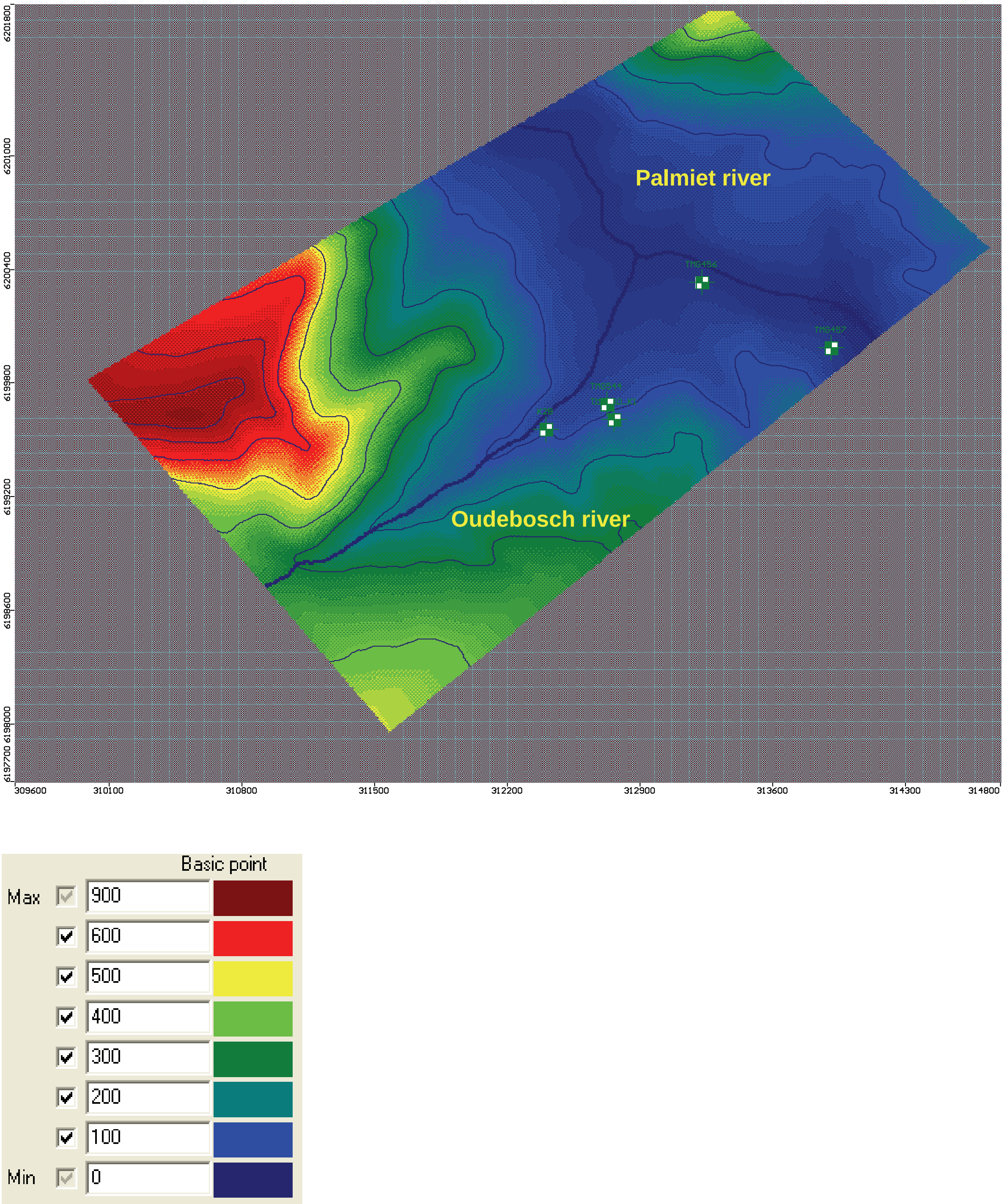

Figure 35

Topographic map of the Oudebosch catchment obtained from interpolated data points, observational boreholes and river boundaries (thick blue lines) in MODFLOW. Coordinate units and contour values in the legend are in m

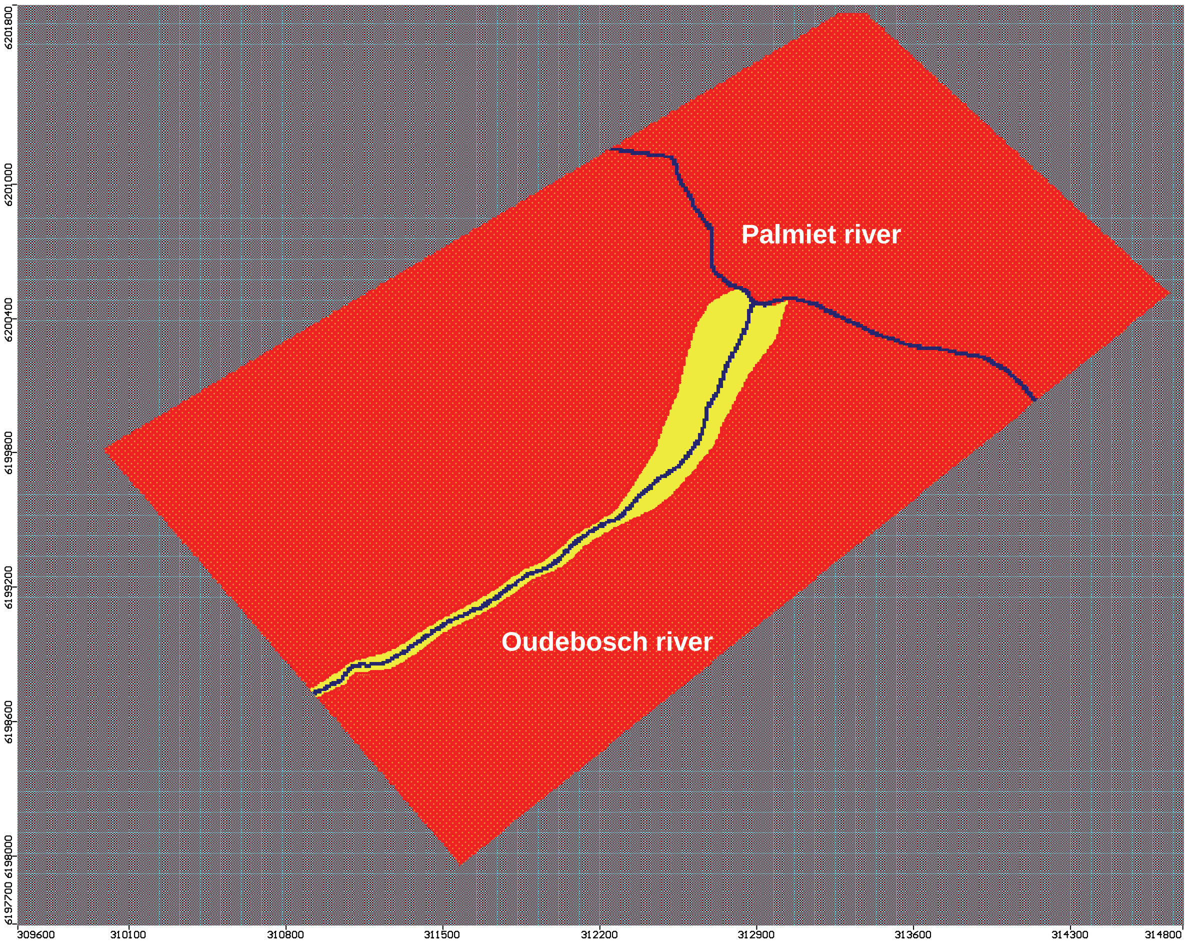

Figure 36

Two areas of delineated hydraulic properties (saturated hydraulic conductivity and porosity) in the Oudebosch catchment based on the soil and terrain map in Figure 18: i) alluvial area along the Oudebosch stream and ii) remaining area on the hillslopes

7.5 Groundwater flow model calibration

In order to simulate groundwater flow with MODFLOW realistically, a thorough calibration is required. In this study, simulated data of groundwater heads were compared to observations for calibration purposes. Input data of groundwater recharge were varied until a satisfactory statistical performance of model simulations was obtained compared to observations.

It is usually extremely difficult to simulate groundwater flow in a complex geological environment, like fractured sandstone, with MODFLOW. It is preferable to calibrate the model for localized areas, where conceptual knowledge of the system and responses exist.

Because of the complexity of the system, the calibration was focused on two boreholes as an example, namely TMG 544 (located on the southern hillslope of the Oudebosch catchment) and TMG457 (located on the western hillslope of the Palmiet river). The output map of equipotential groundwater heads obtained with MODFLOW is shown in Figure 37. Figure 38 shows the velocity vector map, indicating the direction and velocity of groundwater flow in the spatial dimension. Figures 39 and 40 are screen printouts of MODFLOW outputs, which compare simulated and observed groundwater level data. The statistical analyses in Figures 39 and 40 gave an indication of the performance of the model (mean error, mean absolute error, standard error of the estimate, root mean squared error and normalized root mean squared error). The closer the data points to the 1:1 line, the better the prediction and performance of the model. Also, the lower the statistical indicators, the better the prediction and performance of the model. All groundwater heads in this document are expressed as m above mean sea level.

The following considerations were made based on the calibration and the simulation results:

- The model predicted equipotential heads generally well, in terms of contours that sharply decrease towards the lower reaches of the Oudebosch and Palmiet river (Figure 37).
- The velocity vectors showed dominant directions towards the rivers, and velocities tended to increase in the vicinity of rivers where groundwater discharge may occur (Figure 38).
- The output results exhibited very high sensitivity to hydraulic properties, in particular K_{sat} (Deliverable 7 of this project).
- The model predicted groundwater heads localized at two boreholes (TMG544 and TMG457) in a satisfactory manner (Figures 39 and 40), both in terms of absolute values and temporal trends. The mean absolute error was about 1 m over almost three years of simulation for both boreholes. Using daily time steps could have improved the simulations, but at the expense of time.
- Calibrated groundwater recharge for the simulated period was 470 mm, or 20% of total rainfall (Table 14). Comparatively, runoff was previously estimated to vary between 100 and 200 mm a^{-1} (Wu, 2005). Previous estimates of recharge were > 100 mm a^{-1} (Wu, 2005) and > 65 mm a^{-1} (Vegter, 1995), which amounts to 8-12% of annual rainfall.
- ***It should be noted that the calibrated estimate of groundwater recharge was based on two boreholes (TMG544 and TMG457) that displayed distinct fluctuations in groundwater level. Other boreholes did not display fluctuations in groundwater level and, if used for calibration, they would have likely***

resulted in much lower values of calibrated recharge. Estimates of recharge therefore depend on the specific boreholes used in the calibration. A more realistic estimate of recharge would have been obtained by averaging responses of boreholes over the whole study area.

7.6 Conclusions

The following conclusions and recommendations can be drawn from the groundwater flow modelling at Oudebosch:

- An accurate conceptualization of the system is required before starting groundwater flow modelling.
- The fractured rock environment is a very complicated system to simulate.
- Model calibration was successful for localized areas where responses of groundwater levels to rainfall, evapotranspiration and recharge processes were evident, and for a relatively long time span (almost three years).
- Calibration is an on-going process as data become available.
- Hydraulic properties, in particular hydraulic conductivity, need to be accurately estimated to be used in modelling with satisfactory results. This is particularly true in complex systems with dual porosity and preferential flow paths.
- Evapotranspiration measurements (Chapter 4) were invaluable in estimating ET of fynbos and account for it in the calibration of groundwater recharge.

Potential sources of error were identified to be:

- The complexity of the system, including preferential flow paths along fractures and faults.
- The interpolation of raster data in the set-up of the spatial model. The density of raster data may not have been sufficient to describe the topographic details at specific locations.
- Very little geological and borehole construction data were available. Detailed descriptions of the geology, geo-referenced faults and major fractures, as well as other information emanating from a geological survey could be useful to inform and improve the groundwater flow model.
- The basement was assumed to be at mean sea level.
- Some physical properties of the layers used to construct the model referred to literature data obtained in similar environments, as no actual measurements were available for storativity and specific yield.
- Conductance at the river boundary and river bed information was estimated.

- No other boundary conditions were considered, e.g. faults, because their exact location and/or behaviour were not known.
- No vegetation and land use patterns were considered.

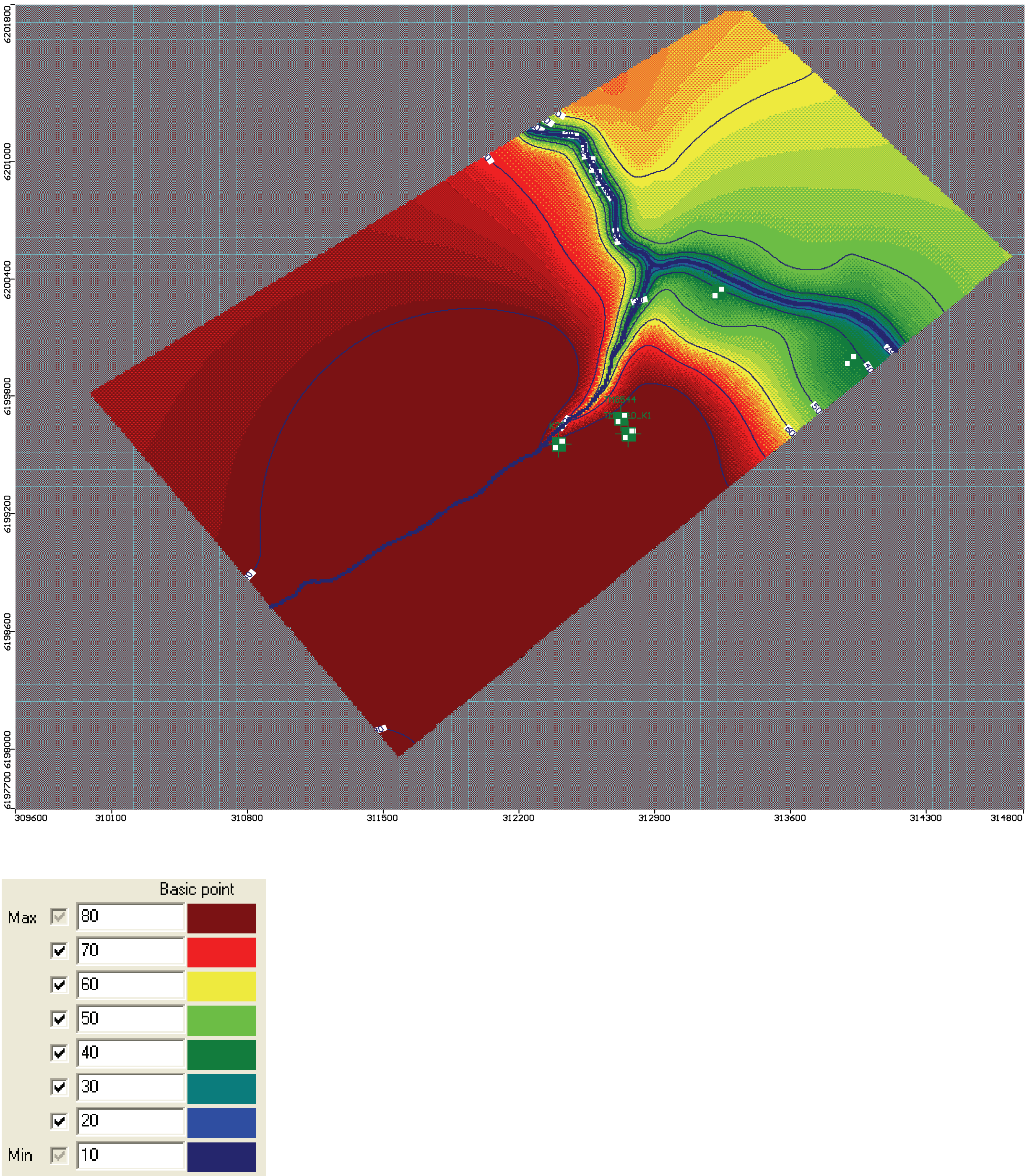

Figure 37

MODFLOW output of groundwater head equipotentials in the Oudebosch catchment obtained from interpolated data points and observational boreholes

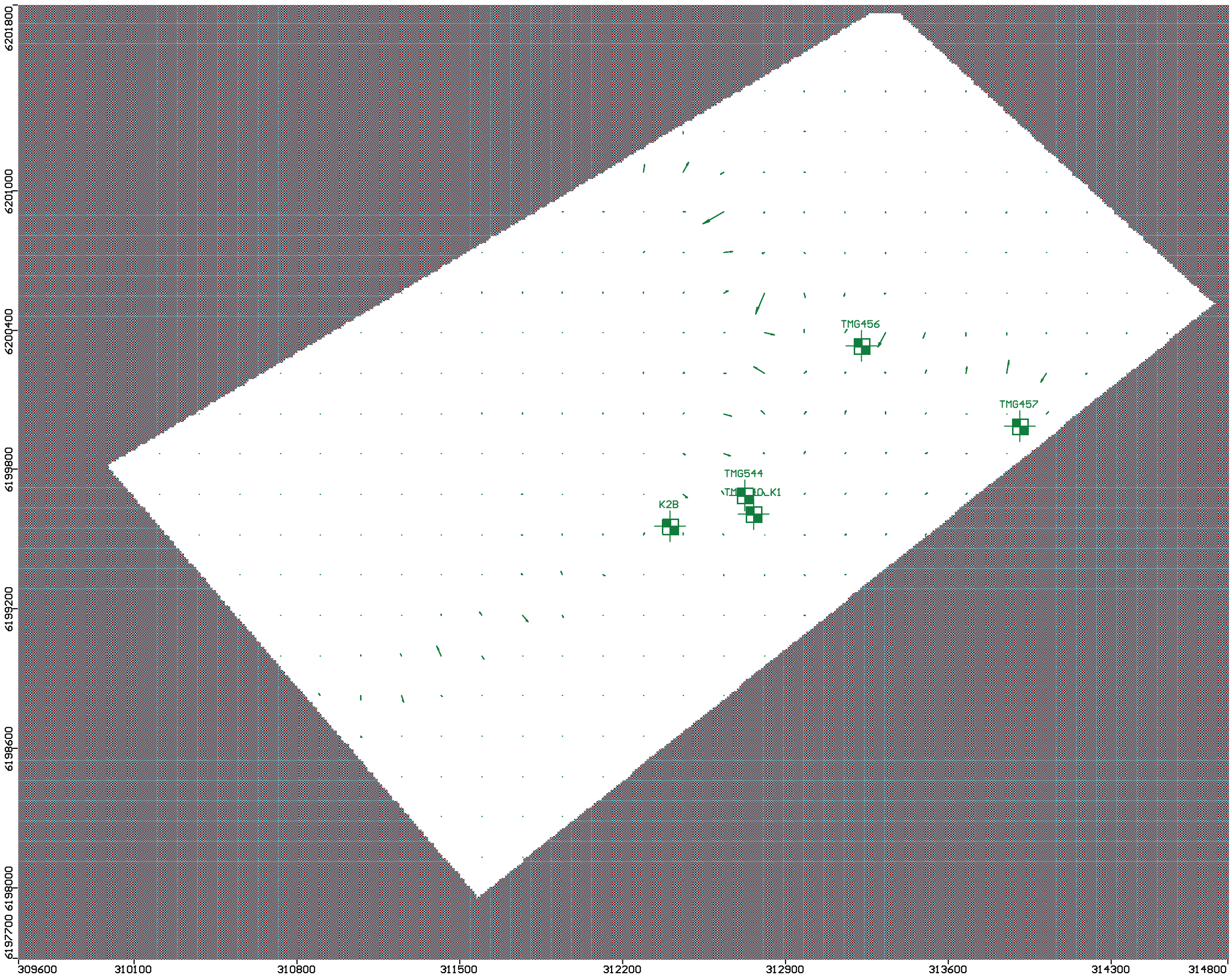

Figure 38

MODFLOW output of velocity vector map of the Oudebosch catchment and observational boreholes

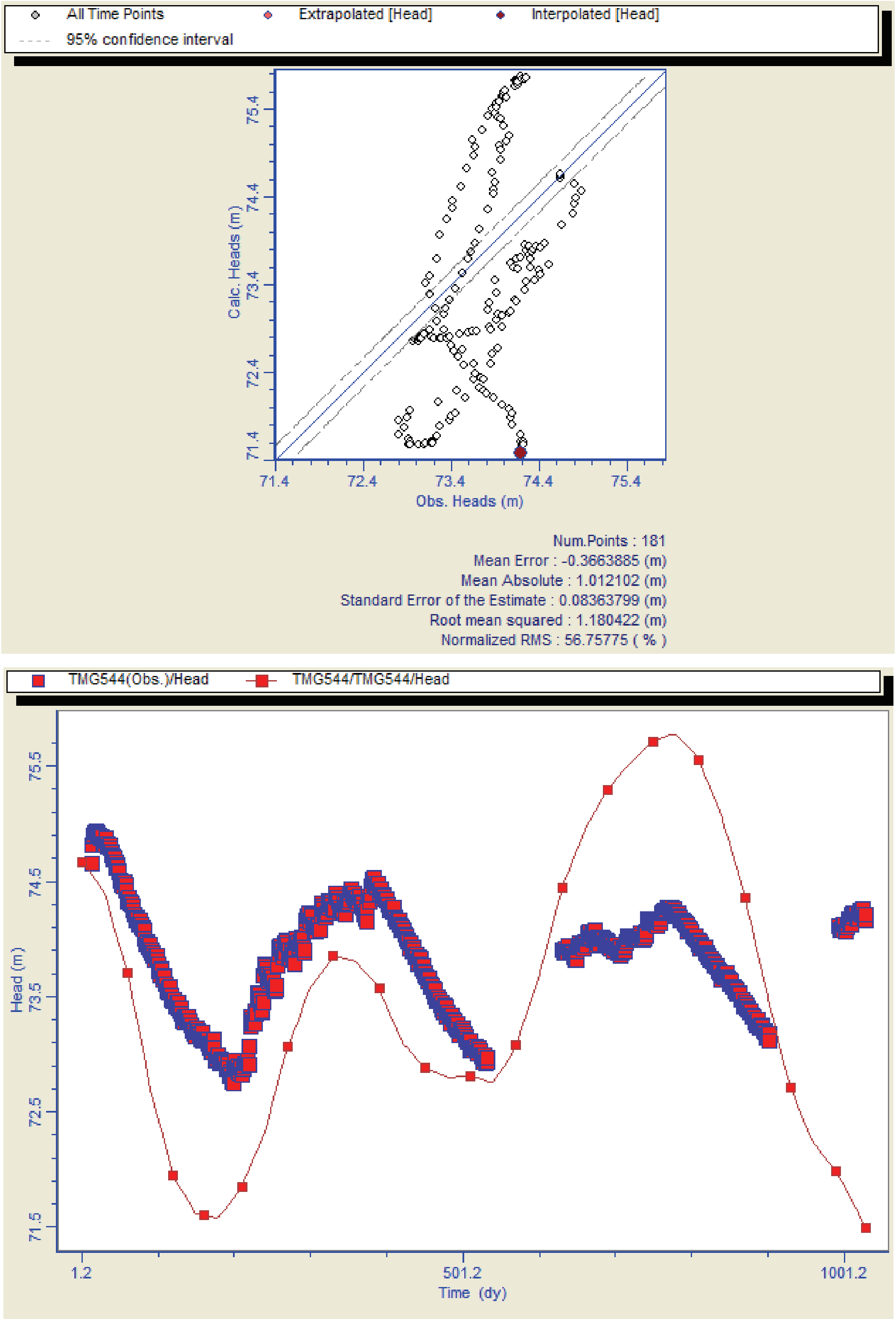

Figure 39

MODFLOW output of calculated vs. observed groundwater heads in the Oudebosch catchment for borehole TMG544 (top: 1:1 scatter plot; bottom: groundwater heads over time)

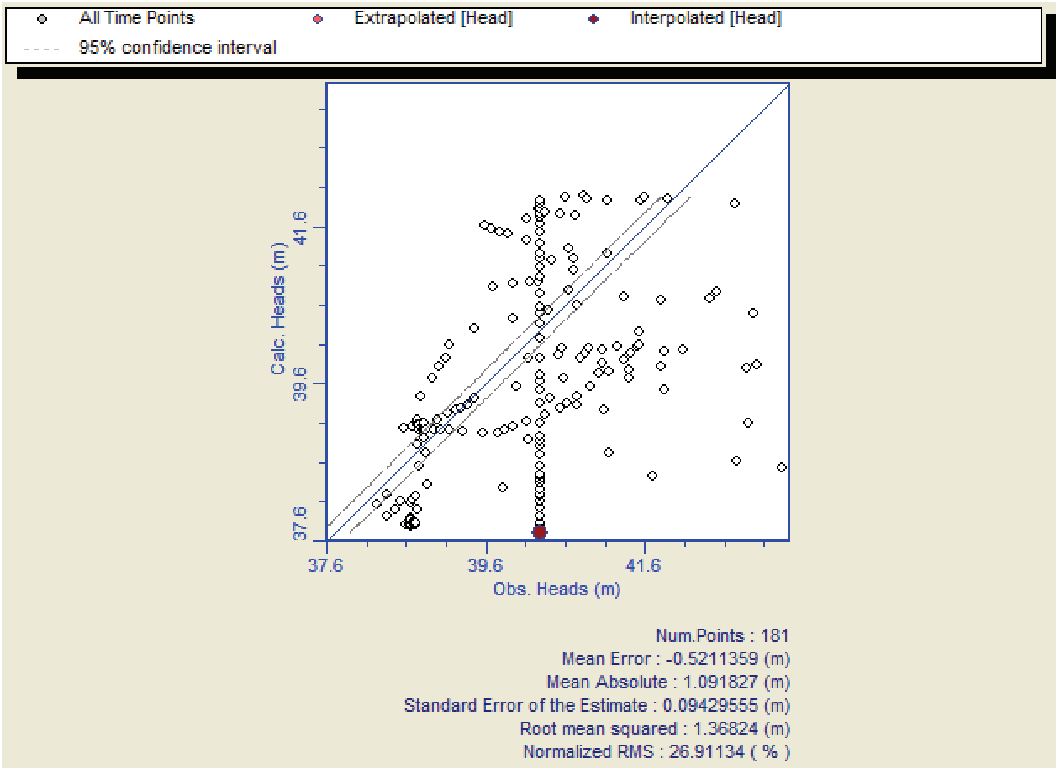

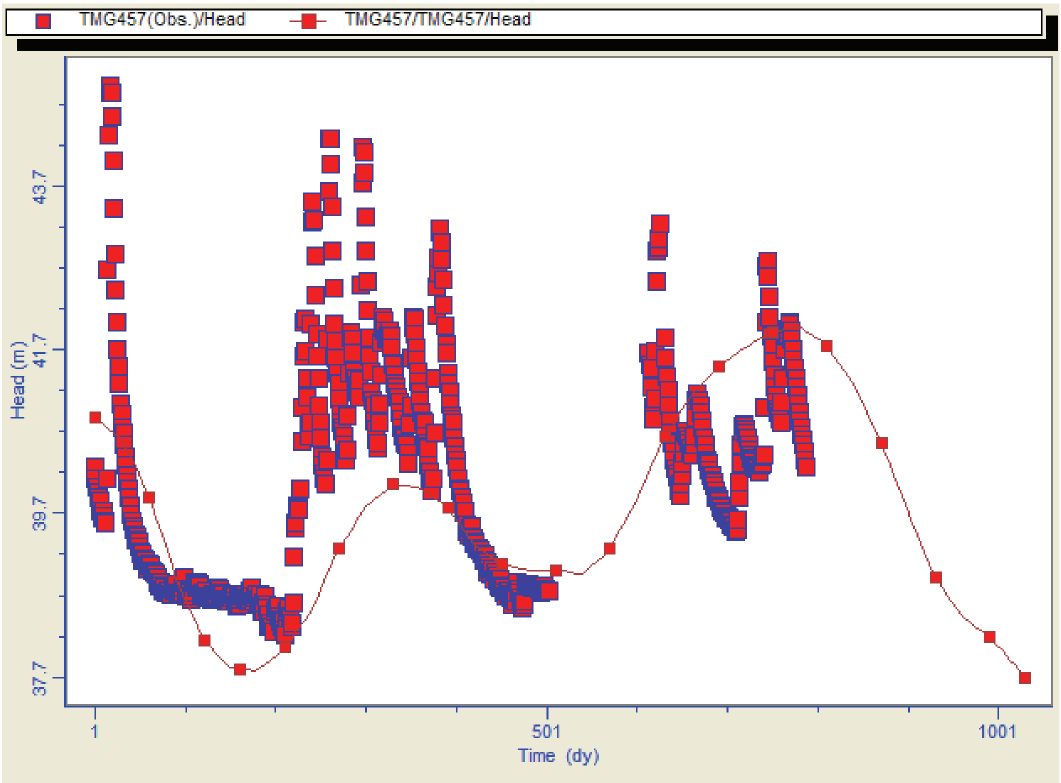

Figure 40

MODFLOW output of calculated vs. observed groundwater heads in the Oudebosch catchment for borehole TMG457 (top: 1:1 scatter plot; bottom: groundwater heads over time)

8 CASE STUDY 3: RAINFALL INFILTRATION BREAKTHROUGH (RIVERLANDS AND OUDEBOSCH)

8.1 Introduction

The coupling of dedicated models (e.g. atmospheric, unsaturated zone, saturated zone) is usually very data-intensive. A simpler method, called Rainfall Infiltration Breakthrough (RIB) was therefore proposed in this study in addition to complex physical process models. The method calculates groundwater recharge based on historic rainfall and fluctuations of groundwater tables. The model is applicable at locations where groundwater levels respond distinctly to rainfall and infiltration. This approach is less data-intensive but it requires long series of groundwater level and rainfall data, as well as a sound knowledge of aquifer characteristics. The RIB software, written in Excel, was applied both at Riverlands and Oudebosch to estimate daily recharge. ***The main purpose of using this model was to obtain quick estimates of groundwater recharge time series with a limited amount of input data.***

8.2 Theoretical overview

The RIB model is an Excel-based software for the estimation of groundwater recharge of aquifers (accommodating for pores, fractures and their combination) where groundwater level fluctuations (ΔS_{gw}) occur resulting from rainfall recharge (Xu and Beekman, 2003; Healy and Scanlon, 2011):

$$R = \Delta S_{gw} = S_y \, \Delta H / \Delta t$$

R – Groundwater recharge (m)
S_y – Specific yield
H – Water table height (m)
t – Time (d)

For estimating recharge, ΔH corresponds to the difference between the peak of the rise and the level of extrapolated antecedent recession curve at time of peak. For estimating change in storage (net recharge), ΔH corresponds to the difference in water levels at any two times. S_y can be estimated as

$$S_y = PD - S_r$$

PD – Porosity

S_r – Specific retention equivalent to field capacity

The RIB method is a box model where the input is rainfall (P), the transfer (convolution) function is a dynamic weighting factor and the output is the rainfall infiltration breakthrough (RIB) (Xu and Beekman, 2003):

$$RIB\,(i)_m^n = \sum_{i=m}^{n} P_i \cdot \left(r - \frac{2rP_i\,(n-m)}{\sum_m^n P_i} + r\,\frac{P_t}{P_{av}} \right)$$

r – Recharge percentage (fraction of cumulative rainfall departure that contributes to rainfall infiltration breakthrough)

P_{av} – Average rainfall over the entire rainfall time series (mm)

P_t – Threshold value representing aquifer boundary conditions, determined during the simulation process (ranging from 0 for a closed aquifer to P_{av} for an open aquifer) (mm)

i – Sequential number of rainfall events

m, n – Start and end of time series (determined using a Solver in Excel)

Calculated RIB is related to groundwater level fluctuations based on catchment area, specific yield and known losses like abstraction and discharge. Rainfall time series are generally a combination of random events and trends (e.g. periodic seasonal events). If rainfall events from P_m to P_n don't show trends, cumulative rainfall averages are equal to P_{av} and the RIB(i) function reduces to cumulative rainfall departure (CRD) (Bredenkamp *et al.*, 1995).

8.3 Software interface

The RIB programme makes use of an Excel platform (Microsoft 2007). The programming language is Visual Basic Application (VBA) and the programme enables to manipulate, analyze and display data. The programme calculates groundwater recharge based on observed groundwater level and rainfall time series, and it can also fill groundwater level data gaps and predict the groundwater level with the available rainfall and abstraction data. An example of screen printout of the RIB user interface is shown in Figure 41.

The time scale needs to be defined before starting data inputs into the programme. This depends on the type of data available (daily, monthly or annual). The time scale can be chosen by clicking the “Start” button.

The definition of symbols used in the RIB programme is summarized in Table 15 along with units and type of data (e.g. input/output, one value/time series, etc.). Input data are time series of rainfall, sink/sources of groundwater, observed groundwater level fluctuations, specific yield (S_y), area of the catchment (A) and parameters for fitting the time lag between rainfall and recharge events. The sink/source terms ($Q_{\_other}$, Q_{out}, $Q_{\_pumpage}$) can be left vacant if data are absent. Groundwater levels and recharge can be calculated by pressing the "Graph" button (Figure 41). The programme generates a chart that is updated automatically. The chart displays rainfall, observed groundwater levels and calculated groundwater recharge with the RIB and CRD methods.

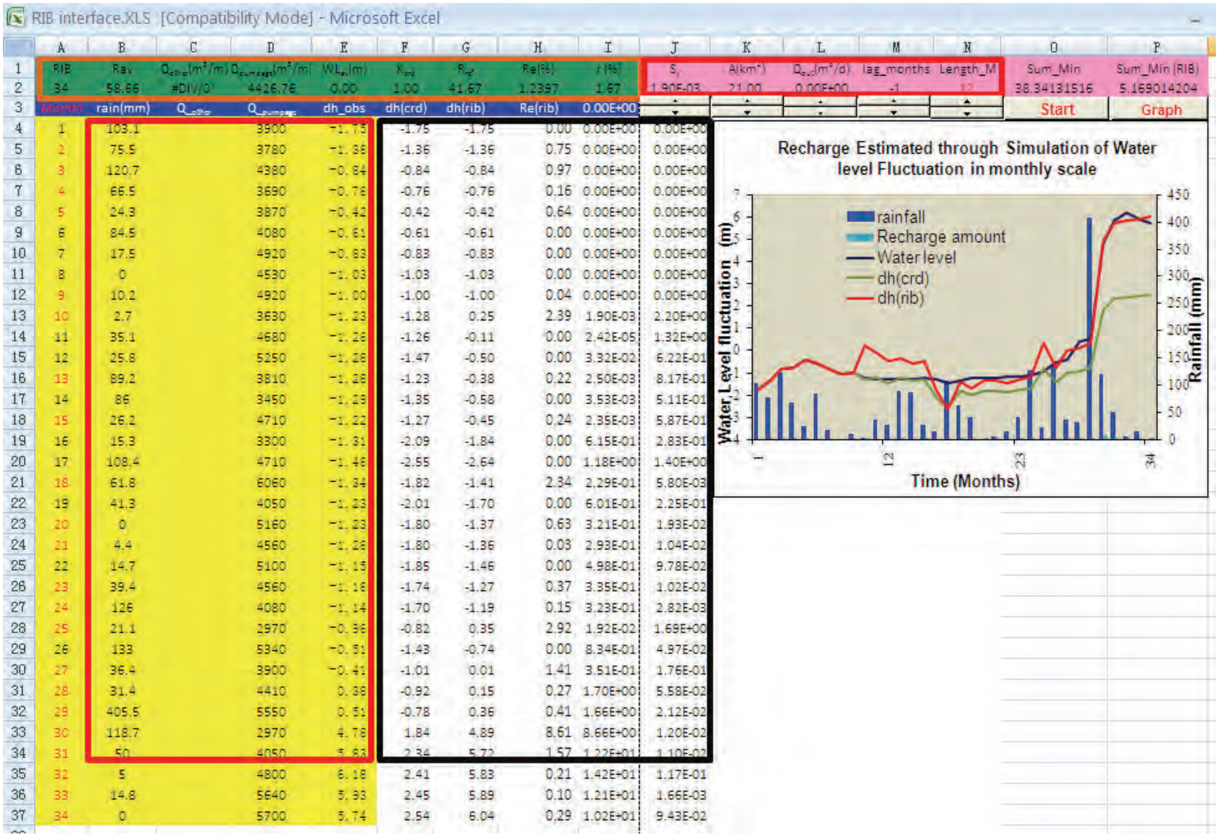

Figure 41

Screen printout of RIB user interface

TABLE 15
INPUT/OUTPUT DATA IN THE RAINFALL INFILTRATION BREAKTHROUGH (RIB) MODEL

Input/output	Symbol	Units	Definition	Type of data
Input	Dayi	-	Day of simulation	Time series (from 1 to n)
	rain	mm	Daily rainfall	Time series
	Q_other	m^3 per time[a]	Source/sink of water other than through abstraction	Time series (positive value means groundwater sink, negative value means groundwater source)
	Q_pumpage	m^3 per time[a]	Abstraction of groundwater	Time series
	dh_obs	m	Observed water level fluctuation (current – WL_{AV})	Time series
	S_y	-	Specific yield	One value
	A	km^2	Surface area of watershed	One value
	Q_{out}	$m^3\ d^{-1}$	Constant volume of groundwater sink (e.g. baseflow)	One value
	lag_Days	time[a]	Time delay between rainfall events and recharge	One value
	Length_D	time[a]	Parameter that characterizes rain sequences and antecedent conditions	One value
Output	R_{AV}	mm per time[a]	Average rainfall	One value
	WL_{AV}	m	Average groundwater level	One value
	K_{crd}	-	Parameter of the CRD[b] method	One value
	R_{ref}	-	Threshold value representing aquifer boundary conditions	One value corresponding to P_t as defined in Section 5.2 (ranging from 0 for a closed aquifer to R_{AV} for an open aquifer system)
	Re	-	Ratio of recharge to rainfall	One value
	r	-	Parameter of the RIB[c] method	One value
	dh(crd)	m	Calculated water level with the CRD[b] method	Time series
	dh(rib)	m	Calculated water level with the RIB[c] method	Time series
	Re(rib)	mm per time[a]	Calculated recharge	Time series

[a] Day, month or year

[b] Cumulative rainfall departure method

[c] Rainfall infiltration breakthrough method

8.4 Examples of application

Daily simulations of groundwater recharge were done with the RIB model for boreholes that displayed distinct seasonal groundwater level fluctuations. These boreholes were RVLD6 and RVLD8 at Riverlands and TMG544 at Oudebosch.

A sensitivity analysis indicated that the model results are particularly sensitive to the input value of S_y. Table 16 summarizes the results of the sensitivity analysis for three boreholes and three values of S_y. The simulations were carried out using time series of available data of rainfall and groundwater levels. The lengths of simulations were 1603 d for RVLD6 and RVLD8 (from 01/05/2007 to 19/09/2011) and 928 d for TMG544 (from 01/01/2008 to 16/07/2010; a gap in rainfall data occurred after this period). No abstraction or other sink/sources were entered in the programme. The simulated surface area was 0.1 km^2 for Riverlands and 3.4 km^2 for the Oudebosch catchment.

The resulting values of groundwater recharge (Table 16) can be interpreted as realistic ranges depending on the hydraulic properties of the aquifer. Figures 42-44 show the output graphs of the sensitivity analysis to S_y. The graphs plot daily rainfall inputs and calculated daily groundwater recharge in mm as bars. Observed groundwater levels as well as groundwater recharge calculated with the cumulative rainfall departure method (dh(crd)) and the RIB method (dh(rib)) are plotted as lines. Daily groundwater recharge decreased with decreasing S_y. Groundwater recharge calculated with CRD and RIB fitted closely the observed values of groundwater level by calibrating lag_Days and Length_D (Table 15). Lag days varied from 0 at Riverlands to 82 at Oudebosch. Length_D was 82 at Riverlands and 84 at Oudebosch. The results from two boreholes at Riverlands were very similar (Figures 42 and 43).

TABLE 16
RESULTS OF GROUNDWATER RECHARGE SENSITIVITY ANALYSIS TO SPECIFIC YIELD WITH THE RIB MODEL

Borehole	Specific yield	Groundwater recharge
RVLD6	0.125	41%
	0.05	16%
	0.025	8%
RVLD8	0.125	37%
	0.05	15%
	0.025	7.5%
TMG544	0.105	26%
	0.042	10%
	0.021	5%

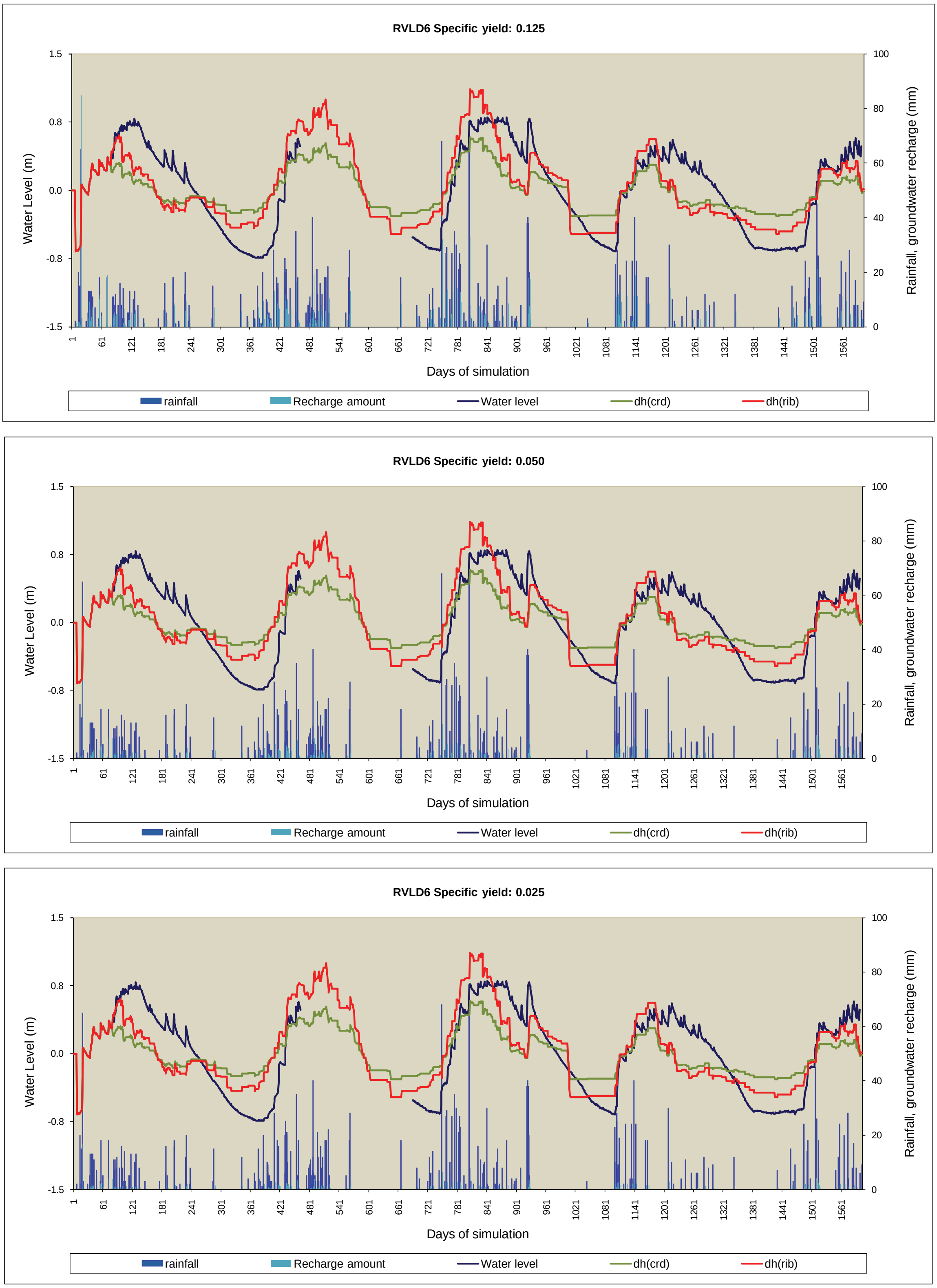

Figure 42

Daily rainfall and groundwater recharge in mm, observed groundwater level as well as groundwater recharge calculated with the cumulative rainfall departure method (dh(crd)) and the RIB method (dh(rib)) for borehole RVLD6 at Riverlands

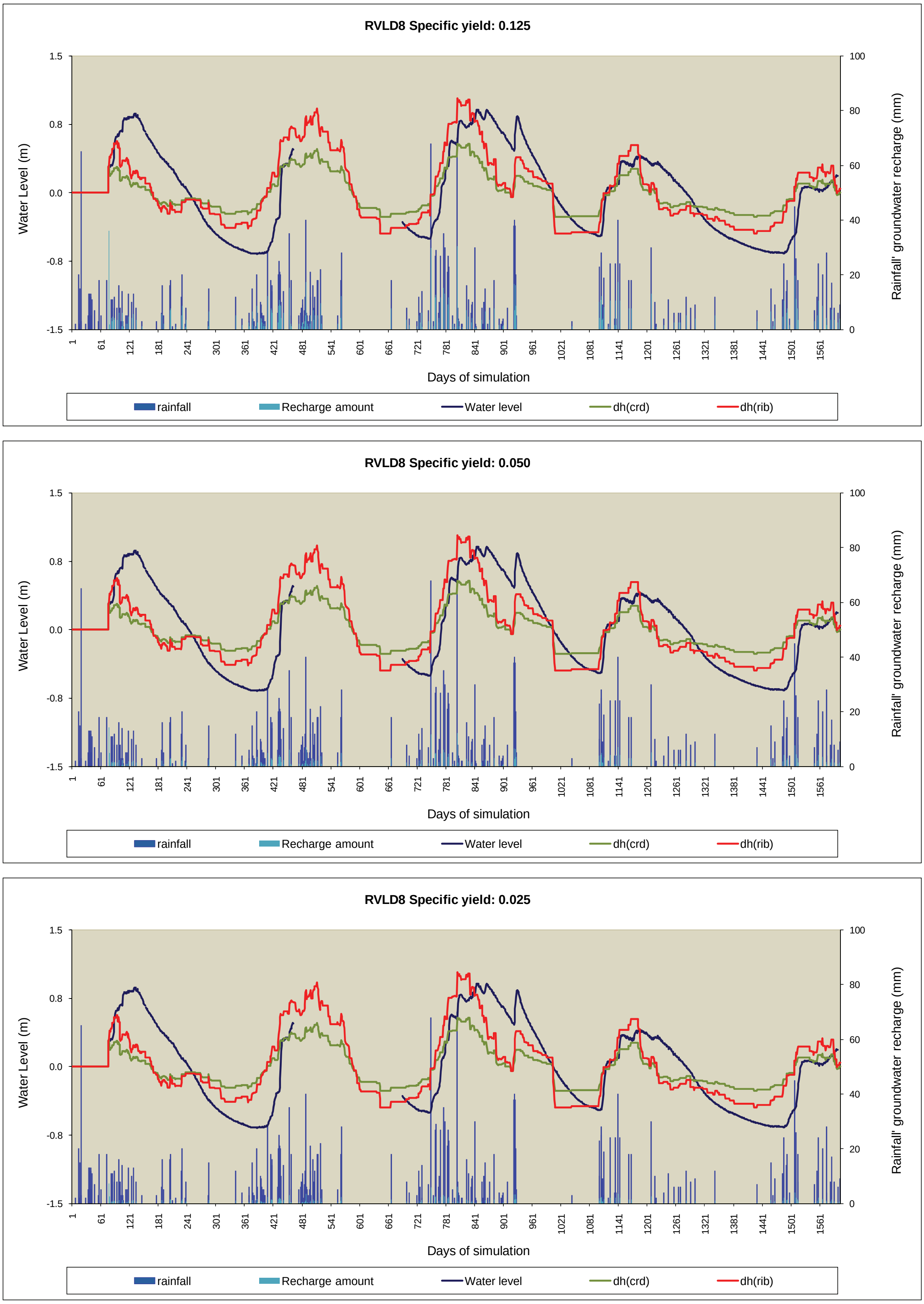

Figure 43

Daily rainfall and groundwater recharge in mm, observed groundwater level as well as groundwater recharge calculated with the cumulative rainfall departure method (dh(crd)) and the RIB method (dh(rib)) for borehole RVLD8 at Riverlands

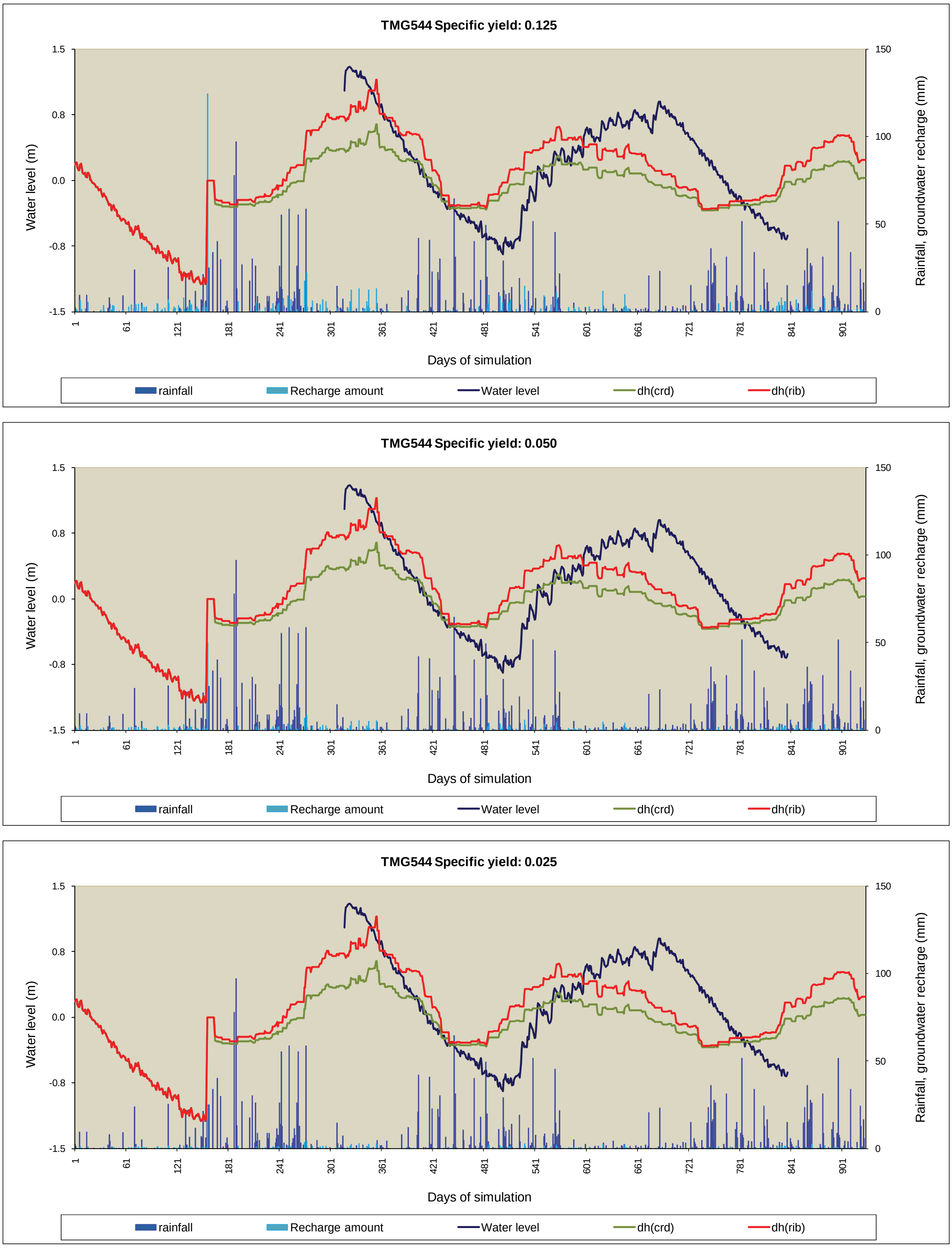

Figure 44

Daily rainfall and groundwater recharge in mm, observed groundwater level as well as groundwater recharge calculated with the cumulative rainfall departure method (dh(crd)) and the RIB method (dh(rib)) for borehole TMG544 at Oudebosch

8.5 Uncertainty analysis

8.5.1 Introduction and purpose

The purpose of this section is to introduce uncertainty analysis into the estimation procedures for groundwater recharge. In general, uncertainty is defined as a state of having limited knowledge where it is impossible to exactly describe the existing state, a future outcome, or more than one possible outcome. Uncertainty is a measure of the 'goodness' of a result. Without such a measure, it is impossible to judge the fitness of the value as a basis for making decisions relating to scientific excellence (Refsgaard *et al*., 2007; Montanari, 2007). The science of environmental modelling is a discipline in which considerable uncertainty is inherent. Over the past two decades, in response to the increasing need to make predictions where observations are not available or of poor quality, it has become unavoidable to consider uncertainty in modeling research (Hughes et al., 2011). There are many different stages in the model-based water resources assessment process at which uncertainty manifests. The most significant sources of uncertainty in modeling are the errors inherent in the input data used to drive the models, the structure of the models and the parameterization of the models (Walker *et al.*, 2003; Brugnach *et al.*, 2008; Gupta *et al.*, 2005).

The measurement of uncertainty is usually done through the provision of a set of possible states or outcomes where probabilities are assigned to each possible state or outcome, and this also includes the application of a probability density function to continuous variables. An analysis of uncertainty is important in water resource management as it aids the decision making process by presenting a range of variability expected in the element under consideration.

8.5.2 Material and methods

In this study, analysis of uncertainty was applied to the RIB model for the estimation of recharge of aquifers. Two inputs to the RIB method are daily values of rainfall (in mm) and water level (in m amsl). In trying to understand the uncertainty related to the estimation of groundwater recharge, the input uncertainty was propagated through the model (using a simple sampling procedure such as Monte Carlo) to generate an ensemble of outputs whose range represents the uncertainty in recharge. The uncertainty related to water levels was considered in this exercise.

The basic tenet of the analysis of uncertainty in the estimation of recharge is to assume some uncertainty in the input data that are used to drive the model. The rationale is that, if the frequency distribution properties of the input data can be established, then it is possible to describe the distribution characteristics of the model output. After successfully defining probability distribution functions for the input data, we can sample from these distributions to define distributions for the modelled recharge. Ideally, each term of that time series of daily water levels has to be considered a random variable with its own probability distribution and related parameters. For instance, each term of the daily time series could have a Gaussian (or normal) probability distribution with central value (or mean value) equal to the observed value and standard deviation (representing the level of uncertainty related to the value) equal to 10% of the observed value (Passarella *et al*., 2006). A similar approach was adopted in this study. However, a uniform distribution was adopted with perturbations of between ±20 and ±50% about the observed value. The two additional time series therefore represent the extremes/boundaries (minimum and maximum) of the uniform distribution. These minimum and maximum time series were run through the model. The model outputs gave a range of variability of recharge, and this range defined the expected uncertainty based on the inputs.

8.5.3 Results and discussion

The uncertainty analysis was performed at three borehole sites – RVLD6, RVLD8 (S_y = 0.05) and TMG544 (S_y = 0.105). The time series data available at these sites were daily values covering the period from January 2008 to July 2010 for TMG544 and May 2007 to September 2011 for the other two boreholes. The data records are continuous with very few gaps indicating missing values. Figures 45, 46 and 47 show the flow duration curves of simulated recharge at the three sites using observed data and limits determined by perturbing the observed values by 50% below and above the observations. The limits do not give a huge range of uncertainty over the simulation periods. This is probably because the observed water levels do not exhibit huge variations. There are long periods with estimated zero recharge. While there are quite huge calculated daily recharge values, the mean values are relatively low (Table 17) given the zero values.

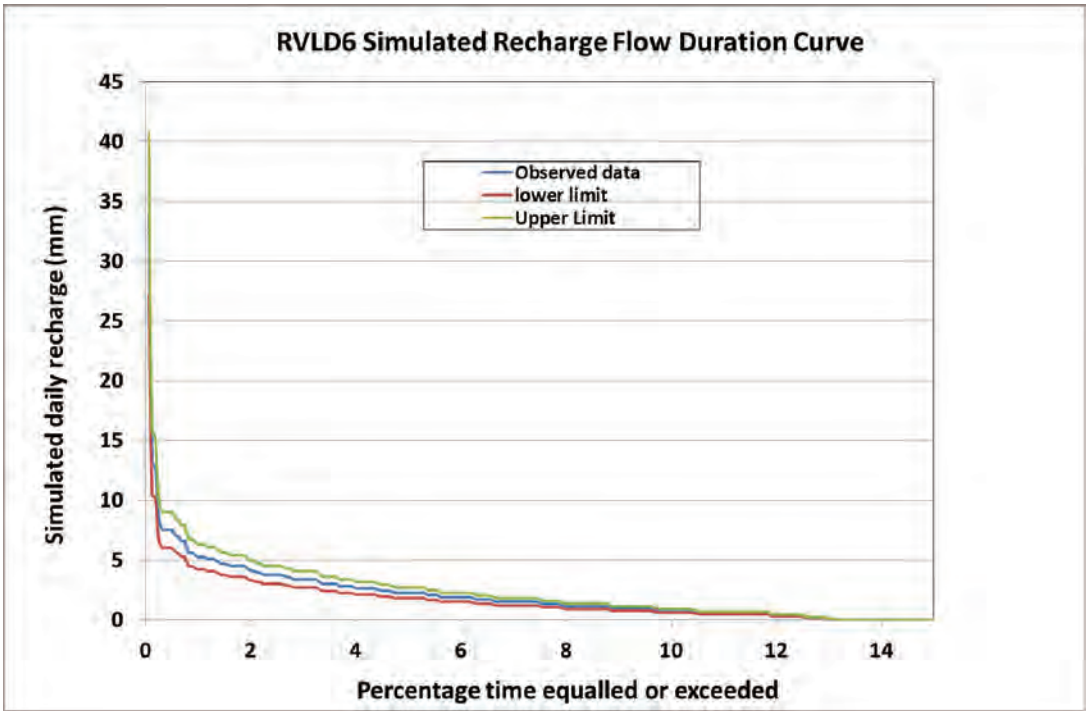

Figure 45

Flow duration curve for simulated recharge at RVLD6 over the simulation period

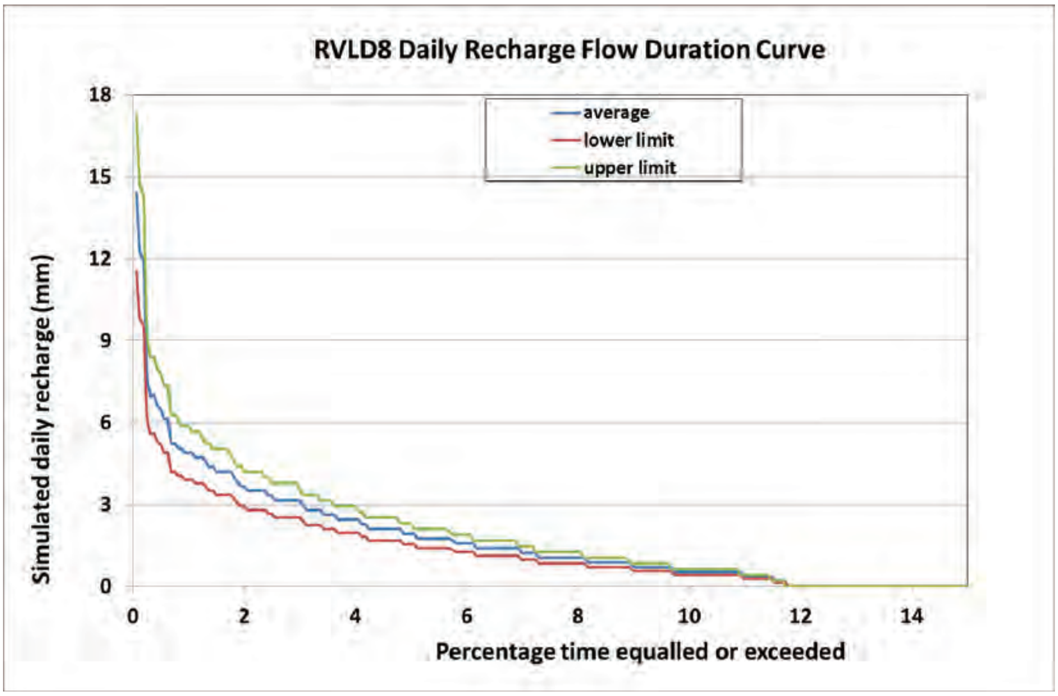

Figure 46

Flow duration curve for simulated recharge at RVLD8 over the simulation period

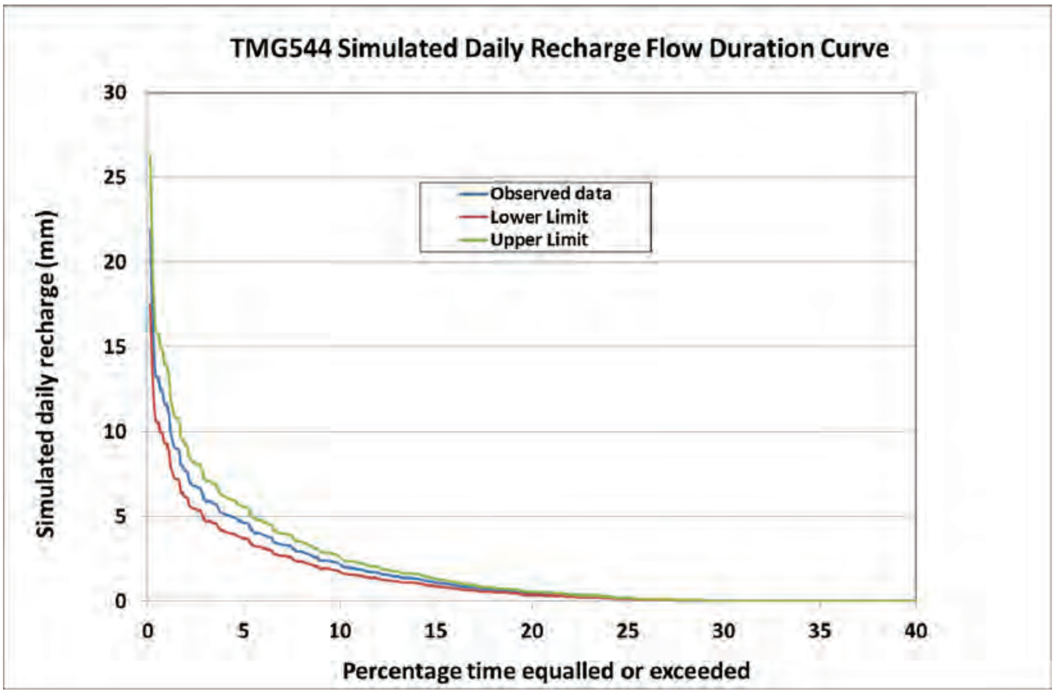

Figure 47

Flow duration curve for simulated recharge at TMG544 over the simulation period

Table 17 shows the results of the range of values of recharge simulated by the RIB method. In the Table, two perturbations of the observed water levels were used, and the results are given as average daily recharge values (in mm), their annual equivalents (in mm) and the recharge values as a percentage of mean annual precipitation (MAP) measured at the boreholes.

TABLE 17
SUMMARY OF OUTPUTS OF THE UNCERTAINTY ANALYSIS OF GROUNDWATER RECHARGE CALCULATED WITH THE RIB MODEL

	Model Outputs (±20% Perturbation)		
Borehole	**Mean daily recharge range (mm)**	**Mean Annual Recharge range (mm)**	**% of MAP**
RVLD6	0.253-0.379	92.254-138.380	14.6-21.9
RVLD8	0.208-0.308	75.945-112.539	12.0-17.8
TMG544	0.556-0.833	202.877-304.315	34.5-51.7
	Model Outputs (±50% Perturbation)		
RVLD6	0.158-0.467	57.658-170.398	9.1-26.9
RVLD8	0.130-.0385	47.466-140.674	7.5-22.2
TMG544	0.347-1.042	126.798-380.394	21.6-64.7

The results show that there is a larger variability at TMG544 borehole (Oudebosch) than the other two (Riverlands). A perturbation of the water level time series data for TMG544 by a factor 20% results in a range of recharge of 34.5-51.7% of MAP and 21.6-64.7% of MAP when the perturbation is higher (indicating more uncertainty). The other two boreholes have a maximum of 26.9% of MAP for both levels of perturbations. These results are expected given the two different environments which host the boreholes. TMG544 is in the Table Mountain Group (TMG) geology with a heterogeneous and fractured rock system. With water flowing through the cracks, fissures, interstices and fractures, it is reasonable to expect higher variability (even between boreholes located close to each other). On the other hand RVLD6 and RVLD8 are sandy aquifers that are more homogeneous. Thus, one would expect the larger uncertainties in the TMG than the sandy aquifer. As in the case of study 2, the estimates of recharge depend on the boreholes considered, in particular with regard to the TMG aquifer where different boreholes displayed different responses to rainfall.

It is prudent to note that the model outputs presented here are point analyses based on individual boreholes, so it was not possible to compare the values with, e.g., GRAII database, DWAF (2006), which are regionalised and are given as basin averages.

8.6 Abstraction scenarios

The Kogelberg Nature Reserve was identified as one of a set of sites that was suitable for the groundwater exploration programme run by the City of Cape Town. Simulations were therefore run with RIB in order to predict trends of groundwater level under different scenarios of abstraction. Borehole TMG544 was used for this purpose and the calibration data from Chapter 8.4. Three scenario simulations were run:

1) Baseline conditions (without abstraction): measured rainfall; S_y = 0.042 (in the absence of measured data, this value was selected from Table 16 for demonstration purposes); aquifer area = 3.40 km^2
2) Abstraction of 3 ML d^{-1}: measured rainfall; S_y = 0.042; aquifer area = 3.40 km^2
3) Abstraction of 3 ML d^{-1} from 1/10 of the aquifer area: measured rainfall; S_y = 0.042; aquifer area = 0.34 km^2

The resulting groundwater levels were plotted in Figure 48. Abstraction of 3 ML d^{-1} did not affect the groundwater level drastically. The groundwater level with abstraction was 0.02 m lower that the baseline without abstraction. The effect of abstraction was small because of the relatively large area of the aquifer (3.40 km^2). However, if the draining area for a borehole is reduced by 1/10 (i.e. 10 abstraction boreholes are used over the same area), the effect on the groundwater level was predicted to be much larger (0.21 m lower than the baseline).

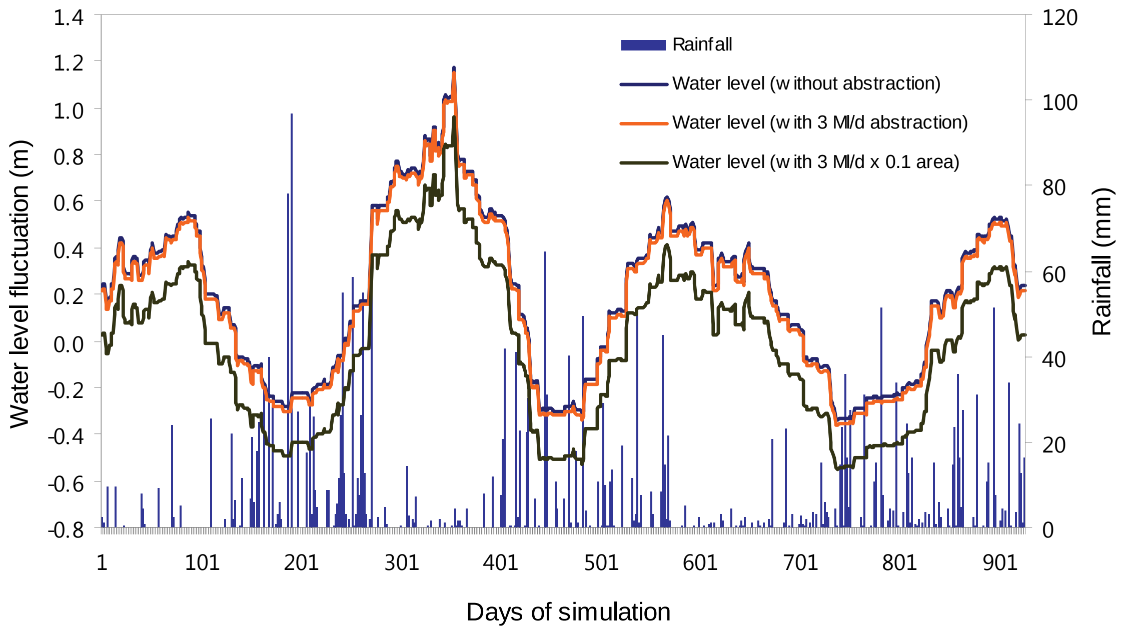

Figure 48

Measured rainfall and groundwater levels (baseline conditions, with 3 ML d^{-1} abstraction and with abstraction from 1/10 of the surface area of the aquifer) for borehole TMG544 in the Oudebosch catchment

8.7 Climate scenario

A second set of scenario simulations was run for TMG544 at Kogelberg in order to predict the effects of climate change on groundwater levels, in particular changes in rainfall. The following scenarios were run:

1) Baseline conditions: measured rainfall; S_y = 0.042 (Table 16); aquifer area = 3.40 km^2
2) Reduction in measured rainfall by 10%
3) Reduction in measured rainfall by 20%

The scenario simulations of groundwater level are shown in Figure 49. It is visible in the graph that, in the initial period of simulation, reduced rainfall did not affect groundwater levels. However, the effects became visible over time. After almost three years, the groundwater level dropped by 0.07 m with 10% rainfall reduction and by 0.13 m with 20% rainfall reduction compared to the baseline.

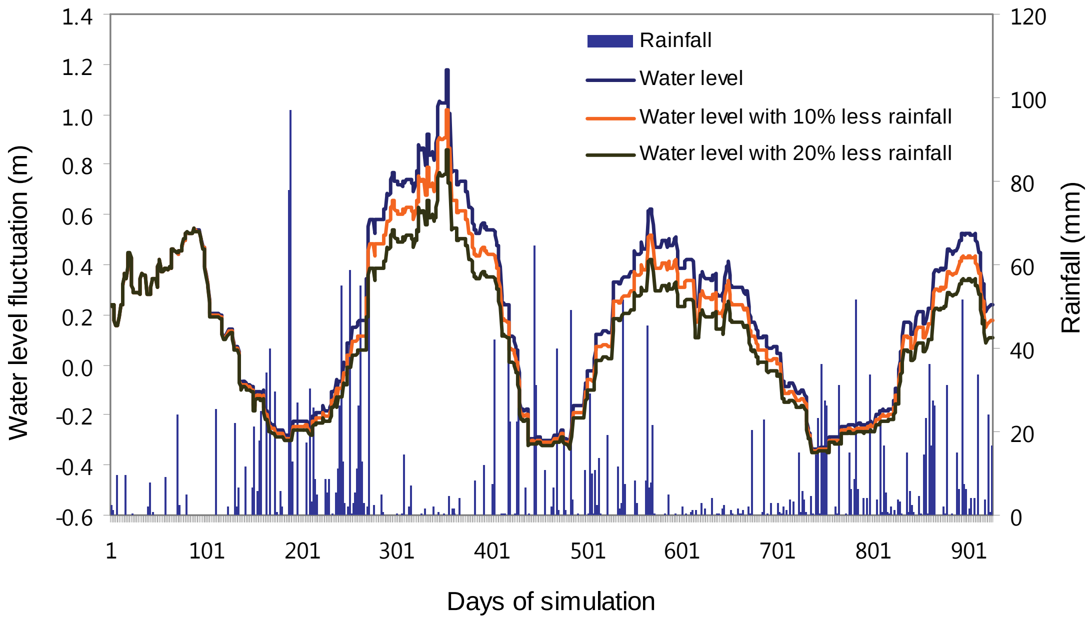

Figure 49

Measured rainfall and groundwater levels (baseline conditions, with 10% and 20% less rainfall) for borehole TMG544 in the Oudebosch catchment

8.8 Conclusions

The RIB model is useful for quick estimates of groundwater recharge at locations where groundwater levels respond distinctly to rainfall. It is not a data-intensive method but a good conceptualization of the system and knowledge of the hydraulic properties of the aquifer are required. The model was found to be particularly sensitive to specific yield as input. Given a range of S_y between 0.021 and 0.125, groundwater recharge was estimated to be between 7.5% and 41% at Riverlands, and between 5% and 26% at Oudebosch. Comparatively, groundwater recharge estimated by coupling an atmospheric model and HYDRUS-2D at Riverlands was 25% (ranging from 15% to 35% per year). At Kogelberg, groundwater recharge calibrated with MODFLOW was 20%.

Uncertainties in groundwater recharge model simulations were assessed at both sites. The ranges of average values of groundwater recharge were calculated as a measure of the uncertainty related to the estimation method used. For the TMG borehole, there was greater variability, indicating more uncertainty, than the boreholes in the sandy aquifer.

The technique used in the uncertainty analysis showed that error propagation method is a useful technique for analysing the influence of input data on the simulated groundwater recharge. The extreme boundaries of a uniform distribution can give the lower and upper limits of simulated recharge which are useful for giving an idea of the extent of the simulation uncertainty. However, more robust sampling from the probable inputs space should give a better representation of the output space. Also, more robust distribution functions for the inputs can be used, but it cannot at the moment be determined how these could improve the uncertainty analysis.

While the uncertainties were higher in the TMG aquifer, this had nothing to with the estimation method but rather with the kind of geological formation that we dealt with. This was easy to see given that the same model was used in the sandy aquifer and resulted in less uncertainty. However, this suggested that when modelling in the TMG, one needs to allow for higher levels of uncertainty. This has implications not only on the recharge estimation, but also on management decision-making and risk associated with the groundwater resource.

Scenario simulations indicated that the effects of abstraction on groundwater levels depend mainly on the volumes of abstraction, the watershed area and number of boreholes. Climate change scenarios for Oudebosch (borehole TMG544) indicated that reduction in rainfall by 20% could cause a drop in groundwater level by 0.13 m over almost three years.

There are ample opportunities for application of the RIB model. In this study, only a few relevant examples were shown. The RIB model should be tested using data collected under different hydrogeological conditions, in different climatic areas and for longer time series of data (rainfall and groundwater levels). A comprehensive sensitivity analysis is recommended before application of the model at a particular site. An analysis of differences between daily, monthly and yearly simulations is also recommended for data sets that include longer time series of input data compared to this study.

9 CONCLUSIONS

The specific conclusions regarding the individual experiments, measurements and modelling exercises were reported at the end of each relevant section. Some general conclusions that emanated from the research are highlighted here.

Evapotranspiration measurements were invaluable in gaining understanding of the water use and water balance in two types of fynbos. It was the first time that measurements of ET were done on Atlantis Sand Plain Fynbos and Kogelberg Sandstone Fynbos. Evapotranspiration depended on weather conditions, vegetation (root distribution and canopy cover) and soil water storage capacity. ET usually followed trends of ETo and rainfall. It was affected by soil water storage; it was lower on shallow stony soils on the Kogelberg slopes compared to the alluvial area of the Oudebosch stream. Less canopy cover resulted in lower ET (e.g. vegetation on Kogelberg slopes). A well-developed root system at Riverlands allowed the vegetation to tap the shallow groundwater and keep ET high.

Soil hydraulic properties, in particular K_{sat} and preferential flow patterns, play a large role in groundwater recharge. Hydraulic conductivities are essential inputs in hydrological models and they need to account for preferential flow characteristics. Statistically significant differences were observed in K_{sat} in the fractured rock system at Kogelberg and large variabilities in preferential flow occurred especially as funnel between large stones, through channels of least resistance, throughout the depth of the profile. Preferential flow may affect a substantial portion of soil profiles and the plant available water is thus expected to be low as the profile drains. The dye experiment also served the purpose of defining the possible fate of conservative and mobile contaminants in the environment and impacts on groundwater quality. Less variability in the hydraulic properties of Riverlands soils was evident compared to Kogelberg.

Geophysical methods, e.g. resistivity tomography, showed potential in defining preferential pathways for water in the sub-soil and they should be investigated further. However, the applicability of this methodology is specific to a site because the resistivity readings also depend on salinity and geological characteristics.

The continuous long-term monitoring of weather, soil water content, vegetation and groundwater was very beneficial in terms of model calibration. Both process models used in the case studies were successful in predicting water balance components (both absolute values and temporal trends). In particular, HYDRUS-2D predicted well seasonal variations in soil water content at Riverlands, whilst MODFLOW was calibrated for two localized areas where conceptual knowledge of the system existed. The RIB model proved to be useful for quick estimates of groundwater recharge at locations where groundwater levels respond distinctly to rainfall. It is not a data-intensive method but a good conceptualization of the system and knowledge of the hydraulic properties of the aquifer are required.

Simulated average groundwater recharge was 25% of rainfall for the alluvial aquifer at Riverlands, ranging from 15 to 35% per year. Capillary rise from shallow groundwater was far higher than recharge during the rainy season. Groundwater recharge calibrated for the Oudebosch catchment was 20% of total rainfall. It should be noted that this estimate of groundwater recharge depended on the boreholes selected for calibration. In this study, boreholes that displayed distinct responses to rainfall were used for calibration. Values of recharge may have been overestimated. A more realistic estimate of recharge can be obtained by averaging responses of boreholes over the whole study area, including those that do not display a response to rainfall.

Given a range of specific yield between 0.021 and 0.125, groundwater recharge with the RIB model was estimated to be between 7.5% and 41% at Riverlands, and between 5% and 26% at Oudebosch. These values of groundwater recharge were within the range of those obtained in other studies. Scenario simulations with the RIB model allowed to quantify possible impacts of abstraction and climate change (reduction in rainfall) on the groundwater resource.

The uncertainty of the estimates of groundwater recharge depends on the accuracy of measured input data into the model (e.g. scintillometer measurements, weather instrumentation, etc.) and variability in environmental factors (rainfall, groundwater levels, vegetation, hydraulic properties, etc.). The technique used in the uncertainty analysis showed that the error propagation method is useful for analysing the influence of input data on the simulated groundwater recharge. Uncertainties in groundwater recharge simulations obtained with the RIB model were assessed at both study sites. Greater environmental variability and more uncertainty occurred in the TMG environment compared to the sandy aquifer. This has implications not only on the recharge estimation, but also on management decision-making and risk associated with the groundwater resource.

10 RECOMMENDATIONS

The following recommendations emanated from the research:

- An accurate conceptualization of the system is required for the estimation of groundwater recharge.
- Selection of methods for groundwater recharge estimation depends on the objectives, the spatial and temporal scale of application, the assumptions, budget and time frame as well as data availability.
- A combination of techniques (physical methods, tracers and numerical models) is recommended for the estimation of recharge.
- The concept of atmospheric demand-soil water supply should be employed in the quantification of actual evapotranspiration.
- A daily time step is recommended in the calculation of water balance variables relevant to groundwater recharge to account for daily actual evapotranspiration and rainfall distribution. In some instances, the high temporal resolution of the daily time step can be traded off for speed of calculation (e.g. numerical models like HYDRUS-2D and MODFLOW) and the monthly time step can be adopted to account at least for the seasonality of rainfall and other water balance components.
- An accurate spatial description of environmental variables is essential (e.g. vegetation, soil properties, etc.).
- A combination of methods (GIS and remote sensing techniques, pedotransfer functions and surveying methods) facilitates the spatial conceptualization of catchment hydrology and spatial delineation of soils based on their hydraulic properties.
- For the estimates of preferential flow, a combination of resistivity tomography during rainfall events, tracer studies and groundwater level monitoring are recommended.
- Continuous long-term monitoring of all environmental components (weather, soil water content, vegetation and groundwater) is invaluable for understanding natural systems and calibrating models.
- Model calibration is an on-going process as data become available.
- Model sensitivity analyses are essential in order to identify and measure accurately inputs to which model outputs are particularly sensitive. For example, these inputs were found to be root distribution, soil properties and potential evapotranspiration in HYDRUS-2D, saturated hydraulic conductivity in MODFLOW and specific yield in the RIB model.

- As it is usually extremely difficult to simulate complex systems (e.g. fractured rock TMG systems) with finite-difference models like MODFLOW, it is preferable to focus on areas where good conceptual and physical knowledge of the system exist. However, the selection of boreholes to be used for calibration is fundamental as they need to be representative of the entire area.
- Assumptions, limitations and potential sources of error of groundwater recharge methods need to be known (e.g. complexity of systems, interpolation of spatial data, lack and patchiness in input data, etc.).
- Process models are generally preferable in terms of quantifying catchment processes, in particular because computers are able to handle more and more detailed information.
- The RIB model, as a low data-intensity tool, can be used for quick estimates of groundwater recharge at locations where groundwater levels respond distinctly to rainfall, where a good conceptualization of the system and knowledge of hydraulic properties exist.
- No single approach can be recommended for quantification of uncertainties. This depends on the objectives, data constraints, spatial and temporal scales of application.
- The extreme boundaries of a uniform distribution can give the lower and upper limits of simulated groundwater recharge and this is a useful measure of uncertainty. Robust sampling of inputs and robust distribution functions can improve the estimation of uncertainty.

Recommended actions for further research include:

- Data collection and monitoring is a pre-requisite in order to gain understanding of natural systems and predict catchment processes accurately. The usefulness of continuous and long term (at least five years) monitoring was proved again in this project.
- Tools for spatial description of environmental variables (e.g. vegetation, soil properties, etc.) need to be refined and made available.
- Remote sensing tools and products are becoming more and more popular in the estimation of water cycle variables of relevance to groundwater recharge. These need to be validated and investigated further.
- Geophysical methods (e.g. resistivity tomography) showed potential in defining preferential pathways for water in the sub-soil and they should be investigated

further. However, the applicability of this methodology is specific to a site because the resistivity readings also depend on salinity and geological characteristics.

- The quantification of uncertainties in catchment hydrology needs to be investigated further given the large number of tools and methods available. Long-term monitoring data are required for this purpose.

11 LIST OF REFERENCES

AKAY O, FOX GA and SIMUNEK J (2009) Numerical simulation of flow dynamics during macropore-subsurface drain interactions using HYDRUS. *Vadose Zone Journal* **7** 909-918.

ALLEN RG, PEREIRA LS, RAES D and SMITH M (1998) Crop Evapotranspiration: Guidelines for Computing Crop Water Requirements. United Nations Food and Agriculture Organization, Irrigation and Drainage Paper 56. Rome, Italy, 300 pp.

ALLEY WM, HEALY RW, LABAUGH JW and REILLY TE (2002) Flow and storage in groundwater systems. *Science* **296** 1985-1990.

ARBOGAST T (1987) The double porosity model for single phase flow in naturally fractured reservoirs. *Inst. Math. Appl.* 295.

ASANO Y, UCHIDA T and NOBUHITO O (2002) Residence times and flow paths of water in steep unchannelled catchments, Tanakami, Japan. *Journal of Hydrology* **261** 173-192.

ASANO Y, UCHIDA T and NOBUHITO O (2002) Residence times and flow paths of water in steep unchannelled catchments, Tanakami, Japan. *Journal of Hydrology* **261** 173-192.

ASTON T (2007) Geohydrological characteristics of Table Mountain Group aquifer-fed seeps and the plant ecophysiological consequences. Unpublished MSc Thesis, Botany Department, University of Cape Town.

BARKER R (1992) A simple algorithm for electrical imaging of the subsurface. *First Break* **10(2)** 53-62.

BARKER R and MOORE J (1998) The application of time-lapse electrical tomography in groundwater studies. *Leading Edge* **17(10)** 1454-1458.

BASTIAANSEN W, MENENTI R, FEDDES R and HOLTSLAG A (1998) A remote sensing surface energy balance algorithm for lands (SEBAL) 1. Formulation. *Journal of Hydrology* **212-213** 198-212.

BETTS RA, BOUCHER O, COLLINS M, COX PM, FALLOON PD, GEDNEY N, HEMMING DL, HUNTINGFORD C, JONES CD, SEXTON DMH, and WEBB MJ (2007)

Projected increase in continental runoff due to plant responses to increasing carbon dioxide. *Nature* **448** 1037-1042.

BINLEY A, HENRY-POULTER S and SHAW B (1996) Examination of solute transport in an undisturbed soil column using electrical resistance tomography. *Water Resources Research* **32(4)** 763-769.

BIRP (1999) Birds in Reserves Project. Site Summary for Riverlands Nature Reserve. Avian Demography Unit, University of Cape Town (adu@adu.uct.ac.za).

BLAKE GR and HARTGE KH (1986) Particle density. In MA Klute (ed.) *Methods of soil analysis. Physical and mineralogical methods: Part 1* (2nd ed.), Soil Science Society of America, Madison, Wisconsin, 377-382.

BLANEY HF and CRIDDLE WD (1950) Determining water requirements in irrigated areas from climatological and irrigation data. USDA Soil Conserv. Serv. SCS-TP96. 44 pp.

BOSCH DD and KING KW (eds.) (2001) Preferential Flow, Water Movement and Chemical Transport in the Environment, Proc. 2nd Int. Symp. (3-5 January 2001, Honolulu, Hawaii, USA), St. Joseph, Michigan: ASAE, ISBN: 1-892769-14-X.

BOUCHER C (1978) Cape Hangklip area. II. The vegetation. *Bothalia* **12(3)** 455-497.

BREDENKAMP D, BOTHA LJ, VAN TONDER GJ and JANSE VAN RENSBURG H (1995), Manual on Qualitative Estimation of Groundwater Recharge and Aquifer Storativity, Based on Practical Hydrological Methods. Water Research Commission report No TT 73/95, Pretoria, South Africa.

BREDENKAMP DB and VANDOOLAEGHE MAC (1982) Die Ontginbare Grondwaterpotensiaal van die Atlantisgebied. Department of Water Affairs and Forestry, Geohydrology Division, Technical report No. Gh 3227, Pretoria, South Africa.

BROWNING D and DUNIWAY M (2011) Digital soil mapping in the absence of field training data: a case study using terrain attributes and semiautomated soil signature derivation to distinguish ecological potential. *Applied and Environmental Soil Science*, 1-12, doi:10.1155/2011/421904.

BRUGNACH M, PAHL-WOSTL C, LINDENSCHMIDT KE, JANSSEN JAEB, FILATOVA T, MOUTON A. HOLTZ G, VAN DER KEUR P and GABER N (2008) Complexity and Uncertainty: Re-Thinking the Modelling Activity. *Developments in Integrated Environmental Assessment* **3** 49-68.

BRYDON J and DAY J (1970) Use of the Fieldes and Perrot sodium fluoride test to distinguish the B horizons of podzols in the field. *Can. J. Soil Sci.* **50** 35-41.

CAVE L, BEEKMAN HE and WEAVER J (2002) Impact of climate change on groundwater resources. In: Managing Water Related Issues on Climate Variability and Climate

Change, R. Schulze (ed.), Proceedings Thukela Dialogue Workshop, University of Natal, Pietermaritzburg, 24 July 2002.

CLARKE R, LAWRENCE A and FOSTER S (1996) Groundwater: A Threatened Resource. United Nations Environment Programme Environment Library No. 15, Nairobi, Kenya.

COLVIN C, RIEMANN K, BROWN C, LE MAITRE D, MLISA A, BLAKE D, ASTON T, MAHERRY A, ENGELBRECHT J, PEMBERTON C, MAGOBA R, SOLTAU L and PRINSLOO E (2009) Ecological and Environmental Impacts of Large-Scale Groundwater Development in the Table Mountain Group (TMG) Aquifer System. Water Research Commission Report No. 1327/1/08, Pretoria, South Africa.

COOK PG and BOHLKE JK (1999) Determining timescales for groundwater flow and solute transport. In: Cook PG, Herczeg AL (eds.) Environmental Tracers in Subsurface Hydrology. Kluwer, Dordrecht, 1-30.

COOK PG and SOLOMON DK (1997) Recent advances in dating young groundwater: chlorofluorocarbons, $^{3}H/^{3}He$ and ^{85}Kr. *Journal of Hydrology* **191** 245-265.

COPPOLA A, KUTILEK M and FRIND EO (2009) Transport in preferential flow domains of the soil porous system: Measurement, interpretation, modelling, and upscaling. *Journal of Contaminant Hydrology* **104** 1-3.

CWCFPA (2005) Business Plan. Cape West Coast Fire Protection Association (CWCFPA), June 2005.

DAILY W, RAMIREZ A, LABRECQUE D and NITAO J (1992) Electrical resistivity tomography of vadose water movement. *Water Resources Research* **28(5)** 1429-1442.

DE COURSEY D, AHUJA L, HANSON J, SHAFFER M, NASH R, HEBSON C and ROJAS K (1992) Root Zone Water Quality Model: version 1.0: Technical documentation. USDA-ARS, GPSR Technical Report No. 2., Great Plains Systems Research Unit, Ft. Collins, Colorado.

DE VRIES JJ and SIMMERS I (2002) Groundwater recharge: an overview of processes and challenges. *Hydrogeology Journal* **10** 5-17.

DEL ROSARIO K, DU TOIT WH and VERSTER H (2005) The application of geostatistics to analyze monitoring data. Proceedings from the Biennial Groundwater Conference, ISBN 0-620-33659-5, Pretoria, South Africa.

DENMEAD OT and SHAW RH (1962) Availability of soil water to plants as affected by soil moisture content and meteorological conditions. *Agronomy J.* **54** 385-390.

DESTOUNI G, DARRACQ A, JARSJO J, PRIETO C and SHIBUO Y (2009) Evapotranspiration in a warming climate: model uncertainty and role for climate adaptation. IOP Conf. Series: Earth and Environmental Science 6, 052014, doi:10.1088/1755-1307/6/5/052014.

DIODATO N and CECCARELLI M (2009) Computational uncertainty analysis of groundwater recharge in catchment. *Ecological Informatics* **1** 377-389.

DOMENICO PA and SCHWARTZ FW (1990) Physical and Chemical Hydrogeology. John Wiley and Sons Inc., New York. 824 pp.

DUSEK J, GERKE HH and VOGEL T (2009) Surface boundary conditions in two-dimensional dual-permeability modeling of tile drain bromide leaching. *Vadose Zone Journal* **7** 1287-1301.

DWAF (2006) Groundwater Resource Assessment II: Recharge Literature Review Report 3aA. Project No. 2003-150. Department of Water Affairs and Forestry, Pretoria, South Africa.

EBEL BA and NIMMO JR (2009) Estimation of unsaturated zone travel times for Rainier Mesa and Shoshone Mountain, Nevada Test Site, Nevada, using a source-responsive preferential-flow model: U.S. Geological Survey Open-File Report 2009-1175, pp. 74.

EVERSON CS, MOLEFE GL and EVERSON TM (1998) Monitoring and Modelling Components of the Water Balance in a Grassland Catchment in the Summer Rainfall Area of South Africa. Water Research Commission Report No.493/1/98, Pretoria, South Africa.

FAO (1998) World Reference Base for Soil Resources. United Nations Food and Agricultural Organization. Rome, Italy.

FAVROT J-C (1981) Pour une approche raisonnee du drainage agricole en France: La methode des secteurs de reference. *Comptes-Rendus des Seances de l'Academie d'Agriculture de France* **8** 716-723.

FETTER CW (1993) Contaminant Hydrogeology. MacMillan Publishing Co., New York. 458 pp.

FLUHLER H, URSINO N, BUNDT M, ZIMMERMAN U and STAMM C (2001) The preferential flow syndrom – A buzzword or a scientific problem. In: DD Bosch and KW King (eds.) Preferential Flow, Water Movement and Chemical Transport in the Environment, Proc. 2nd Int. Symp. (3-5 January 2001, Honolulu, Hawaii, USA), St. Joseph, Michigan: ASAE 701P0006, 21-24.

FREEZE RA and CHERRY JA (1979) Groundwater. Prentice-Hall Inc. Englewood Cliffs, New Jersey. 604 pp.

FUCHS JW, FOX GA, STORM DE, PENN CJ and BROWN GO (2009) Subsurface transport of phosphorus in riparian floodplains: Influence of preferential flow paths. *Journal of Environmental Quality* **38** 473-484.

GAUDET JP, JEGAT H, VACHAUD G and WIERENGA PJ (1977) Solute transfer with exchange between mobile and stagnant water through unsaturated sand. *Soil Science Society of America Journal* **41** 665-671.

GEE G and BAUDER J (1986) Particle-size analysis. p. 383-411. In MA Klute (ed.) Methods of soil analysis: Physical and mineralogical methods: Part 1 (2nd ed.), Soil Science Society of America, Madison, Wisconsin.

GERKE HH (2006) Review article: preferential-flow descriptions for structured soils. *J. Plant Nutr. Soil Sci.* **169** 1-19.

GERKE HH, RAY C and VOGEL T (2001) Effects of aggregate skins on flow and transport in structured soil. In: DD Bosch and KW King (eds.) Preferential Flow, Water Movement and Chemical Transport in the Environment, Proc. 2nd Int. Symp. (3-5 January 2001, Honolulu, Hawaii, USA), St. Joseph, Michigan: ASAE 701P0006, 293-296.

GERMANN PF (2001) Preferential flow in field soils. In: DD Bosch and KW King (eds.) Preferential Flow, Water Movement and Chemical Transport in the Environment, Proc. 2nd Int. Symp. (3-5 January 2001, Honolulu, Hawaii, USA), St. Joseph, Michigan: ASAE 701P0006, 11-20.

GIAMBELLUCA TW, LOAGUE K, GREEN RE and NULLET MA (1996) Uncertainty in recharge estimation: impact on groundwater vulnerability assessments for the Pearl Harbor Basin, O'ahu, Hawai'i, U.S.A. *Journal of Contaminant Hydrology* **23(1-2)** 85-112.

GLASS RJ, NICHOLL MJ, RAMIREZ AL and DAILY WD (2002) Liquid phase structure within an unsaturated fracture network beneath a surface infiltration event: field experiment. *Water Resour. Res.* **38** 1199-1135.

GLEESON T, NOVAKOWSKI K and KYSER K (2009) Extremely rapid and localized recharge to a fractured rock aquifer. *Journal of Hydrology* **376** 496-509.

GOLDBLATT P and MANNING J (2000) Cape Plants. A conspectus of the Cape flora of South Africa. Strelitzia 9, South African National Biodiversity Institute, Pretoria.

GRELLIER S, BOUYÉ J, GUÉRIN R, ROBAIN H and SKHIRI N (2005) Electrical Resistivity Tomography (ERT) applied to moisture measurements in bioreactor: principles, in situ measurements and results, *International Workshop Hydro-Physico-Mechanics of Landfills*, Grenoble, France, 21-22 March 2005.

GUPTA HV, BEVEN KJ and WAGENER T (2005) Model calibration and uncertainty estimation. In: Anderson, M,G. (ed.), *Encyclopaedia of Hydrologic Sciences*. Wiley, Chichester.

HAGEDORN F and BUNDT M (2002) The age of preferential flow paths. *Geoderma* **108(1)** 119-132.

HANGENA E, GERKE HH, SCHAAF W and HUTTL RF (2003) Flow path visualization in a lignitic mine soil using iodine-starch staining. *Geoderma* **120** 142-151.

HANSEN M, BROWN D, DENNISON P, GRAVES S and BRICKLEMYER R (2009) Inductively mapping expert-derived soil-landscape units within dambo wetland catenae using multispectral and topographic data. *Geoderma* **150** 72-84.

HARGREAVES GH (1983) Discussion of 'Application of Penman wind function' by Cuenca, R.H. and Nicholson, M.J. *J. Irrig. and Drain. Eng*. *ASCE* **109(2)** 277-278.

HEALY RW and SCANLON BR (2011) Estimating groundwater recharge. Africa Groundwater Academy series short course, 14-16 November 2011, Cape Town, South Africa.

HENDRICKX JMH and FLURY M. (2001) Uniform and preferential flow mechanisms in the vadose zone. In: Conceptual Models of Flow and Transport in the Fractured Vadose Zone, Washington, D.C., National Academy Press, 149-187.

HENSLEY M, LE ROUX P, GUTTER J. and ZERIZGHY M (2007) A Procedure for an Improved Soil Survey Technique for Delineating Land for Rainwater Harvesting. Water Research Commission Report No. TT311/07. Pretoria, South Africa.

HOLMAN IP (2007) Sources of uncertainty in climate change impacts on groundwater recharge. *Eos Trans. AGU,* **88(52)**, Fall Meet. Suppl., Abstract.

HSIEH PA (2001) TopoDrive and ParticleFlow – two computer models for simulation and visualization of ground-water flow and transport of fluid particles in two dimensions. Open File Report 01-286, United States Geological Survey, Menlo Park, California.

HUGHES DA, KAPANGAZIWIRI E, MALLORY SJL, WAGENER T and SMITHERS JC (2011) Incorporating Uncertainty in Water Resources Simulation and Assessment Tools in South Africa. Water Research Commission Report No. 1838/1/11, Pretoria, South Africa.

HUISMAN JA, SPERL C, BOUTEN W and VERSTRATEN JM (2001) Soil water content measurements at different scales: accuracy of time domain reflectometry and ground-penetrating radar*. Journal of Hydrology* **245** 48-58.

HUPET F, BOGAERT P and VANCLOOSTER M (2004) Quantifying the local-scale uncertainty of estimated actual evapotranspiration. *Hydrological Processes* **18(17)** 3415-3434.

JANSSEN M and LENNARTZ B (2009) Characterization of preferential flow pathways through paddy bunds with dye tracer tests. *Soil Science Society of America Journal* **72** 1756-1766.

JARMAIN C, EVERSON CS, SAVAGE MJ, MENGISTU MG, CLULOW AD WALKER S and GUSH MB (2009) Refining tools for evaporation monitoring in support of water resources management. Water Research Commission Report No. K5/1567/1/08, Pretoria, South Africa.

JARVIS NJ (1994) The MACRO model (Version 3.1): Technical description and sample simulations. Reports and Dissert. 19, Dept. Soil Sci., Swedish Univ. Agric. Sci., Uppsala, Sweden, pp. 51.

JENSEN ME and HAISE HR (1963) Estimating evapotranspiration from solar radiation. *J.Irrig. and Drain. Div. ASCE* **89** 15-41.

JOEL A and MESSING I (2001) Infiltration rate and hydraulic conductivity measured with rain simulator and disc permeameter on sloping arid land. *Arid Land Research and Management* **15** 371-384.

JOVANOVIC NZ, HON A, ISRAEL S, LE MAITRE D, RUSINGA F, SOLTAU L, TREDOUX G, FEY MV, ROZANOV A and VAN DER MERWE N (2009a) Nitrate Leaching from Soils Cleared of Alien Vegetation. Water Research Commission Report No. 1696/09, Pretoria, South Africa.

JOVANOVIC NZ, ISRAEL S, TREDOUX G, SOLTAU L, LE MAITRE D, RUSINGA F, ROZANOV A and VAN DER MERWE N (2009b) Nitrogen dynamics in land cleared of alien vegetation (*Acacia saligna*) and impacts on groundwater at Riverlands Nature Reserve (Western Cape, South Africa). *Water SA* **35(1)** 37-44.

KAY AL and DAVIES HN (2008) Calculating potential evaporation from climate model data: A source of uncertainty for hydrological climate change impacts. *Journal of Hydrology* **358** 221-239

KITE G and DROOGERS P (2000) Comparing estimates of actual evapotranspiration from satellites, hydrological models, and field data: A case study from Western Turkey. International Water Management Institute Research Report no. 42, 32 pp.

KLUTE M (ed.) (1986) Methods of Soil Analysis Part 1 (2 ed.). Soil Science Society of America, Madison, Wisconsin.

KROES JG and VAN DAM JC (2003) Reference Manual SWAP version 3.0.3. Wageningen, Alterra, Green World Research. Alterra Rep. No. 773, pp. 211.

KUNG K-JS (1990) Preferential flow in a sandy vadose zone. 1. Field observation. *Geoderma* **46** 51-58.

LEAVSLEY GH, LICHTY RW, TROUTMAN BM and SAINDON LG (1983) Precipitation-runoff modelling system – User's manual. US Geological Survey Water Resources Investigation Report 83-4238, Denver, Colorado, USA.

LE ROUX PAL, VAN TOL JJ, KUENENE BT, HENSLEY M, LORENTZ SA, EVERSON CS, VAN HUYSSTEEN CW, KAPANGAZIWIRI E and RIDDEL E (2011) Hydropedological Interpretations of the Soils of Selected Catchments with the Aim of

Improving the Efficiency of Hydrological Models. Water Research Commission Report No. 1748/1/10, Pretoria, South Africa.

LIN H, MCINNES K, WILDING L and HALLMARK C (1999) Effects of soil morphology on hydraulic properties: II. Hydraulic Pedotransfer Functions. *Soil Sci. Soc. Am. J.* **63** 955-961.

LIN HS, KOGELMANN W, WALKER C and BRUNS MA (2006) Soil moisture patterns in a forested catchment: A hydropedological perspective. *Geoderma* **131** 345-368.

LOKE M (2001) A practical guide to RES2DINV ver. 3.4; Rapid 2-D Resistivity & IP inversion using the least squares method. Geoelectrical Imaging 2-D & 3D, Allied Associates, Dunstable, UK.

LORENTZ S (2007) Interim annual report on data collection at local, field and catchment scale for each pollutant type, Wartburg research catchment. Report to Sigma Beta Consulting on Development of an Intergrated Modelling Approach for the Prediction of Agricultural Non-Point Source (NPS) Pollution from Field to Catchment Scales for Selected Agricultural NPS Pollutants. Water Research Commission Project No. K5/1467, Pretoria, South Africa.

LUO L and LIN H (2009) Lacunarity and fractal analyses of soil macropores and preferential transport using micro-X-ray computed tomography. *Vadose Zone Journal* **8** 233-241.

LUXMOORE RJ (1992) On preferential flow and its measurement. US Department of Energy Contract No. DE-AC05-840R21400.

MANNING J and GOLDBLATT P (1996) West Coast. South African Wild Flower Guide 7. Botanical Society of South Africa, Kirstenbosch.

McCARTHY GW and ANGIER J (2001) Impact of preferential flow pathways on ability of riparian wetlands to mitigate agricultural pollution. In: DD Bosch and KW King (eds.) Preferential Flow, Water Movement and Chemical Transport in the Environment, Proc. 2nd Int. Symp. (3-5 January 2001, Honolulu, Hawaii, USA), St. Joseph, Michigan: ASAE 701P0006, 53-56.

MCDONALD MG and HARBAUGH AW (1988) A Modular Three-Dimensional Finite Difference Ground-Water Model. U.S. Geological Survey Techniques of Water Resource Investigations, Book 6, 586 pp.

McINTOSH GC and SHARRATT BS (2001) Over winter stability of macropores in the Northern US corn belt. In: DD Bosch and KW King (eds.) Preferential Flow, Water Movement and Chemical Transport in the Environment, Proc. 2nd Int. Symp. (3-5 January 2001, Honolulu, Hawaii, USA), St. Joseph, Michigan: ASAE 701P0006, 221-224.

MIDGLEY J and SCHAFER G (1992) Correlates of water colour in streams rising in Southern Cape catchments vegetated by fynbos and/or forest. *Water SA* **18** 93-100.

MILEWSKI A, SULTAN M, YAN E, BECKER R, ABDELDAYEM A, SOLIMAN F and GELI KA (2009) A remote sensing solution for estimating runoff and recharge in arid environments. *Journal of Hydrology* **373** 1-14.

MISHRA S (2009) Uncertainty and sensitivity analysis techniques for hydrologic modeling. *Journal of Hydroinformatics* **11(3-4)** 282-296.

MOENCH AF (1984) Double-porosity models for a fissured groundwater reservoir with fracture skin. *Water Resources Research* **20** 831-846.

MOHNATY BP, CASTIGLIONE P, SHOUSE PJ and VAN GENUCHTEN MTh (2001) Measurement and modelling of preferential flow under controlled conditions. In: DD Bosch and KW King (eds.) Preferential Flow, Water Movement and Chemical Transport in the Environment, Proc. 2nd Int. Symp. (3-5 January 2001, Honolulu, Hawaii, USA), St. Joseph, Michigan: ASAE 701P0006, 77-80.

MONTANARI A (2007) What do we mean by 'uncertainty'? The need for a consistent wording about uncertainty assessment in hydrology. *Hydrological Processes Journal*, **21** 841-845.

MOORE RJ (2007) The PDM rainfall-runoff model. *Hydrology and Earth System Sciences* **11** 483-499.

NASH JE and SUTCLIFFE JV (1970) River flow forecasting through conceptual models part I — A discussion of principles. *Journal of Hydrology* **10(3)** 282-290.

NIEBER JL (2001) The relation of preferential flow to water quality, and its theoretical and experimental quantification. In: DD Bosch and KW King (eds.) Preferential Flow, Water Movement and Chemical Transport in the Environment, Proc. 2nd Int. Symp. (3-5 January 2001, Honolulu, Hawaii, USA), St. Joseph, Michigan: ASAE 701P0006, 1-10.

NIMMO JR (2007) Simple predictions of maximum transport rate in unsaturated soil and rock. *Water Resources Research* **43** W05426, doi:10.1029/2006WR005372.

NIMMO JR, PERKINS KS, SCHMIDT KM, MILLER DM, STOCK JD and SINGHA K (2009) Hydrologic characterization of desert soils with varying degrees of pedogenesis: 1. Field experiments evaluating plant-relevant soil water behavior. *Vadose Zone Journal* **8** 480-495.

OR D and HANKS RJ (1992) Spatial and temporal soil water estimation considering soil variability and evapotranspiration uncertainty. *Water Resources Research* **28(3)** 803-814.

PACHEPSKY Y, RAWLS W and LIN H (2006) Hydropedology and pedotransfer functions. *Geoderma* **131** 308-316.

PARSONS R (2002) Development of groundwater resources for the Arabella Country Estate. In: A synthesis of the hydrogeology of the Table Mountain Group – Formation of a research strategy. In K Pietersen and R Parsons (eds.) Water Research Commission Report No. TT 158/01, Pretoria, South Africa.

PASSARELLA G, BARCA E, LO PRESTI R, MASCIALE R and VURRO M (2006) Candelaro River Basin, Italy. A HarmoniRiB Case Study. Water Research Institute of the National Research Council, Bari, Italy (CNR-IRSA), www.harmonirib.com accessed on 31/01/2012.

PENMAN HL (1948) Natural evaporation from open water, bare soil and grass. *Proc. Roy. Soc. London A(194), S.* 120-145.

PEROZZI L and HOLLIGER K (2008) Detection and Characterization of Preferential Flow Paths in the Downstream Area of a Hazardous Landfill. *Journal of Environmental Engineering Geophysics* **13(4)** 343-350.

PERRET J, PRASHER SO, KANZTAS A and LANGFORD C (2001) A two-domain approach to model solute transport in an undisturbed soil column using X-ray CAT scanning. In: DD Bosch and KW King (eds.) Preferential Flow, Water Movement and Chemical Transport in the Environment, Proc. 2nd Int. Symp. (3-5 January 2001, Honolulu, Hawaii, USA), St. Joseph, Michigan: ASAE 701P0006, 109-112.

PETERSEN CT, JENSEN HE, HANSEN S and BENDER KOCH C (2001) Susceptibility of a sandy loam soil to preferential flow as affected by tillage. *Soil and Tillage Research* **58** 81-89.

POOL DR and EYCHANER JH (1995) Measurements of aquifer-storage change and specific yield using gravity surveys *Ground Water* **33**, 425-432.

PRAASMA T, NOVAKOWSKI K and KYSER K (2009) Using stable isotopes and hydraulic head data to investigate groundwater recharge and discharge in a fractured rock aquifer. *Journal of Hydrology* **366** 35-45.

PRIESTLEY CHB and TAYLOR RJ (1972) On the assessment of surface heat flux and evaporation using large scale parameters. *Mon. Weath. Rev*. **100** 81-92.

RAWLINS MA, FROLKING S, LAMMERS RB and VOROSMARTY CJ (2006) Effects of uncertainty in climate inputs on simulated evapotranspiration and runoff in the Western Arctic. *Earth Interactions* 10(18) 1-18.

RAWLS WJ, PACHEPSKY YA and LIN HS (2001) Evaluation of methods to estimate macropore characteristics in montmorillonitic clay soils. In: DD Bosch and KW King (eds.) Preferential Flow, Water Movement and Chemical Transport in the Environment, Proc. 2nd Int. Symp. (3-5 January 2001, Honolulu, Hawaii, USA), St. Joseph, Michigan: ASAE 701P0006, 233-236.

REBELO AG, BOUCHER C, HELME N, MUCINA L and RUTHERFORD MC (2006) Fynbos biome. In L Mucina and MC Rutherford (eds.) The Vegetation of South Africa, Lesotho and Swaziland. Strelitzia 19. South African National Biodiversity Institute, Pretoria, 53-219.

REFSGAARD JC, VAN DER SLUIJS JP, HOLBERG AL and VANROLLEGHEM PA (2007) Uncertainty in the environmental modelling process – A framework and guidance. *Environmental Modelling & Software* **22** 1543-1556.

RHOADES J (1996) Salinity: Electrical conductivity and total dissolved solids. In: DL Sparks (ed.) Methods of soil analysis: Chemical methods: Part 3. Soil Science Society of America, Madison, Wisconsin, 417-435.

RHOADES J (1996) Salinity: Electrical conductivity and total dissolved solids. In: DL Sparks (ed.) Methods of soil analysis: Chemical methods: Part 3. Soil Science Society of America, Madison, Wisconsin, 417-435.

RITCHIE JT (1972) Model for predicting evaporation from a row crop with incomplete cover. *Water Resources Research* **8** 1204-1213.

ROSENBERG NJ, BLAD BL and VERMA SB (1983) Microclimate: The Biological Environment. 2nd edition. Wiley, New York, 495 pp.

SAAYMAN IC, BEEKMAN HE, ADAMS S, CAMPBELL RB, CONRAD J, FEY MB, JOVANOVIC N, THOMAS A and USHER BH (2007) Assessment of aquifer vulnerability. Water Research Commission report No. 1432/1/07, Pretoria, South Africa.

SAMOUELIAN A, COUSIN I, RICHARD G, TABBAGH A and BRUAND A (2003) Electrical resistivity imaging for detecting soil cracking at the centimetric scale. *Soil Science Society of America Journal* **67(5)** 1319-1326.

SANDERSON JS and COOPER DJ (2008) Ground water discharge by evapotranspiration in wetlands of an arid intermountain basin. *Journal of Hydrology* **351** 344-359.

SAVAGE MJ, EVERSON CS, ODHIAMBO GO, MENGISTU MJ and JARMAIN C (2004) Theory and practice of evaporation measurement, with special focus on SLS as an operational tool for the estimation of spatially-averaged evaporation. Water Research Commission Report No. 1335/1/04, Pretoria, South Africa.

SAXTON K and RAWLS W (2006) Soil water characteristic estimates by texture and organic matter for hydrologic solutions. *Soil Sci. Soc. Am. J.* **70** 1569-1578.

SCANLON BR, HEALY RW and COOK PG (2002) Choosing appropriate techniques for quantifying groundwater recharge. *Hydrogeology Journal* **10** 18-39.

SCHENK HJ and JACKSON RB (2009) Mapping the global distribution of deep roots in relation to climate and soil characteristics. *Geoderma* **126** 129-140.

SCHULZE RE (1994) Hydrology and agrohydrology: a text to accompany the ACRU-300 agrohydrological modelling system. Agricultural Catchments Research Unit, Department of Agricultural Engineering, University of Natal.

SCHULZE RE (2005) Climate change and water resources in Southern Africa. Water Research Commission report No 1430/1/05, Pretoria, South Africa.

SEYLER H, DODMAN A, WEBB, M, RIEMANN K and HARTNADY CJ (2011) Groundwater modelling for aquifer management and yield limit determination – Gateway Wellfield Hermanus, South Africa.

SHIRMOHAMMADI A, MONTAS H, BERGSTROM L, COYNE K, WEI S and GISH T (2001) Deterministic and stochastic prediction of atrazine transport in soils displaying macropore flow. In: DD Bosch and KW King (eds.) Preferential Flow, Water Movement and Chemical Transport in the Environment, Proc. 2nd Int. Symp. (3-5 January 2001, Honolulu, Hawaii, USA), St. Joseph, Michigan: ASAE 701P0006, 133-136.

SIMIC E and DESTOUNI G (2001) Significance of preferential flow for contaminant transport by groundwater in an integrated soil-groundwater system. In: DD Bosch and KW King (eds.) Preferential Flow, Water Movement and Chemical Transport in the Environment, Proc. 2nd Int. Symp. (3-5 January 2001, Honolulu, Hawaii, USA), St. Joseph, Michigan: ASAE 701P0006, 29-32.

SIMUNEK J, SEJNA M and VAN GENUCHTEN MTh (1999) The HYDRUS-2D software package for simulating two-dimensional movement of water, heat, and multiple solutes in variably-saturated media, Version 2.0. U.S. Salinity Laboratory, USDA, ARS, Riverside, California.

SIVAPALAN M (2003a) Process complexity at hillslope scale, process simplicity at the watershed scale: is there a connection? *Hydrological Processes* **17** 1037-1041.

SIVAPALAN M (2003b) Prediction in ungauged basins: a grand challenge for theoretical hydrology. *Hydrological Processes* **17** 3163-3170.

SOIL CLASSIFICATION WORKING GROUP (1991) Soil Classification – A Taxonomic System for South Africa. Memoirs on the agricultural natural resources of South Africa No. 15. Department of Agricultural Development. Pretoria, South Africa.

SOIL CLASSIFICATION WORKING GROUP (1991) Soil Classification – A Taxonomic System for South Africa. Memoirs on the agricultural natural resources of South Africa No. 15. Department of Agricultural Development. Pretoria, South Africa.

SOPHOCLEOUS M and PERKINS SP (2000) Methodology and application of combined watershed and ground-water models in Kansas. *Journal of Hydrology* **236** 185-201.

SPARKS DL (ed.) (1996) Methods of Soil Analysis Part 3 (2 ed.), Soil Science Society of America, Madison, Wisconsin.

STARR JL (2001) Estimating preferential infiltration and redistribution from real-time measurements of soil water content. In: DD Bosch and KW King (eds.) Preferential Flow, Water Movement and Chemical Transport in the Environment, Proc. 2nd Int.

Symp. (3-5 January 2001, Honolulu, Hawaii, USA), St. Joseph, Michigan: ASAE 701P0006, 97-100.

THOMAS G (1996) Soil pH and soil acidity. In D Sparks (ed.). Methods of Soil Analysis: Chemical Methods. Part 3. Soil Science Society of America, Madison, Wisconsin, 475-490.

THORNTHWAITE CW (1948) An approach toward a rational classification of climate. *Geograph. Rev*. **38** 55.

TICEHURST J, CRESSWELL H, MCKENZIE N and GILOVER M (2007) Interpreting soil and topographic properties to conceptualise hillslope hydrology. *Geoderma* **137** 279-292.

TIETJEN B, ZEHE E and JELTSCH F (2009) Simulating plant water availability in dry lands under climate change: A generic model of two soil layers. *Water Resources Research* **45** W01418, doi:10.1029/2007WR006589.

TYNER JS, BROWN GO and HUNTLEY D (2001) Applying chloride mass balance to quantify preferential flow at multiple sites. In: DD Bosch and KW King (eds.) Preferential Flow, Water Movement and Chemical Transport in the Environment, Proc. 2nd Int. Symp. (3-5 January 2001, Honolulu, Hawaii, USA), St. Joseph, Michigan: ASAE 701P0006, 101-104.

VAN DEN BRINK C, ZAADNOORDIJK WJ, BURGERS S and GRIFFIOEN J (2008) Stochastic uncertainties and sensitivities of a regional-scale transport model of nitrate in groundwater. *Journal of Hydrology* **361** 309-318.

VAN DER KAMP G and SCHMIDT R (1997) Monitoring of total soil moisture on a scale of hectares using groundwater piezometers. *Geophys. Res. Lett*. **24** 719-722.

VAN DER LEE J and GEHRELS JC (1997) Modelling of groundwater for a fractured dolomite aquifer under semi-arid conditions. In IAH-recharge of Phreatic Aquifers in semi-arid areas (ed. I. Simmers), A.A. Balkema/Rotterdam, 129-144 pp.

VAN HUYSSTEEN C, HENSLEY M, LE ROUX P, ZERE T and DU PREEZ C (2005) The Relationship between Soil Water Regime and Soil Profile Morphology in the Weatherley Catchment, an Afforestation Area in the North-Eastern Eastern Cape. Water Research Commission Report No. K5/1317. Pretoria, South Africa.

VAN HUYSSTEEN CW (1995) The relationship between subsoilcolour and degree of wetness in a suite of soils in the Grabouw district, Western Cape. MSc Thesis, Stellenbosch University, South Africa.

VEGTER JR (1995) *An Explanation of a Set of National Groundwater Maps*. Water Research Commission report No. TT74/95, Pretoria, South Africa.

VOLTZ M and GOULARD M (1994) Spatial interpolation of soil moisture retention. *Geoderma* **62** 109-123.

WAHR J, MOLENAAR M and BRYAN F (1998) Time-Variability of the Earth's Gravity Field: Hydrological and Oceanic Effects and Their Possible Detection Using GRACE. *J. Geophys. Res.* **103** 30205 30230.

WALKER WE, HARREMOES P, ROTMANS J, VAN DER SLUIJS JP VAN ASSELT MBA JANSSEN P and KRAYER VON KRAUSS MP (2003) Defining uncertainty a conceptual basis for uncertainty management in model-based decision support. *Integrated Assessment* **4(1)** 5e1,

WANG ZR and WANG WY (2001) An improved Darcy's model of soil water movement with preferential paths. In: DD Bosch and KW King (eds.) Preferential Flow, Water Movement and Chemical Transport in the Environment, Proc. 2nd Int. Symp. (3-5 January 2001, Honolulu, Hawaii, USA), St. Joseph, Michigan: ASAE 701P0006, 125-128.

WATERLOO HYDROGEOLOGIC Inc. (1999) User's manual for Visual MODFLOW. Waterloo Hydrogeologic Inc., Waterloo, Ontario, Canada.

WEILER M and McDONNELL JJ (2007) Conceptualizing lateral preferential flow and flow networks and simulating the effects on gauged and ungauged hillslopes. *Water Resources Research* **43**, W03403, doi:10.1029/2006WR004867.

WEILER M and NAEF F (2002) Simulating surface and subsurface initiation of macropore flow. *Journal of Hydrology* **273** 139-154.

WILLMOTT CJ (1981) On the validation of models. *Phys. Geogr.* **2** 184-194.

WOODFORD AC (2007) Preliminary Assessment pf Supplying Eskom's Ankerlig Power Station with Water from Local Groundwater Resources. SRK Consulting report No. 374624, Cape Town, South Africa.

WU Y (2005) Groundwater recharge estimation in Table Mountain Group aquifer systems with a case study of Kammanassie area. D. Phil. Thesis, University of the Western Cape, South Africa.

XU Y and BEEKMAN HE (2003) A box model for estimating recharge – The RIB method. In Y Xu and HE Beekman (eds.) *Groundwater Recharge Estimation in Southern Africa*, UNESCO IHP Series No. 64, UNESCO, Paris, 81-88.

XU Y, LIN L and JIA H (2009) Groundwater flow conceptualisation and storage determination of the Table Mountain Group (TMG) aquifers. Water Research Commission Report No. 1419/1/09, Pretoria, South Africa.

XU Y, WU Y and DUAH A (2007) Groundwater recharge estimation of Table Mountain Group aquifer systems with case studies. Water Research Commission report No. 1329/1/07, Pretoria, South Africa.

YE M, POHLMANN K, CHAPMAN J and SHAFER D (2006) On Evaluation of Recharge Model Uncertainty: a Priori and a Posteriori. American Nuclear Society. Las Vegas, Nevada.

YELENIK SG, STOCK WD and RICHARDSON DM (2004) Ecosystem level impacts of invasive *Acacia saligna* in the South African fynbos. *Restoration Ecology* **12(1)** 44-51.

ZHENG C (1993) Extension of the method of characteristics for simulation of solute transport in three dimensions. *Ground Water* **31(3)** 456-465.

ZHENG C and WANG PP (1999) MT3DMS: A modular three-dimensional multi-species model for simulation of advection, dispersion and chemical reactions of contaminants in groundwater systems: Documentation and user's guide, SERDP-99-1, U.S. Army Engineer Research and Development Centre, Vicksburg, MS.

ZHENG C, HILL MC, HSIEH PA (2001) MODFLOW-2000, the U.S. Geological Survey modular ground-water model – User guide to the LMT6 package, the linkage to MT3DMS for multispecies mass transport modelling, U.S Geological Survey Open-File Rep. 01-82, 43 pp.

ZHOU QY, SHIMADA J and SATO A (2001) Three-dimensional rainfall infiltration process in heterogeneous soil. In: DD Bosch and KW King (eds.) Preferential Flow, Water Movement and Chemical Transport in the Environment, Proc. 2nd Int. Symp. (3-5 January 2001, Honolulu, Hawaii, USA), St. Joseph, Michigan: ASAE 701P0006, 257-260.